OPERATION KOMOREBI

REALIZATION CALCULUS

CORE SERIES VII

Quantum Seeds and Effective Dynamics

Symmetry, geometric transport, quantum channels, and bounded refinement towers

A quantum seed generates a space through an operator grammar. Packets resolve how symmetry, evolution, geometry, and hidden degrees of freedom change that space.

Komorebi P.

Modern Monograph • 18 October 2026

How to use this volume

Part I. The finite quantum seed calculus develops the packet language and states the precise scope of the archived formal proof.
Part II. The strengthened development extends this language through seventy-nine theorem, proposition, lemma, and corollary proofs.
Part III. Six supplements give the detailed mathematical constructions behind the formal proofs, followed by three alternative derivations.
Part IV. Forty worked visual pages connect the formulas to finite models and identify the hypotheses needed at each continuum boundary.

Reading this edition

A seed is useful only together with the operators allowed to act on it. Paper VII follows that principle through symmetry packets, quantum circuits, moving projectors, channels, effective dynamics, and refinement. The finite calculus in Part I supplies the common language. The strengthened development in Part II gives broader bounded constructions and limit criteria. Part III retains the detailed proof completions rather than reducing them to a status summary.

The original finite item numbers keep the prefix I. The strengthened development has the prefix II, and the supplementary constructions have the prefix III. All nine mathematical source parts are retained. This edition revises their explanatory prose while preserving the mathematical expressions, hypotheses, proof steps, and statement inventory. The accompanying report records the changes. Overlapping statements and proofs are retained because their hypotheses and uses differ. Their total is not a count of independent discoveries.

The selected archived formal checkpoint covers nineteen scoped manuscript items. It records 323 explicit theorem declarations across twenty-five active Lean proof modules. These are different units. The strengthened Part II is outside that nineteen-item contract. The formal evidence comes from the archived checkpoint of 6 September 2026. The present prose revision does not report a fresh Lean compilation. Exact hypotheses, declarations, inherited compiler records, and reproduction instructions appear in the Lean companion.

Five explicitly named conjectures remain open in the finite core: anomaly-free refinement, uniform Feshbach control, Lorentzian reconstruction, the Einstein infrared limit, and massless spin-two packets. Bounded direct limits and norm limits provide useful criteria. Each physical target still needs the additional structure stated in its conjecture.

Four distinctions to keep in view

A seed's algebraic orbit is different from a unitary state-preparation orbit. Compression is different from an effective resolvent. A normalized channel is different from an unnormalized error family. A finite spectrum is different from a continuum particle interpretation. Keeping these distinctions visible makes the later results easier to use.

Read Part I first for the packet grammar and the finite statements. Turn to Part II for bounded operator transport, spectral and channel constructions, and refinement towers. Use Part III when the geometric bundle construction or a formal specialization needs more detail. The visual atlas follows the same topics through explicit examples. It illustrates the statements with finite data and does not replace their proofs.

Contents

Reading this edition i

I Corrected finite quantum seed calculus **1**

Three exact finite models 1
I.1 The quantum seed realization 4
I.2 Quantum seed rank and cyclicity 5
I.2.1 Finite observable algebras 5
I.2.2 A computational-basis seed 6
I.3 Cyclic symmetry packets 7
I.3.1 Character projectors 7
I.3.2 Tensor refinement 7
I.4 Quantum circuits as packet paths 9
I.5 Symmetry-resolved Hamiltonians and leakage 10
I.5.1 Leakage under broken symmetry 11
I.6 Moving packets, connections, and curvature 12
I.6.1 Moving quantum coordinates 12
I.6.2 A canonical projector connection 13
I.6.3 Projector curvature 14
I.7 Measurements and quantum channels 16
I.7.1 Packet measurements 16
I.7.2 Kraus transfer 17
I.8 Quantum error correction as obstruction-packet annihilation 19
I.9 Exact effective dynamics 21
I.9.1 Schur–Feshbach reduction 21
I.9.2 The hidden packet as memory 22
I.10 Finite quantum geometry 23
I.10.1 A projector-resolved geometry 23
I.10.2 Euclidean transfer 24
I.11 Spectral dimension and continuum diagnostics 25
I.11.1 The circle dispersion bound 26
I.11.2 One- and two-dimensional plateaus 27
I.12 Constraint packets and the quantum-spacetime boundary 28
I.13 Numerical certificates 30
I.15 Conclusion 32

II Strengthened quantum packet calculus and continuum towers **33**

II.1 Introduction 33
II.2 Quantum seeds and observable algebras 35
II.3 Symmetry packets and selection rules 38
II.3.1 Cyclic charge packets 39
II.3.2 Tensor refinement 39
II.4 Quantum circuits as packet paths 41
II.5 Symmetry resolved dynamics and leakage 43
II.6 Moving packets and geometric transport 45
II.6.1 Discrete packet transport 47

II.6.2 Local frames and curvature . . . 48
II.7 Operator packets, measurements, and quantum channels . . . 50
II.7.1 Channel superblocks . . . 52
II.7.2 Covariance and coherence order . . . 52
II.7.3 Quantum dynamical semigroups . . . 54
II.8 Quantum error correction as a compression obstruction . . . 55
II.9 Feshbach effective dynamics and hidden packet memory . . . 60
II.9.1 Time memory . . . 62
II.9.2 Stability across models . . . 65
II.10 Euclidean transfer and finite reflection positivity . . . 65
II.11 Finite spectral geometry and diffusion dimension . . . 68
II.11.1 Periodic lattices . . . 69
II.12 Constraint closure and anomaly packets . . . 71
II.12.1 Constraint refinement . . . 73
II.13 Quantum refinement towers . . . 74
II.13.1 Exact bounded direct limits . . . 75
II.13.2 Norm summable approximation . . . 76
II.14 Continuum milestones and exact boundary . . . 78
II.15 Conclusion . . . 79

III Mathematical proof completions and retained derivations 81
III.1 Exact packets and arbitrary circuit length . . . 81
III.1.1 Circuit paths: source Theorem 4.1 . . . 81
III.1.2 Adjoint conservation: source Theorem 4.2 . . . 82
III.2 Symmetry and measurement . . . 82
III.2.1 Exact symmetry: source Theorem 5.1 . . . 82
III.2.2 Measurements: source Theorem 7.1 . . . 83
III.3 Corrected Feshbach resolvent . . . 83
III.3.1 Correct statement: source Theorem 9.1 . . . 83
III.3.2 Provenance and limits . . . 84
III.4 Dispersion with an explicit spacing condition . . . 84
III.4.1 Checked stronger statement . . . 84
III.4.2 What this does not establish . . . 85
III.5 A constraint diagnostic that vanishes automatically . . . 85
III.5.1 Compressed vanishing without operator closure . . . 86
III.5.2 Interpretation for the paper . . . 86
III.6 One seed for the computational basis . . . 86
III.7 Tensor and polyphase refinement . . . 87
III.8 Differentiated moving coordinates . . . 88
III.9 The canonical packet connection . . . 89
III.10 Finite Kraus channels and full amplification . . . 90
III.11 Actual orbits and sharp seed counts . . . 91
III.11.1 Several seeds: both necessity and construction . . . 91
III.11.2 Simultaneous generation in a direct sum . . . 91
III.12 Schmidt rank and the reduced state . . . 92
III.12.1 An independent definition of Schmidt rank . . . 92
III.12.2 The actual partial trace and its support . . . 92

III.13 Constructed cyclic character projectors . . . 93
III.13.1 Exact coefficient formula . . . 93
III.13.2 Algebraic identities . . . 93
III.13.3 Orthogonality of the projectors . . . 94
III.14 The actual Euclidean transfer exponential . . . 94
III.14.1 Connecting power series and spectral calculus . . . 94
III.14.2 The minimum eigenvalue . . . 94
III.14.3 Positivity, semigroup composition, and the interval . . . 95
III.15 Quantitative leakage from the actual exponential . . . 95
III.15.1 Deriving the estimate by differentiation . . . 95
III.15.2 Checked consequences . . . 96
III.16 Actual projected differentiation and curvature . . . 96
III.16.1 Differentiated projector and section identities . . . 96
III.16.2 Retaining the bracket of vector fields . . . 97
III.16.3 Tensor properties and the remaining global boundary . . . 97
III.17 A constructive and total syndrome recovery . . . 97
III.17.1 Constructing the recovery on the whole ambient space . . . 97
III.17.2 Exact correction, including coherent errors . . . 98
III.18 The precise finite channel statement . . . 98
III.18.1 Necessary and sufficient conditions . . . 99
III.18.2 Including degenerate cases . . . 99
III.19 From Gram data to an actual total recovery . . . 99
III.19.1 Null directions are removed by proof . . . 100
III.19.2 A channel on the whole ambient space . . . 100
III.20 Deriving the Gram matrix from recovery . . . 100
III.20.1 Rank-one rigidity of the corrected channel . . . 101
III.20.2 Trace-preserving recovery supplies the original Gram data . . . 101
III.21 Density matrices, all operators and finite references . . . 101
III.21.1 Normalization is not an extra assumption . . . 102
III.21.2 Complex polarization reaches the whole operator space . . . 102
III.21.3 An arbitrary finite reference system . . . 102
III.22 Coherent combinations and normalization . . . 103
III.22.1 Cross terms for the original errors . . . 103
III.22.2 Every normalized channel in the same span . . . 103
III.22.3 The equivalence for unnormalized error families . . . 103
III.23 Exact examples, trust audit and remaining work . . . 104
III.23.1 Singular, nonorthogonal errors are accepted . . . 104
III.23.2 A genuine channel can still be uncorrectable . . . 104
III.24 The global projected connection . . . 104
III.25 Local products constructed from the projector . . . 104
III.25.1 An invertible intertwiner near each anchor . . . 105
III.25.2 The mutually inverse local maps . . . 105
III.25.3 Smooth overlap maps and rank . . . 105
III.26 A connection on the constructed bundle . . . 105
III.26.1 Connection axioms and smoothness . . . 106
III.26.2 Smoothness of sections in bundle coordinates . . . 106
III.26.3 The local connection and its change of coordinates . . . 106
III.27 From differentiated projectors to the two-form . . . 106

III.27.1 The flat ambient identity is proved in charts . . . 106
III.27.2 Projector and section identities are derived . . . 107
III.27.3 Cancellation of the second derivatives . . . 107
III.27.4 Geometry and scalar conventions . . . 107
III.27.5 An explicit smooth atlas . . . 107
III.28 Earlier compact derivations retained as alternatives . . . 108
III.28.1 Duhamel proof of leakage from a fixed packet . . . 108
III.28.2 Proof of projected curvature with exterior forms . . . 108
III.28.3 Restricted low-mode proof . . . 109

IV Worked visual atlas **110**
References . . . 150

List of Figures

1 The figure displays exact coefficient matrices for $d = 2$, $m = 3$. The combined row support of two seeds has rank three. The bar heights record algebraic orbit dimensions and should not be read as probabilities of unitary state preparation. 1
2 This rational model uses two coordinates to illustrate block inversion. Both the eliminated block and the full operator are invertible, and the plotted values are exact fractions. The example shows why direct compression and resolvent elimination give different results. 2
3 The figure shows exact weights for one supported code state. The normalized map preserves trace one, while the unnormalized positive map has output trace four. The illustration records this finite scaling distinction and does not assert a general recovery construction. 3
4 The diagram shows the quantum realization of the common sequence of operators in the seed calculus. The same finite packet language describes states, gates, Hamiltonians, channels, geometric projectors, and effective dynamics. 4
5 The eight computational packets of three qubits refine the two total-parity packets exactly. 8
6 The Bell state generated from the seed $|00\rangle$. 10
7 Circuit reconstruction as a sum over packet paths. 10
8 The Hamiltonian becomes exactly block diagonal when the even and odd basis vectors are grouped. 11
9 A perturbation that breaks parity creates nonzero transfer between the packets. The measured leakage remains below the commutator bound. 12
10 The equation in the moving frame holds to numerical precision only when the connection term is retained. 13
11 The curvature of the Bloch projector, evaluated by finite differences, is compared with the exact density $\frac{1}{2}\sin\theta$. 16
12 Amplitude damping transfers population from the excited packet to the ground packet while preserving trace and positivity. 18
13 The four orthogonal syndrome packets of the three-qubit bit-flip code. Each packet identifies one correctable error without resolving the encoded logical state. 21
14 Exact Feshbach reduction versus bare truncation. 22
15 Norms of packet Green-function blocks. 22
16 The diagram organizes a conjectural nested packet tower for quantum geometry. It does not provide a numerical reconstruction of physical spacetime. 24
17 Positive spectrum of the Euclidean transfer operator. 25
18 Ground-state volume packet in the controlled toy model. 25
19 The figure shows the finite Euclidean kernel for volume transfer. Positivity and semigroup composition hold exactly in the finite model. Its gravitational interpretation remains provisional. 26
20 The first nonzero circle mode converges at second order and remains below the proved dispersion bound. 27
21 The curves show intermediate windows of spectral dimension for a finite cycle and a finite two-dimensional torus. Departures in the ultraviolet and infrared reflect the finite size of the models rather than additional dimensions. 28
22 The proof boundary. Finite packet, circuit, leakage, Feshbach, connection, and spectral identities are established here. Constraint closure and the physical continuum claims remain conjectural. 30

23 The finite mathematical layers developed in the article and the separate limit criteria needed at the continuum boundary. . . . 35
24 The dimension reached by all local operators is linear in Schmidt rank. . . . 37
25 An operator of charge one moves each cyclic packet to the next packet and has no other transfer blocks. . . . 40
26 A circuit block is the coherent sum of its allowed packet paths. Selection rules remove forbidden paths before amplitudes are evaluated. . . . 43
27 Exact transition amplitude in a two packet model and the linear commutator bound. . . . 44
28 A moving rank one packet on the Bloch sphere. The Kato evolution transports the range without choosing a phase convention for its eigenvector. . . . 48
29 A density matrix or observable carries two packet addresses. Diagonal packets contain populations and internal observables. Off diagonal packets contain coherences. . . . 51
30 Amplitude damping transfers population and contracts the coherence packet. . . . 54
31 The syndrome packets of the three qubit repetition code. Each packet has dimension two and carries the full logical state. . . . 59
32 The zeros of the Feshbach determinant recover the eigenvalues of the full finite Hamiltonian away from the hidden spectrum. . . . 61
33 A finite hidden spectrum produces an oscillatory memory kernel. The retained dynamics therefore depend on the history of the retained state. . . . 64
34 Eigenvalues of a finite reflection positive Gram matrix. Small numerical negative values would signal either roundoff or failure of the transfer assumptions. . . . 67
35 Finite periodic lattices show an intermediate dimension window. The ultraviolet and infrared limits return to zero because the state space is finite. . . . 71
36 The closure obstruction lives in a quotient by the constraint span. Physical compression is automatic for self adjoint constraints and cannot replace this quotient. . . . 72
37 A refinement tower carries Hamiltonians, packets, constraints, and transfer data. Each family has its own compatibility defect. . . . 74
38 The finite identities occupy the first step. Every later step needs a separate convergence or reconstruction theorem. . . . 79

Part I Corrected finite quantum seed calculus

A route through this section

The finite core starts with seed rank, then resolves symmetry and circuit transfer into packets. Its geometric statements use the actual range bundle, including the Lie-bracket term. Its channel and Feshbach statements keep normalization and invertibility visible. The three examples below introduce those distinctions with exact finite data.

Three exact finite models

A seed remembers multiplicity support

For $M_2(\mathbb{C}) \otimes I_3$, a coefficient matrix with rank one generates an orbit of dimension two. A matrix of rank two generates an orbit of dimension four. Neither single seed spans the full space of dimension six, because a 2×3 matrix cannot have rank three. Two seeds can nevertheless cover all three multiplicity coordinates together. The example illustrates the finite seed rank formula with $d = 2$ and $m = 3$.

Seed rank measures the available multiplicity support

```
C1 = [[1, 0, 0], [0, 0, 0]]

C2 = [[1, 0, 0], [0, 1, 0]]

C3 = [[0, 0, 1], [0, 0, 0]]

C2 and C3 cover all 3 columns.
```

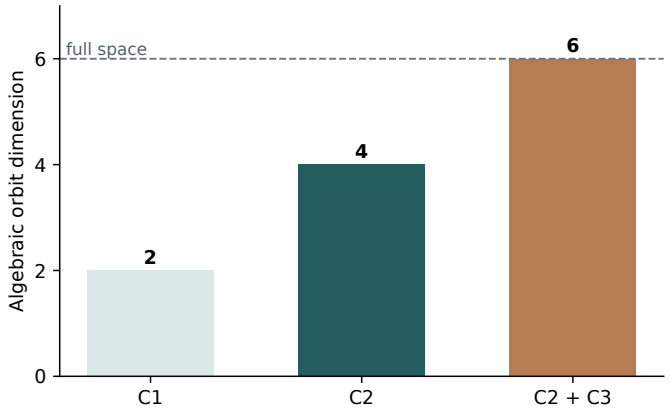


Figure 1. The figure displays exact coefficient matrices for $d = 2, m = 3$. The combined row support of two seeds has rank three. The bar heights record algebraic orbit dimensions and should not be read as probabilities of unitary state preparation.

An eliminated coordinate still contributes

Take $H = \left(\begin{smallmatrix} 2 & 1 \\ 1 & 3 \end{smallmatrix}\right)$ and retain its first coordinate. The eliminated block is invertible and the Schur complement of H is $2 - 1/3 = 5/3$. Its inverse is $3/5$, exactly the retained entry of H^{-1}. Inverting the compressed entry alone gives $1/2$. The difference records the contribution of a path through the eliminated coordinate. Direct compression omits that contribution, while block inversion retains it.

Block inversion includes the discarded coordinate

```
H = [[2, 1], [1, 3]]

Schur complement of H:

2 - 1/3 = 5/3

Retained entry of H inverse:

(5/3) inverse = 3/5
```

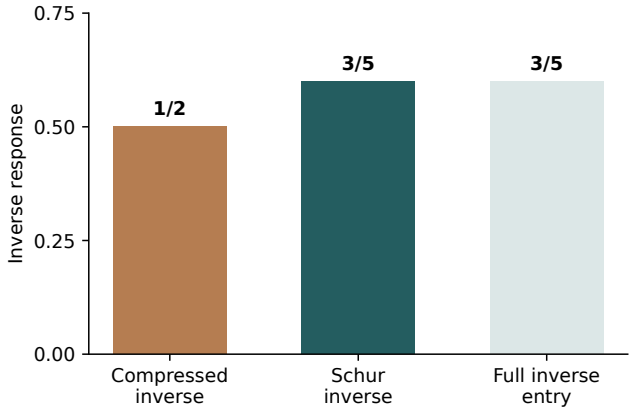


Figure 2. This rational model uses two coordinates to illustrate block inversion. Both the eliminated block and the full operator are invertible, and the plotted values are exact fractions. The example shows why direct compression and resolvent elimination give different results.

Normalization changes the map

Let $P = |0\rangle\langle 0|$ on $\mathbb{C}^2$ and $Z = \mathrm{diag}(1, -1)$. The normalized Kraus family $\sqrt{3/4}\, I$, $\sqrt{1/4}\, Z$ satisfies $\sum_j K_j^* K_j = I$ and maps P to P. The unnormalized family $\sqrt{3}\, I$, Z satisfies $\sum_j E_j^* E_j = 4I$ and maps P to $4P$. The two families have the same relative weights, but their total normalization differs. Both outputs are proportional to the same projector, but their traces differ.

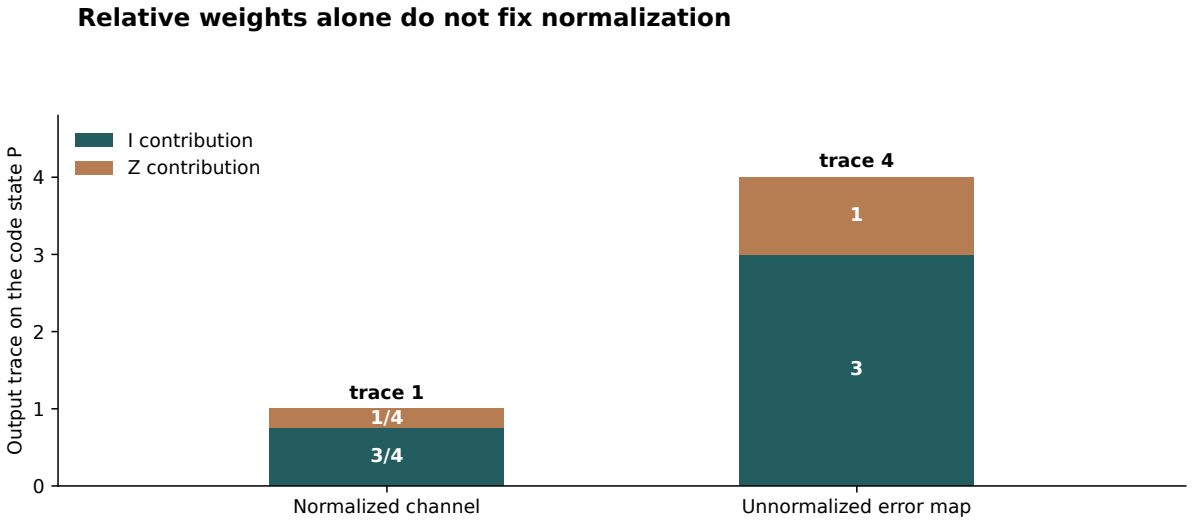


Figure 3. The figure shows exact weights for one supported code state. The normalized map preserves trace one, while the unnormalized positive map has output trace four. The illustration records this finite scaling distinction and does not assert a general recovery construction.

I.1 The quantum seed realization

Conventions. Unless the zero space is explicitly included as a boundary case, quantum state spaces are nonzero complex Hilbert spaces of finite dimension. A complete packet family is a finite collection satisfying

$$P_\alpha^* = P_\alpha, \qquad P_\alpha P_\beta = \delta_{\alpha\beta} P_\alpha, \qquad \sum_\alpha P_\alpha = I.$$

All operator norms in the analytic estimates are induced by the norm on the Hilbert space. The estimates do not use the entrywise maximum norm or the Frobenius norm. We write $[A, B] = AB - BA$ and use units with $\hbar = 1$. Parameter derivatives are real derivatives. A matrix X is supported on a code projector P when $PXP = X$.

The common operator sequence of the series becomes

$$\boxed{\begin{array}{c}\text{quantum seed} \longrightarrow \text{gate or observable address} \longrightarrow \text{symmetry projection} \\ \longrightarrow \text{packet transfer} \longrightarrow \text{constraint} \longrightarrow \text{refinement} \longrightarrow \text{reconstruction}\end{array}}$$

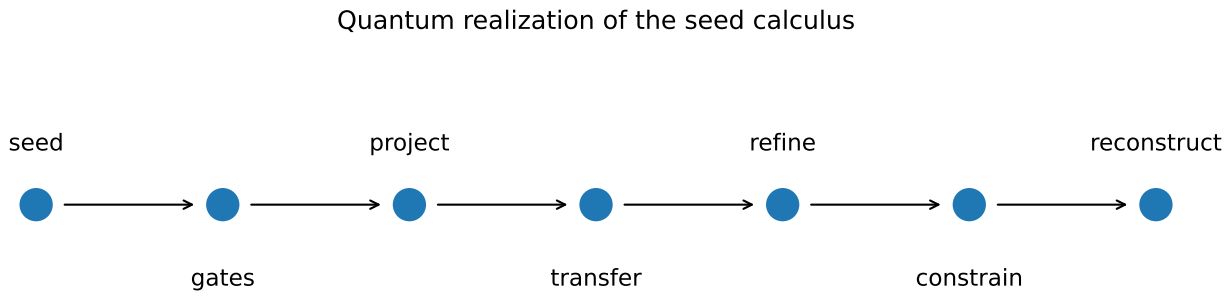


Figure 4. The diagram shows the quantum realization of the common sequence of operators in the seed calculus. The same finite packet language describes states, gates, Hamiltonians, channels, geometric projectors, and effective dynamics.

Definition I.1.1 (Finite quantum seed system)**.** A finite quantum seed system is a tuple

$$\mathfrak{Q} = \left(\mathcal{H}, \psi_0, \mathcal{O}, \mathcal{R}, \{P_{\ell,\alpha}\}, H, \tau\right),$$

where $\mathcal{H}$ is a finite-dimensional Hilbert space, $\psi_0 \in \mathcal{H}$ is a nonzero seed, $\mathcal{O}$ is the declared operator grammar, $\mathcal{R}$ is a collection of algebraic or physical constraints, $\{P_{\ell,\alpha}\}$ is an exact packet system at each refinement level, $H = H^*$ is a Hamiltonian when dynamics are present, and τ specifies the topology used in a later completion.

The generated state space is

$$\mathcal{H}(\psi_0; \mathcal{O}) = \operatorname{span}\left\{O_r \cdots O_1 \psi_0 : O_j \in \mathcal{O},\ r \geq 0\right\}.$$

The quantum seed is cyclic for the grammar when

$$\mathcal{H}(\psi_0; \mathcal{O}) = \mathcal{H}.$$

This is a statement about the pair $(\psi_0, \mathcal{O})$, not about the vector alone. A state may be cyclic for the full matrix algebra and noncyclic for a restricted physical gate set.

I.2 Quantum seed rank and cyclicity

I.2.1 Finite observable algebras

Let a finite-dimensional unital $*$-subalgebra of operators act in its standard multiplicity form

$$\mathcal{A} \cong \bigoplus_{i=1}^{r} \left(M_{d_i}(\mathbb{C}) \otimes I_{m_i} \right)$$

on

$$\mathcal{H} \cong \bigoplus_{i=1}^{r} \left(\mathbb{C}^{d_i} \otimes \mathbb{C}^{m_i} \right).$$

Here every d_i is a positive integer and every multiplicity m_i is a nonnegative integer. An empty block family represents the zero space and has seed rank zero. The maximum over an empty block family is also assigned the value zero. A vector $\psi_i \in \mathbb{C}^{d_i} \otimes \mathbb{C}^{m_i}$ is identified with a $d_i \times m_i$ coefficient matrix C_i.

Theorem I.2.1 (Orbit dimension of one quantum seed). *For integers $d \geq 1$ and $m \geq 0$, consider the action of $M_d(\mathbb{C}) \otimes I_m$ on $\mathbb{C}^d \otimes \mathbb{C}^m$. Let C be the coefficient matrix of a vector ψ. Then*

$$\boxed{\dim \operatorname{span}\{(A \otimes I_m)\psi : A \in M_d(\mathbb{C})\} = d \operatorname{rank} C.}$$

The seed is cyclic if and only if $\operatorname{rank} C = m$*, which is possible only when $m \leq d$.*

Proof. Under the identification by coefficient matrices, $(A \otimes I_m)\psi$ corresponds to AC. Every row of AC lies in the row space of C. Conversely, any $d \times m$ matrix whose rows lie in the row space of C equals AC for a suitable A: choose each row of A to produce the desired row combination. The orbit therefore consists of all matrices with d independently chosen rows in the $\operatorname{rank} C$-dimensional row space of C, and has dimension $d \operatorname{rank} C$. It equals the full dm-dimensional space exactly when $\operatorname{rank} C = m$. □

Theorem I.2.2 (Quantum seed-rank formula). *For*

$$\mathcal{A} = \bigoplus_i (M_{d_i}(\mathbb{C}) \otimes I_{m_i}) \quad \text{on} \quad \mathcal{H} = \bigoplus_i (\mathbb{C}^{d_i} \otimes \mathbb{C}^{m_i}),$$

the minimum number of seeds required to generate $\mathcal{H}$ is

$$\boxed{\operatorname{srank}_{\mathcal{A}}(\mathcal{H}) = \max_i \left\lceil \frac{m_i}{d_i} \right\rceil.}$$

Proof. Each seed contributes a coefficient matrix of rank at most d_i in the ith block. Thus k seeds can cover at most a kd_i-dimensional subspace of the multiplicity factor $\mathbb{C}^{m_i}$, so $k \geq \lceil m_i/d_i \rceil$ for every i.

For the converse, take

$$k = \max_i \left\lceil \frac{m_i}{d_i} \right\rceil.$$

In each block, partition a basis of $\mathbb{C}^{m_i}$ into at most k groups of size at most d_i. Choose the coefficient matrix of seed a so that its nonzero rows span the ath group. The combined row spaces of the k seeds then span $\mathbb{C}^{m_i}$ in every block. The preceding theorem shows that their $\mathcal{A}$-orbits generate the whole direct sum. □

Corollary I.2.3 (Local orbit and Schmidt rank)**.** *Let $\psi \in \mathcal{H}_A \otimes \mathcal{H}_B$, with $\dim \mathcal{H}_A = d_A \geq 1$, and let r be its Schmidt rank. The reduced positive operator on B is $\rho_B = \mathrm{Tr}_A(|\psi\rangle\langle\psi|)$. Normalization of ψ does not affect its support. Then*

$$\boxed{\dim \mathrm{span}\{(A \otimes I_B)\psi : A \in M_{d_A}(\mathbb{C})\} = d_A r.}$$

In particular, local operators on A generate the complete bipartite Hilbert space exactly when the reduced state on B has full support.

Proof. A Schmidt decomposition of length r gives a coefficient matrix of rank r. Applying Theorem I.2.1 gives the orbit dimension $d_A r$. The range of ρ_B is the span of the r Schmidt vectors on B, so full support is equivalent to $r = \dim \mathcal{H}_B$. Because $d_A > 0$, this is equivalent to the orbit having the full bipartite dimension. □

The conclusion concerns the algebraic span obtained from arbitrary local operators. A normalized unitary gate orbit need not contain every vector, and the span statement does not supply a deterministic protocol for preparing arbitrary remote states. Entanglement controls the multiplicity support appearing in that algebraic span.

I.2.2 A computational-basis seed

Theorem I.2.4 (One seed for the computational basis)**.** *For an integer $n \geq 0$, let*

$$\psi_0 = |0\rangle^{\otimes n}$$

and let X_j denote the Pauli X operator on qubit j. Then

$$\{X_1^{a_1} \cdots X_n^{a_n} \psi_0 : (a_1, \ldots, a_n) \in \{0,1\}^n\}$$

is the complete computational basis. Hence the seed is cyclic under the algebra generated by the X_j.

Proof. For a binary address $a = (a_1, \ldots, a_n)$,

$$X_1^{a_1} \cdots X_n^{a_n} |0 \cdots 0\rangle = |a_1 \cdots a_n\rangle .$$

Distinct binary addresses produce distinct orthonormal basis vectors. There are 2^n of them, equal to the dimension of the Hilbert space. □

Recorded Numerical Check I.2.5 (Three-qubit seed orbit). The original numerical implementation generated all eight computational basis states from $|000\rangle$ using the three local X address operators. It reported an orbit rank of $8/8$.

I.3 Cyclic symmetry packets

I.3.1 Character projectors

Let $N \geq 1$ be an integer, and let S be a unitary symmetry whose order divides N:

$$S^N = I.$$

Set $\omega = e^{2\pi i/N}$.

Theorem I.3.1 (Cyclic quantum projectors). *The operators*

$$\boxed{P_j = \frac{1}{N}\sum_{r=0}^{N-1} \omega^{-jr} S^r, \qquad 0 \leq j < N,}$$

are self-adjoint, pairwise orthogonal projectors satisfying

$$P_j P_k = \delta_{jk} P_j, \qquad \sum_{j=0}^{N-1} P_j = I, \qquad S P_j = \omega^j P_j.$$

Proof. Using $S^{r+s} = S^{r+s \bmod N}$ and the finite character orthogonality relation,

$$\frac{1}{N}\sum_{r=0}^{N-1} \omega^{(k-j)r} = \delta_{jk},$$

we obtain $P_j P_k = \delta_{jk} P_j$. Summing over j cancels every term indexed by $r \neq 0$ and retains the $r = 0$ term, which proves completeness. Unitarity and the change of residue $r \mapsto -r$ give

$$P_j^* = \frac{1}{N}\sum_{r=0}^{N-1} \omega^{jr} S^{-r} = P_j.$$

Finally, multiplication by S shifts the summation index and contributes the factor ω^j. □

For parity,

$$S = Z^{\otimes n}, \qquad P_{\text{even}} = \frac{I+S}{2}, \qquad P_{\text{odd}} = \frac{I-S}{2}.$$

I.3.2 Tensor refinement

Fix $N \geq 1$. Suppose every factor a has a complete orthogonal family $P_0^{(a)}, \ldots, P_{N-1}^{(a)}$. The fine tensor packets are

$$P_{\mathbf{j}}^{\text{fine}} = P_{j_1}^{(1)} \otimes \cdots \otimes P_{j_m}^{(m)}.$$

Theorem I.3.2 (Tensor/polyphase refinement). *For each residue $r \in \mathbb{Z}/N\mathbb{Z}$, define*

$$P_r^{\text{coarse}} = \sum_{j_1+\cdots+j_m \equiv r \pmod N} P_{j_1}^{(1)} \otimes \cdots \otimes P_{j_m}^{(m)}.$$

Then the P_r^{coarse} are complete orthogonal projectors, and every coarse packet is the exact sum of its fine descendants.

Proof. The fine tensor projectors are mutually orthogonal and sum to the identity. Grouping the fine addresses by their total residue partitions the full address set. Sums over disjoint sets of orthogonal projectors remain orthogonal projectors, and the union of the residue classes is the full fine address set. □

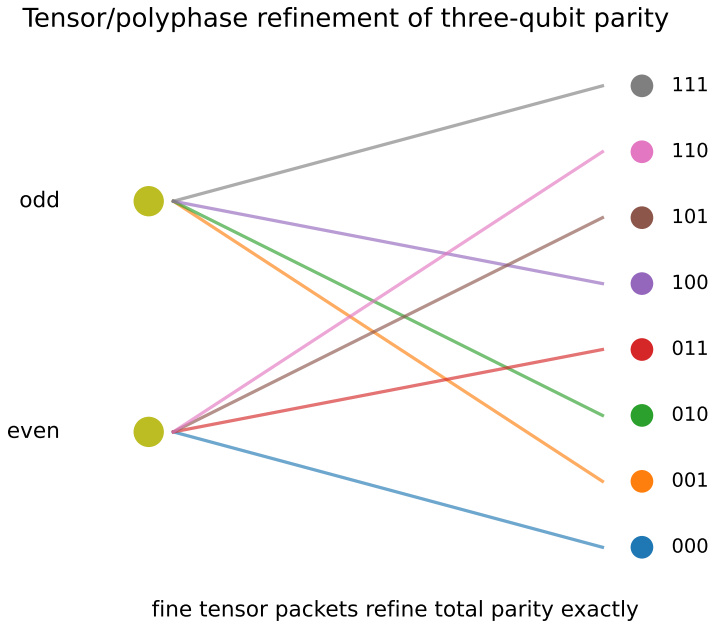


Figure 5. The eight computational packets of three qubits refine the two total-parity packets exactly.

Recorded Numerical Check I.3.3 (Exact parity refinement). For three qubits, the local computational projectors were grouped by the parity of their Hamming weight. The resulting coarse projectors agreed with $(I \pm Z^{\otimes 3})/2$ with residual 0.

I.4 Quantum circuits as packet paths

Let

$$U = U_m U_{m-1} \cdots U_1$$

be a circuit with $m \geq 1$, and let $\{P_\alpha\}$ be a complete packet system. For the empty circuit $m = 0$, set $U = I$. Its boundary block is $P_\beta P_\alpha = \delta_{\beta\alpha} P_\alpha$.

Theorem I.4.1 (Exact circuit path expansion). *For source packet α_0 and target packet α_m,*

$$\boxed{P_{\alpha_m} U P_{\alpha_0} = \sum_{\alpha_1,\ldots,\alpha_{m-1}} P_{\alpha_m} U_m P_{\alpha_{m-1}} \cdots P_{\alpha_1} U_1 P_{\alpha_0}.}$$

Summing over the source and target packets reconstructs the complete circuit operator.

Proof. Insert the identity resolution $I = \sum_\alpha P_\alpha$ between every adjacent pair of gates. Distributing the finite sums gives the path expansion. Summing the left and right boundary projectors reconstructs U. □

Theorem I.4.2 (Packetwise unitarity conservation). *If U is unitary and $U_{\beta\alpha} = P_\beta U P_\alpha$, then*

$$\boxed{\sum_\beta U^*_{\beta\alpha} U_{\beta\gamma} = \delta_{\alpha\gamma} P_\alpha.}$$

Similarly,

$$\sum_\alpha U_{\beta\alpha} U^*_{\delta\alpha} = \delta_{\beta\delta} P_\beta.$$

Proof. Using completeness and unitarity,

$$\sum_\beta U^*_{\beta\alpha} U_{\beta\gamma} = P_\alpha U^* \left(\sum_\beta P_\beta \right) U P_\gamma = P_\alpha P_\gamma.$$

For the second identity, sum over the source packets and use unitarity in the reverse order. □

Example I.4.3 (Bell seed circuit). In this example only, H denotes the Hadamard gate, not a Hamiltonian. Starting from $|00\rangle$,

$$(H \otimes I)\,|00\rangle = \frac{|00\rangle + |10\rangle}{\sqrt{2}},$$

and then

$$\mathrm{CNOT}(H \otimes I)\,|00\rangle = \frac{|00\rangle + |11\rangle}{\sqrt{2}}.$$

The parity packets show that the final state lies entirely in the even sector, while the intermediate circuit path passes through both even and odd addresses.

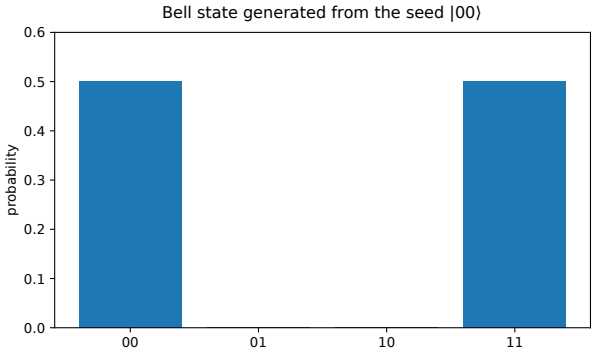


Figure 6. The Bell state generated from the seed $|00\rangle$.

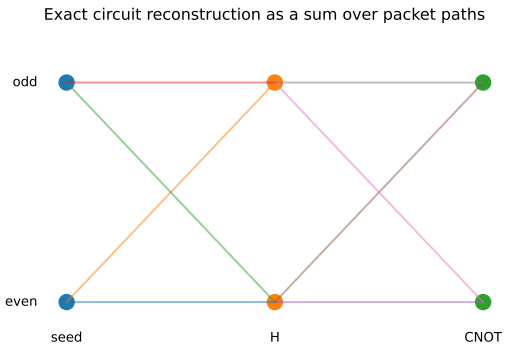


Figure 7. Circuit reconstruction as a sum over packet paths.

Recorded Numerical Check I.4.4 (Bell and path reconstruction). The original numerical implementation reported residuals of 0 for both the Bell state and its complete reconstruction from parity paths.

I.5 Symmetry-resolved Hamiltonians and leakage

Let $H = H^*$ and let P be a packet projector. If $[H, P] = 0$, then $P\mathcal{H}$ is invariant under e^{-itH}.

Theorem I.5.1 (Exact symmetry packets). *If $[H, P_\alpha] = 0$ for every packet, then*

$$H = \sum_\alpha P_\alpha H P_\alpha$$

and

$$e^{-itH} = \sum_\alpha P_\alpha e^{-itH} P_\alpha.$$

No amplitude transfers between distinct packets.

Proof. The commutation relation gives $P_\beta H P_\alpha = 0$ for $\beta \neq \alpha$. Every polynomial in H has the same block form, and the finite-dimensional exponential is the norm limit of its polynomial series. □

For two qubits and real parameters J, h, consider

$$H = JX \otimes X + h(Z \otimes I + I \otimes Z).$$

In the ordered even basis $\{|00\rangle, |11\rangle\}$ and odd basis $\{|01\rangle, |10\rangle\}$,

$$H_{\text{even}} = \begin{pmatrix} 2h & J \\ J & -2h \end{pmatrix}, \qquad H_{\text{odd}} = \begin{pmatrix} 0 & J \\ J & 0 \end{pmatrix}.$$

Therefore

$$\operatorname{Spec} H_{\text{even}} = \{\pm\sqrt{4h^2 + J^2}\}, \qquad \operatorname{Spec} H_{\text{odd}} = \{\pm J\}.$$

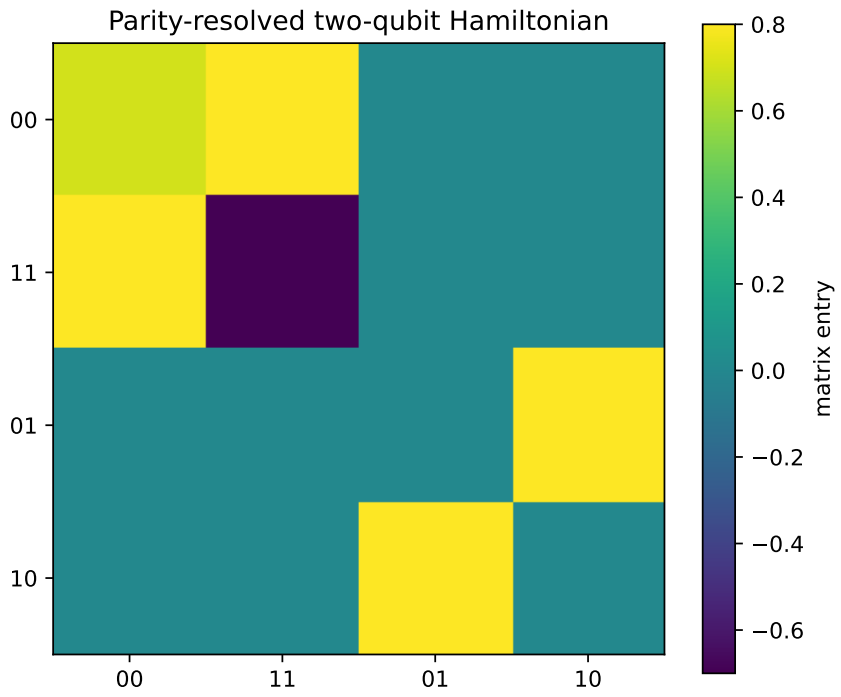


Figure 8. The Hamiltonian becomes exactly block diagonal when the even and odd basis vectors are grouped.

I.5.1 Leakage under broken symmetry

Set $Q = I - P$.

Theorem I.5.2 (Commutator leakage bound)**.** *For every self-adjoint H, orthogonal projector P, and real time t,*

$$\boxed{\left\|Qe^{-itH}P\right\| \le |t|\ \|[H,P]\|\,.}$$

In particular, exact commutation gives zero leakage for all time.

Proof. Set $F(s) = e^{isH}Pe^{-isH}$. Differentiating the exponential gives

$$F'(s) = i\,e^{isH}[H,P]e^{-isH}, \qquad F(0) = P.$$

Unitary conjugation preserves the operator norm, so $\|F'(s)\| = \|[H,P]\|$. The mean-value estimate on the interval between 0 and t yields

$$\|F(t) - P\| \le |t|\,\|[H,P]\|.$$

Finally, $e^{itH}Qe^{-itH}P = (P - F(t))P$ and $\|P\| \le 1$. Left multiplication by e^{itH} preserves the norm and gives the desired inequality. This argument includes positive, negative and zero time. □

Recorded Numerical Check I.5.3 (Symmetry and negative control). For the Hamiltonian that preserves parity, the norm of the block between distinct packets and the maximum measured leakage were both 0. Adding an $X \otimes I$ perturbation broke parity and produced a maximum leakage of approximately 0.79196. The maximum violation of the proved bound remained 0.

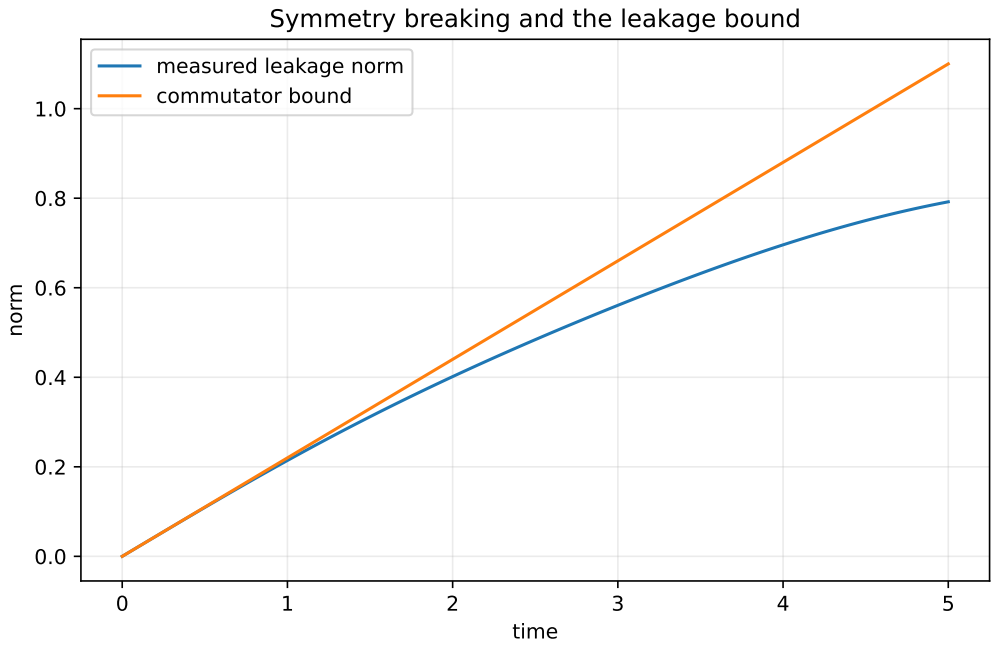


Figure 9. A perturbation that breaks parity creates nonzero transfer between the packets. The measured leakage remains below the commutator bound.

I.6 Moving packets, connections, and curvature

I.6.1 Moving quantum coordinates

Theorem I.6.1 (Moving-frame Hamiltonian). *Let $U(t)$ and $\psi(t)$ be differentiable on an open real time interval, let $U(t)$ be unitary, and let $H(t) = H(t)^*$. Suppose*

$$i\dot{\psi}(t) = H(t)\psi(t).$$

Writing

$$\psi(t) = U(t)y(t)$$

gives

$$\boxed{i\dot{y}(t) = \left(U(t)^*H(t)U(t) - iU(t)^*\dot{U}(t)\right)y(t).}$$

Both the connection term $-iU^*\dot{U}$ and the effective Hamiltonian $U^*HU - iU^*\dot{U}$ are Hermitian.

Proof. Differentiate $\psi = Uy$:

$$i\dot{U}y + iU\dot{y} = HUy.$$

Multiplying by U^* gives the formula. Differentiating $U^*U = I$ shows $U^*\dot{U}$ is skew-Hermitian, so $-iU^*\dot{U}$ is Hermitian. □

Recorded Numerical Check I.6.2 (Moving-frame correction). The reported residual for the complete equation in the moving frame was 1.0645×10^{-10}. Omitting the connection increased the residual to 0.7000.

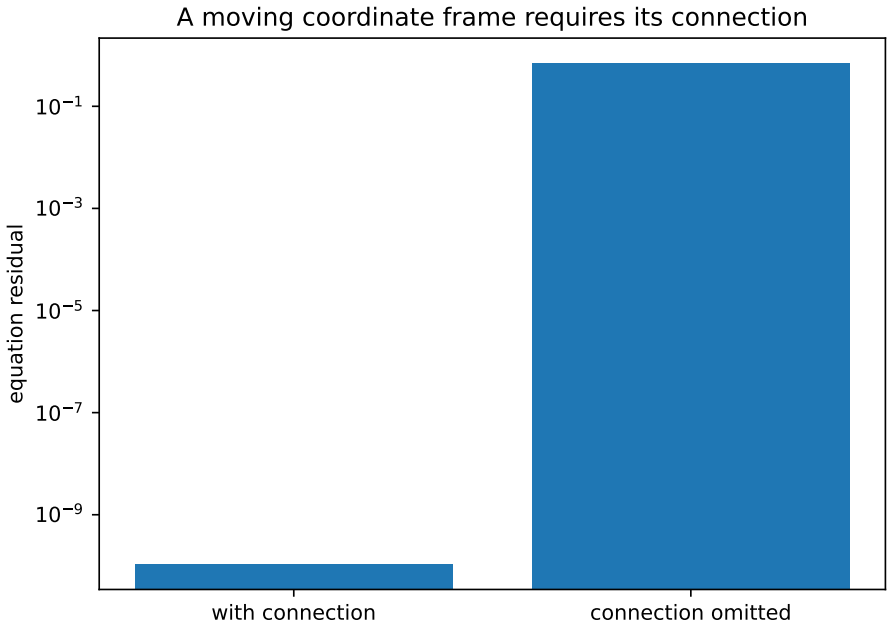


Figure 10. The equation in the moving frame holds to numerical precision only when the connection term is retained.

I.6.2 A canonical projector connection

Let $P_1(t), \dots, P_m(t)$ be differentiable on an open real time interval, with $P_a(t)^* = P_a(t)$ and

$$P_a P_b = \delta_{ab} P_a, \qquad \sum_a P_a = I.$$

Theorem I.6.3 (Canonical packet connection). *Define*

$$\boxed{C(t) = \frac{1}{2} \sum_a [\dot{P}_a(t), P_a(t)] = \sum_a \dot{P}_a(t) P_a(t).}$$

Then

$$C(t)^* = -C(t)$$

and

$$\boxed{[C(t), P_b(t)] = \dot{P}_b(t)}$$

for every packet b.

Proof. Differentiating $P_a^2 = P_a$ gives

$$\dot{P}_a P_a + P_a \dot{P}_a = \dot{P}_a.$$

Summing over a and using $\sum_a \dot{P}_a = 0$ yields

$$\sum_a P_a \dot{P}_a = -\sum_a \dot{P}_a P_a,$$

which proves both displayed formulas for C and its skew-Hermiticity.

For fixed b,

$$CP_b = \dot{P}_b P_b.$$

When $a \neq b$, differentiating $P_b P_a = 0$ gives

$$P_b \dot{P}_a = -\dot{P}_b P_a.$$

Hence

$$P_b C = \sum_a P_b \dot{P}_a P_a = -\dot{P}_b (I - P_b),$$

and subtraction gives $[C, P_b] = \dot{P}_b$. □

The connection generates infinitesimal transport of the moving packet frame. The packet family determines it directly, so its construction does not require a basis inside any packet.

I.6.3 Projector curvature

Classical Input I.6.4 (Projected connection). Let M be a smooth finite-dimensional real manifold without boundary, let V be a finite-dimensional real normed vector space, and let $P : M \to \mathrm{End}_{\mathbb{R}}(V)$ be smooth with $P(x)^2 = P(x)$. In the quantum application, V is the underlying real space of a finite complex Hilbert space and P is an orthogonal complex-linear projector.

The rank of P is locally constant. On each open rank region, its ranges form a smooth vector bundle. For a smooth range section s, so that $Ps = s$, define

$$\nabla_X s = P\, ds(X).$$

This is a connection on smooth range sections. For smooth vector fields X, Y, its curvature satisfies

$$\boxed{(\nabla_X \nabla_Y - \nabla_Y \nabla_X - \nabla_{[X,Y]})s = P[dP(X), dP(Y)]P\, s.}$$

Equivalently, its endomorphism-valued curvature is

$$\boxed{F = P(dP \wedge dP)P.}$$

No global frame or globally constant rank is required, and the vector fields need not commute. The geometric formalization concerns real smooth structures. It does not cover complex analytic manifolds or extensions to a boundary.

Proof. Range coordinates. Fix $a \in M$ and put

$$T_a(x) = P(x)P(a) + (I - P(x))(I - P(a)).$$

Then $T_a(a) = I$ and $P(x)T_a(x) = T_a(x)P(a)$. Invertibility is open, so on a neighborhood of a, $T_a(x)$ restricts to an isomorphism from $\mathrm{Ran}\, P(a)$ to $\mathrm{Ran}\, P(x)$. This proves local constancy of rank. The local coordinates and their transitions are

$$(x, v) \longmapsto (x, T_a(x)^{-1} v), \qquad u \longmapsto T_b(x)^{-1} T_a(x) u.$$

Their smoothness follows from smoothness of P and inversion. The transition maps satisfy the cocycle identity by cancellation. These charts construct the smooth range bundles on the open rank regions, including when different connected components have different ranks.

Connection rules. Smoothness of $P\,ds(X)$ and $P^2 = P$ show that $\nabla_X s$ is a smooth range section. Differentiation and projection give

$$\nabla_{X+Y} s = \nabla_X s + \nabla_Y s, \qquad \nabla_{fX} s = f \nabla_X s,$$
$$\nabla_X (s+t) = \nabla_X s + \nabla_X t, \quad \nabla_X (fs) = f \nabla_X s + (Xf)s$$

for smooth real f. The range coordinates above identify ambient smooth range sections with smooth sections of the constructed bundle.

Curvature. Differentiating $P^2 = P$ gives $P(dP(X))P = 0$. Write $D_X s = ds(X)$. For ambient smooth sections,

$$D_X D_Y s - D_Y D_X s - D_{[X,Y]} s = 0.$$

Expansion of the projected derivatives therefore leaves

$$R(X,Y)s = P(dP(X))D_Y s - P(dP(Y))D_X s.$$

Since $Ps = s$, differentiation gives $D_Y s = (dP(Y))s + PD_Y s$. The terms with a middle P vanish. Thus

$$R(X,Y)s = P\big(dP(X)dP(Y) - dP(Y)dP(X)\big)P\,s.$$

This expression is alternating and bilinear in the tangent vectors, and it preserves the range. The ordinary chain rule and the transformation law for the Lie bracket make the local calculations agree on chart overlaps, which gives the global formula. □

For an orthogonal rank-one complex projector, use the scalar connection convention $A = -i\langle u, du\rangle$ in a local unit frame. The associated scalar curvature density is

$$\mathcal{F}_{\mu\nu} = -i \operatorname{Tr}\left(P[\partial_\mu P, \partial_\nu P]\right).$$

On the Bloch sphere,

$$P(\theta,\phi) = \frac{1}{2}\left(I + \mathbf{n}(\theta,\phi)\cdot\sigma\right),$$

where

$$\mathbf{n} = (\sin\theta\cos\phi, \sin\theta\sin\phi, \cos\theta).$$

The Pauli multiplication law gives

$$[\partial_\theta P, \partial_\phi P] = \frac{i}{2}(\partial_\theta \mathbf{n} \times \partial_\phi \mathbf{n})\cdot\sigma.$$

Using $\operatorname{Tr}(P\,\mathbf{a}\cdot\sigma) = \mathbf{n}\cdot\mathbf{a}$ therefore yields

$$\boxed{\mathcal{F}_{\theta\phi} = \frac{1}{2}\mathbf{n}\cdot(\partial_\theta \mathbf{n} \times \partial_\phi \mathbf{n}) = \frac{1}{2}\sin\theta.}$$

The scalar sign changes if the opposite convention for A is chosen. This explicit calculation is not a separate entry among the 19 items in the Lean register.

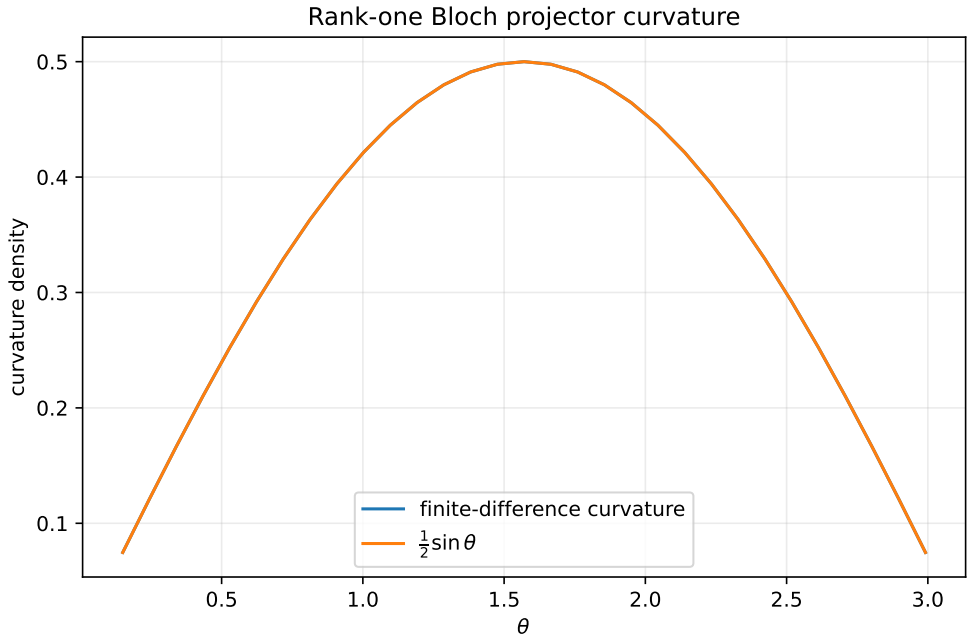


Figure 11. The curvature of the Bloch projector, evaluated by finite differences, is compared with the exact density $\frac{1}{2}\sin\theta$.

Recorded Numerical Check I.6.5 (Geometric packet identities). The canonical connection reconstructed every packet derivative with residual 0. The maximum residual for the Bloch curvature was 2.0803×10^{-11}.

I.7 Measurements and quantum channels

I.7.1 Packet measurements

Let ρ be a density matrix and let $\{E_k\}$ be a POVM:

$$E_k \geq 0, \qquad \sum_k E_k = I.$$

The outcome probabilities are

$$p_k = \mathrm{Tr}(E_k \rho).$$

Theorem I.7.1 (Block-diagonal measurement invariance)**.** *Let $\{P_\alpha\}$ be a complete packet family, and suppose every measurement effect is packet diagonal:*

$$E_k = \sum_\alpha P_\alpha E_k P_\alpha.$$

Define the packet-dephased state

$$\mathcal{D}_P(\rho) = \sum_\alpha P_\alpha \rho P_\alpha.$$

Then

$$\boxed{\mathrm{Tr}(E_k\rho) = \mathrm{Tr}(E_k \mathcal{D}_P(\rho))}$$

for every outcome k.

Proof. Insert the packet decomposition of E_k and use cyclicity of the trace:

$$\mathrm{Tr}(E_k\rho) = \sum_\alpha \mathrm{Tr}(P_\alpha E_k P_\alpha \rho) = \sum_\alpha \mathrm{Tr}(E_k P_\alpha \rho P_\alpha).$$

□

The theorem identifies which coherences a declared measurement can detect. Observables that are diagonal in the packet decomposition cannot detect coherence between distinct packets. Coherence within a packet remains available to such observables.

I.7.2 Kraus transfer

A quantum channel can transfer both populations and coherences between packet addresses. A Kraus representation describes this transfer by summing the contributions of its individual branches. The normalization of those branches ensures that the total trace is preserved.

Classical Input I.7.2 (Finite Kraus channel). Let $K_1, \dots, K_r$ satisfy

$$\sum_a K_a^* K_a = I.$$

Then

$$\boxed{\Phi(\rho) = \sum_a K_a \rho K_a^*}$$

is completely positive and trace preserving.

Proof. Trace preservation follows from

$$\mathrm{Tr}\,\Phi(\rho) = \mathrm{Tr}\left(\rho \sum_a K_a^* K_a\right) = \mathrm{Tr}\,\rho.$$

For any auxiliary dimension and positive matrix X, each term

$$(I \otimes K_a) X (I \otimes K_a)^*$$

is positive, so their sum is positive. This is complete positivity. □

Packet superoperator blocks are defined by

$$\Phi_{\alpha\beta;\gamma\delta}(X) = P_\alpha \Phi(P_\gamma X P_\delta) P_\beta.$$

Summing all four packet indices reconstructs $\Phi(X)$ exactly.

For amplitude damping with a real parameter $0 \le \gamma \le 1$,

$$K_0 = \begin{pmatrix} 1 & 0 \\ 0 & \sqrt{1-\gamma} \end{pmatrix}, \qquad K_1 = \begin{pmatrix} 0 & \sqrt{\gamma} \\ 0 & 0 \end{pmatrix}.$$

The excited state becomes

$$\Phi(|1\rangle\langle 1|) = \gamma\,|0\rangle\langle 0| + (1-\gamma)\,|1\rangle\langle 1|\,.$$

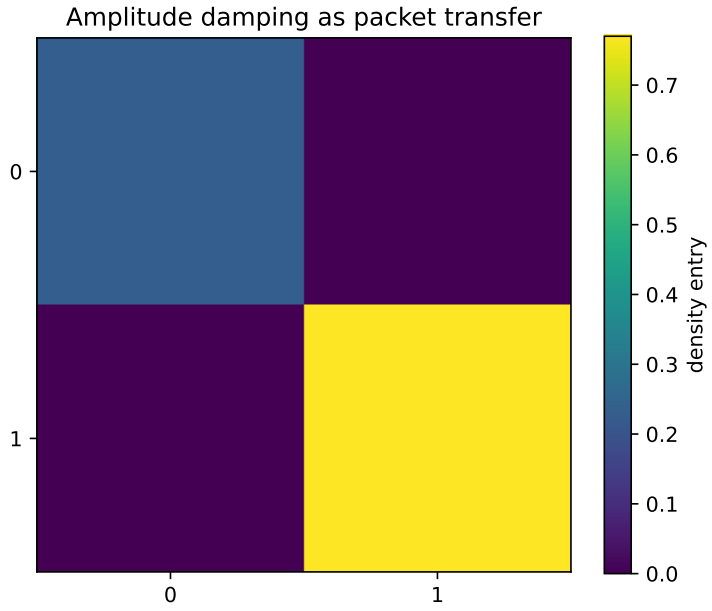


Figure 12. Amplitude damping transfers population from the excited packet to the ground packet while preserving trace and positivity.

Recorded Numerical Check I.7.3 (Channel reconstruction). For $\gamma = 0.23$, the residuals for Kraus completeness and the output trace were 0. The computed output from $|1\rangle\langle 1|$ was $\mathrm{diag}(0.23, 0.77)$. In the Bell state test, packet dephasing left every measurement probability in the computational basis unchanged.

I.8 Quantum error correction as obstruction-packet annihilation

Let $P = P^* = P^2$ project onto a code space $\mathcal{C} \subset \mathcal{H}$, and let $E_1, \dots, E_r$ be a finite family of complex error matrices. Neither a nonzero code nor channel normalization is assumed unless stated. The operators

$$PE_a^* E_b P$$

are the obstruction packets on the code. If they retain information about the logical state beyond one scalar multiple of P, the environment can distinguish logical states and exact correction is impossible.

We call a recovery complete when it is a Kraus map

$$\mathcal{R}(X) = \sum_j K_j X K_j^*, \qquad \sum_j K_j^* K_j = I.$$

The family is *exactly correctable* when one such recovery works for every coherent error combination $A_w = \sum_a w_a E_a$: for every w there is a real $t_w \geq 0$, independent of the logical input, such that

$$PXP = X \quad \Longrightarrow \quad \mathcal{R}(A_w X A_w^*) = t_w X.$$

The coefficient is an unnormalized weight. It is not necessarily a probability for an arbitrary matrix A_w.

Classical Input I.8.1 (Finite Knill–Laflamme criterion). The finite error family is exactly correctable in the sense just defined if and only if there is a positive semidefinite complex matrix $C = (c_{ab})$ such that

$$\boxed{PE_a^* E_b P = c_{ab} P \qquad \text{for every } a, b.}$$

If $\sum_a E_a^* E_a = I$, the equivalent normalized-channel formulation is the existence of a complete recovery satisfying

$$\mathcal{R}\left(\sum_a E_a X E_a^*\right) = X \quad \text{for every } X \text{ with } PXP = X.$$

The zero code and an empty error family are included. An empty family cannot define a channel that preserves trace on a nonzero ambient space.

Proof. Necessity. Fix an error E_a and let $L_j = K_j E_a P$. Perfect recovery on rank-one code operators gives

$$\sum_j |L_j \psi\rangle \langle L_j \psi| = t_a |\psi\rangle \langle \psi| \qquad (\psi \in \mathcal{C}).$$

For every vector orthogonal to ψ, the quadratic form on the left is a sum of nonnegative squared absolute values and equals zero. Each $L_j \psi$ therefore lies in the span of ψ. A linear operator that preserves every line in $\mathcal{C}$ is scalar there: apply it to two independent vectors and their sum. The one-dimensional case is immediate, and the claim is vacuous for the zero code. Consequently

$$K_j E_a P = d_{ja} P.$$

Recovery completeness now gives

$$PE_a^*E_bP = \sum_j (K_jE_aP)^*(K_jE_bP)$$
$$= \left(\sum_j \overline{d_{ja}}d_{jb}\right) P.$$

The coefficients form a Gram matrix, hence are positive semidefinite. For a normalized channel, apply the same rank-one argument to all composite branches K_jE_aP at once to obtain the necessary condition.

Sufficiency. Diagonalize $C = U\,\mathrm{diag}(\lambda_r)U^*$ with U unitary and $\lambda_r \geq 0$. Define compressed transformed errors

$$F_r = \sum_a U_{ar}E_aP.$$

Then $F_rP = F_r$ and $F_r^*F_s = \lambda_r\delta_{rs}P$. If $\lambda_r = 0$, $F_r^*F_r = 0$ forces $F_r = 0$. For positive eigenvalues only, set $V_r = F_r/\sqrt{\lambda_r}$. These satisfy

$$V_rP = V_r, \qquad V_r^*V_s = \delta_{rs}P.$$

Let $S = \sum_{\lambda_r>0} V_rV_r^*$. Orthogonality makes S an orthogonal projector. Use the recovery branches

$$K_r = V_r^*, \qquad K_{\text{unused}} = I - S.$$

They are complete on the whole ambient space because

$$\sum_r K_r^*K_r + K_{\text{unused}}^*K_{\text{unused}} = S + (I-S)^2 = I.$$

The inverse unitary change of coordinates reconstructs each E_aP from the F_r. Every recovery branch of a coherent combination is therefore scalar on the code, while the branch for the unused space vanishes. For all supported matrices, the resulting recovery is

$$\mathcal{R}(A_wXA_w^*) = (w^*Cw)X.$$

This establishes the arbitrary-family statement without assuming normalization. Under $\sum_a E_a^*E_a = I$ and $P \neq 0$, summing the diagonal KL equations gives $\mathrm{Tr}\,C = 1$, so the normalized-channel output is X. When $P = 0$, every supported X is zero and the conclusion is automatic. The recovery is trace preserving by completeness and completely positive at every finite ancillary dimension by the Kraus calculation in Classical Input I.7.2. □

For the three-qubit bit-flip code,

$$|0_L\rangle = |000\rangle\,, \qquad |1_L\rangle = |111\rangle\,,$$

and the error family is

$$I, \quad X\otimes I\otimes I, \quad I\otimes X\otimes I, \quad I\otimes I\otimes X.$$

The four error images of the code are pairwise orthogonal two-dimensional syndrome packets whose projectors sum to the identity on the eight-dimensional Hilbert space.

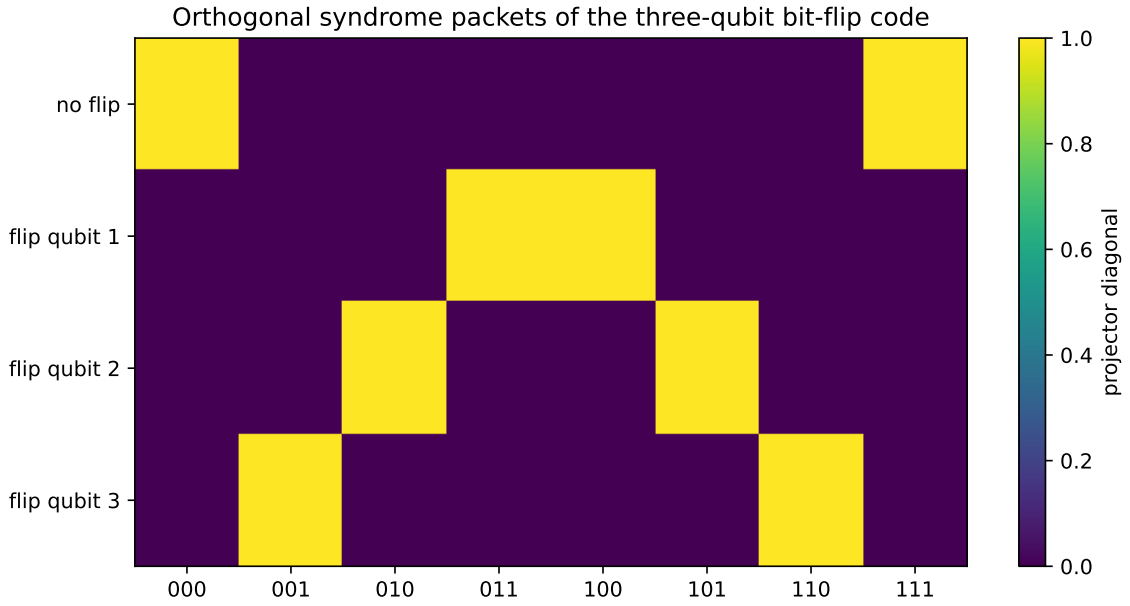


Figure 13. The four orthogonal syndrome packets of the three-qubit bit-flip code. Each packet identifies one correctable error without resolving the encoded logical state.

Recorded Numerical Check I.8.2 (Exact bit-flip correction). The residuals for the Knill–Laflamme condition and completeness of the syndrome packets were both 0. A mixed channel of single bit flip errors, applied to a nontrivial logical superposition, was reversed with a residual of 1.0385×10^{-16} in the density matrix.

I.9 Exact effective dynamics

I.9.1 Schur–Feshbach reduction

Let P be a retained packet projector and $Q = I - P$. In packet coordinates,

$$H = \begin{pmatrix} H_{PP} & H_{PQ} \\ H_{QP} & H_{QQ} \end{pmatrix}.$$

Theorem I.9.1 (Exact Feshbach resolvent). *Assume that both $zI_Q - H_{QQ}$ and $zI - H$ are invertible. Define*

$$\boxed{H_{\text{eff}}(z) = H_{PP} + H_{PQ}(z - H_{QQ})^{-1} H_{QP}.}$$

Then

$$\boxed{P(z - H)^{-1} P = (z - H_{\text{eff}}(z))^{-1}}$$

where the left side is restricted to $P\mathcal{H}$, the right side is an inverse on that retained space, and both are written in the same orthonormal basis. Here $z - H_{QQ}$ and $z - H_{\text{eff}}$ abbreviate the appropriately sized scalar matrices minus the indicated blocks.

Proof. The block in the lower right corner of $z - H$ is $z - H_{QQ}$. Gaussian block elimination produces the Schur complement

$$z - H_{PP} - H_{PQ}(z - H_{QQ})^{-1}H_{QP}.$$

The assumed invertibility of this block and of the full matrix implies that the Schur complement is invertible. The block in the upper left corner of the full inverse is the inverse of that Schur complement, which is exactly the displayed operator. □

The second premise cannot be dropped: at $z = 0$ and $H = \mathrm{diag}(0, -1)$, the eliminated block is 1 but $zI - H$ is singular. This counterexample is also included in the Lean module.

The self-energy

$$\Sigma_P(z) = H_{PQ}(z - H_{QQ})^{-1}H_{QP}$$

contains the complete influence of the eliminated packet. Bare truncation drops $\Sigma_P(z)$ and is therefore exact only when the coupling between packets vanishes or the self-energy cancels for another stated reason.

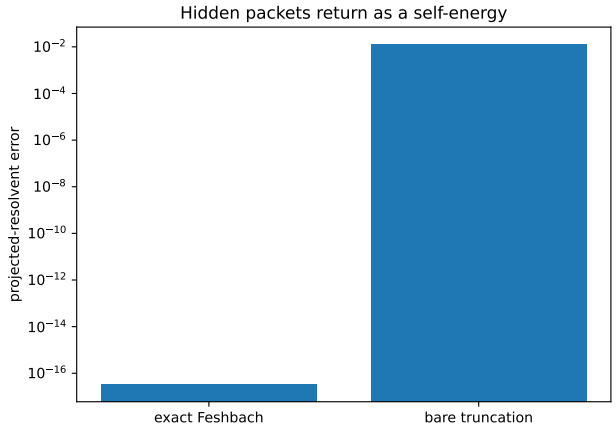


Figure 14. Exact Feshbach reduction versus bare truncation.

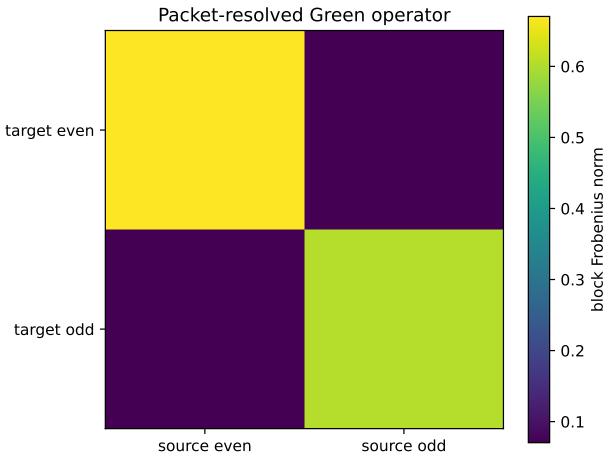


Figure 15. Norms of packet Green-function blocks.

Recorded Numerical Check I.9.2 (Effective resolvent). In the reported test with a random Hermitian matrix of dimension six, the exact Feshbach residual was 3.2291×10^{-17}. The corresponding residual for bare truncation was 1.3091×10^{-2}.

I.9.2 The hidden packet as memory

For a time-independent finite Hamiltonian H and fixed projectors P, Q, write $\psi = x + y$, with $x = P\psi$ and $y = Q\psi$. Then

$$i\dot{x} = H_{PP}x + H_{PQ}y,$$
$$i\dot{y} = H_{QP}x + H_{QQ}y.$$

Solving the second equation gives

$$y(t) = e^{-itH_{QQ}}y(0) - i\int_0^t e^{-i(t-s)H_{QQ}}H_{QP}x(s)\,ds.$$

Substitution yields the exact Volterra equation

$$\boxed{\begin{aligned} i\dot{x}(t) &= H_{PP}x(t) + H_{PQ}e^{-itH_{QQ}}y(0) \\ &\quad - i\int_0^t K(t-s)x(s)\,ds, \end{aligned}}$$

with memory kernel

$$\boxed{K(t) = H_{PQ}e^{-itH_{QQ}}H_{QP}.}$$

The influence of the eliminated degrees of freedom is therefore retained in a self-energy that depends on frequency, or equivalently in an exact memory term. For forward evolution the integral is causal. When the Hamiltonian depends on time, the corresponding propagator between two times replaces the stationary exponential used here. This Volterra derivation is not a separate entry in the finite Lean register.

I.10 Finite quantum geometry

I.10.1 A projector-resolved geometry

At resolution ℓ, define

$$\boxed{\mathfrak{Q}_\ell = \left(\mathcal{A}_\ell, \mathcal{H}_\ell, D_\ell, \{P_{\ell,\alpha}\}, E_\ell, C_\ell, \Pi_\ell^{\text{phys}}, T_\ell\right).}$$

In order, the entries specify the observable algebra, Hilbert space, geometric or Dirac-type operator, packet projectors, embedding into the fine space, reconstruction onto the coarse space, physical constraint projector, and transfer operator. The maps have types $E_\ell : \mathcal{H}_\ell \to \mathcal{H}_{\ell+1}$ and $C_\ell : \mathcal{H}_{\ell+1} \to \mathcal{H}_\ell$. The left inverse relation $C_\ell E_\ell = I$ alone does not imply $C_\ell = E_\ell^*$ or make the embedding isometric.

A coherent refinement should satisfy

$$C_\ell E_\ell = I$$

and

$$\boxed{P_{\ell,\alpha} = C_\ell \left(\sum_{\beta \succ \alpha} P_{\ell+1,\beta}\right) E_\ell.}$$

For an operator D, define the refinement defect

$$\Delta_\ell(D) = C_\ell D_{\ell+1} E_\ell - D_\ell.$$

Exact resolution independence is $\Delta_\ell(D) = 0$. When exact equality is too strong, the correct continuum problem is to prove convergence of the resolvents and uniform control of the effective self-energies.

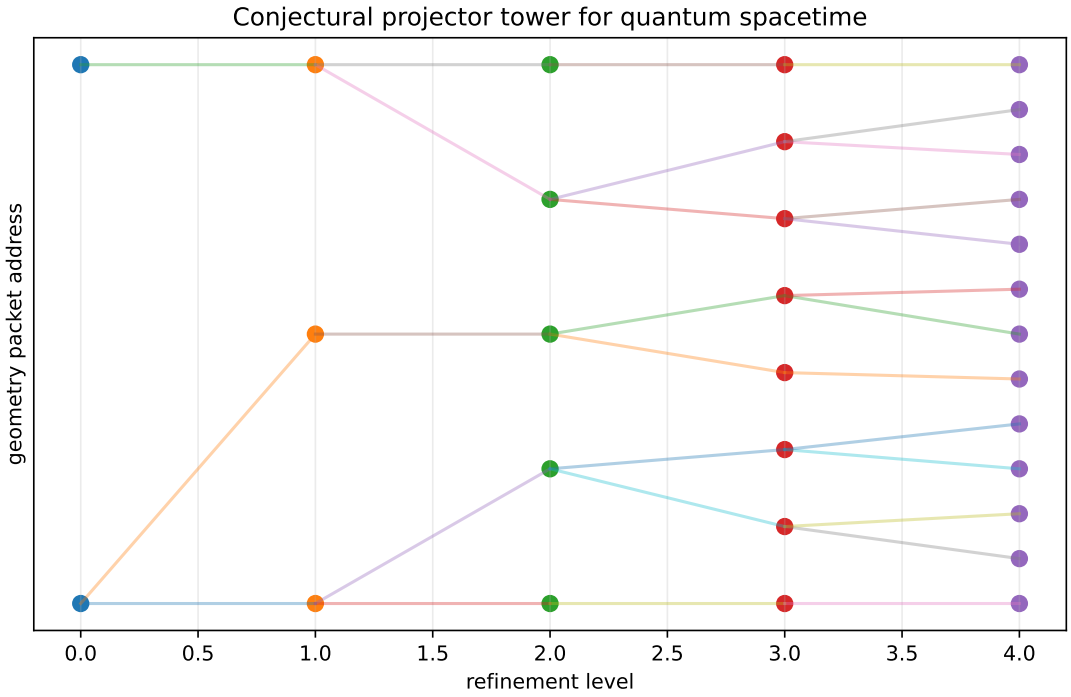


Figure 16. The diagram organizes a conjectural nested packet tower for quantum geometry. It does not provide a numerical reconstruction of physical spacetime.

I.10.2 Euclidean transfer

Theorem I.10.1 (Finite Euclidean transfer). *Let H be Hermitian on a nonzero finite-dimensional Hilbert space. For all real $\tau, \sigma \geq 0$,*

$$T(\tau) = e^{-\tau(H - E_0 I)}, \qquad E_0 = \min \operatorname{Spec} H,$$

is positive definite and satisfies

$$\boxed{T(\tau + \sigma) = T(\tau)T(\sigma).}$$

Its spectrum is contained in $(0, 1]$.

Proof. Diagonalize $H = \sum_j E_j P_j$. Then

$$T(\tau) = \sum_j e^{-\tau(E_j - E_0)} P_j.$$

Every eigenvalue is strictly positive and at most one. Multiplication adds the exponents, proving the semigroup law and $T(0) = I$. Positivity here is operator positivity, not an assertion that every matrix entry is nonnegative. □

The paper tests a controlled volume-state model

$$H_{nn} = 2\kappa + V(n), \qquad H_{n,n+1} = H_{n+1,n} = -\kappa,$$

with $\kappa > 0$ and a real confining potential. This is a finite transfer-matrix test only. Operator positivity alone is not reflection positivity of a Euclidean field measure. It is not derived from a gravitational path integral and is not evidence for a unique microscopic spacetime dynamics.

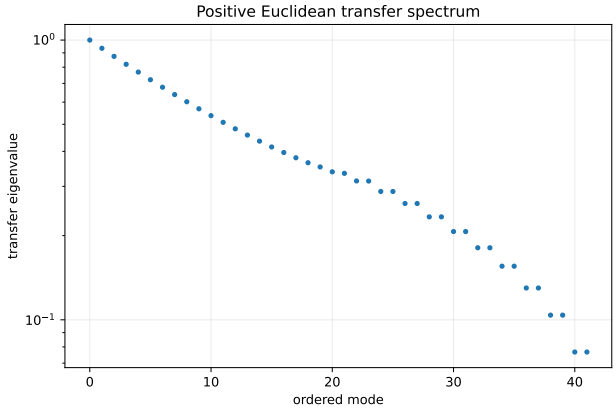


Figure 17. Positive spectrum of the Euclidean transfer operator.

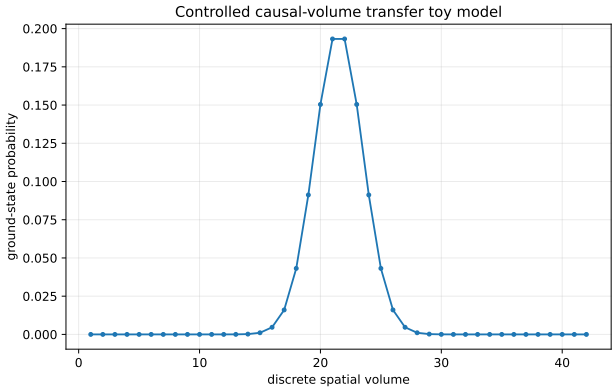


Figure 18. Ground-state volume packet in the controlled toy model.

Recorded Numerical Check I.10.2 (Finite transfer model). The minimum transfer eigenvalue was 0.0767054, the semigroup residual was 0, and reconstruction from four volume-residue packets had residual 0.

I.11 Spectral dimension and continuum diagnostics

Let $L \geq 0$ be a finite Laplacian on $N \geq 1$ states, with eigenvalues λ_j and at least one zero eigenvalue. For diffusion time $\tau > 0$, define the normalized heat trace

$$K(\tau) = \frac{1}{N} \sum_j e^{-\tau \lambda_j}$$

and the scale-dependent spectral dimension

$$\boxed{d_s(\tau) = -2 \frac{d \log K(\tau)}{d \log \tau}.}$$

For a finite system, $d_s(\tau)$ is a diagnostic, not a topological invariant. Indeed, finite differentiation gives

$$d_s(\tau) = 2\tau \frac{\sum_j \lambda_j e^{-\tau \lambda_j}}{\sum_j e^{-\tau \lambda_j}}.$$

It tends to zero as $\tau \downarrow 0$ and, under the stated assumption of a zero mode, as $\tau \to \infty$. If a general positive operator has no zero mode, its behavior at large times is instead asymptotic to $2\tau\lambda_{\min}$. The conclusion for operators with a zero mode therefore does not apply to that case. Inferring a geometric dimension requires a stable intermediate window and a controlled refinement limit.

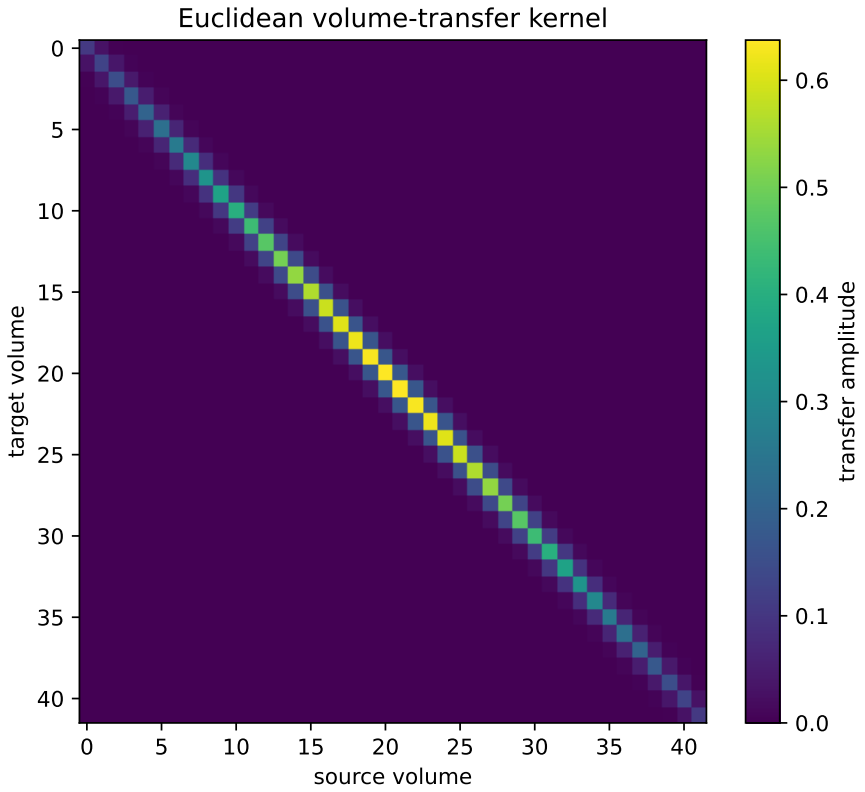


Figure 19. The figure shows the finite Euclidean kernel for volume transfer. Positivity and semigroup composition hold exactly in the finite model. Its gravitational interpretation remains provisional.

I.11.1 The circle dispersion bound

For a periodic grid with spacing $h > 0$ and physical wave number $k \in \mathbb{R}$,

$$\lambda_{k,h} = \frac{4}{h^2} \sin^2\left(\frac{kh}{2}\right).$$

Theorem I.11.1 (Low-mode second-order bound). *For every real k and every nonzero real h, define $\lambda_{k,h} = 4h^{-2}\sin^2(kh/2)$. Then*

$$\boxed{0 \le k^2 - \lambda_{k,h} \le \frac{k^4 h^2}{12}.}$$

Proof. Put $x = kh/2$. The inequalities $|\sin x| \le |x|$ and $|x - \sin x| \le |x|^3/6$, which hold for every real argument, give

$$0 \le x^2 - \sin^2 x = |x - \sin x|\,|x + \sin x| \le \frac{|x|^3}{6}\,2|x| = \frac{x^4}{3}.$$

Multiplying by $4/h^2$ proves both bounds. The estimate holds for every frequency. Its interpretation as convergence of second order keeps k fixed while $h \to 0$, so it does not assert a uniformly small relative error across all grid modes. □

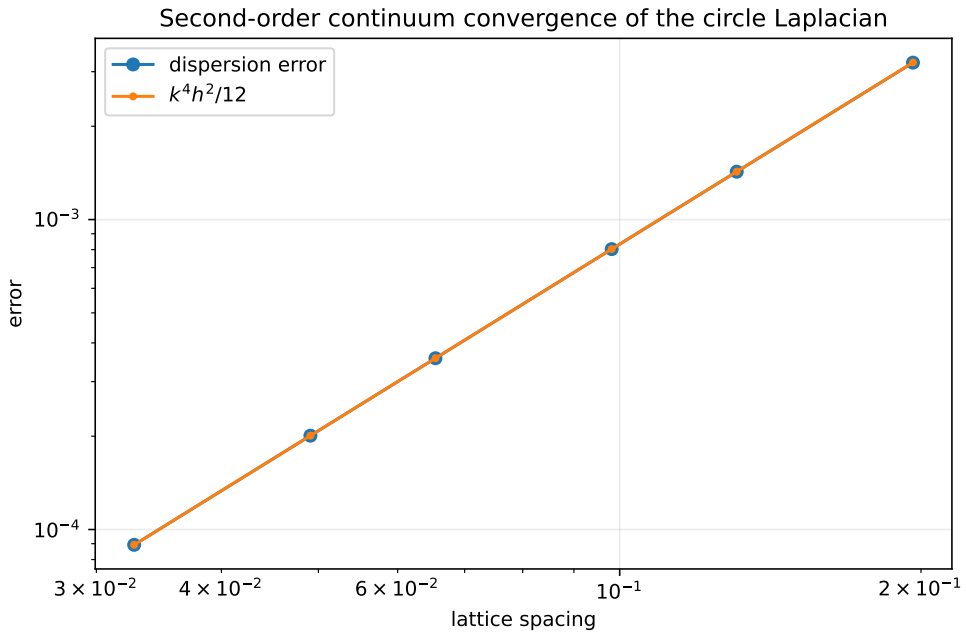


Figure 20. The first nonzero circle mode converges at second order and remains below the proved dispersion bound.

Recorded Numerical Check I.11.2 (Continuum dispersion). The reported convergence order was 1.99936. For every tested mode, the error was below the bound, so none of those tests violated the theorem.

I.11.2 One- and two-dimensional plateaus

At intermediate diffusion times, a finite cycle and a finite torus can exhibit plateaus near the dimensions of their underlying geometries. The following figure and numerical certificate show the reported behavior for these two examples. The plateaus occur between the small and large time regimes in which the spectral dimension returns to zero.

Recorded Numerical Check I.11.3 (Spectral dimension). The median intermediate plateaus were

$$d_s^{(1)} = 1.00062, \qquad d_s^{(2)} = 2.03781.$$

These tests recover the expected dimensions of the chosen finite geometries. They do not select a physical theory of quantum spacetime.

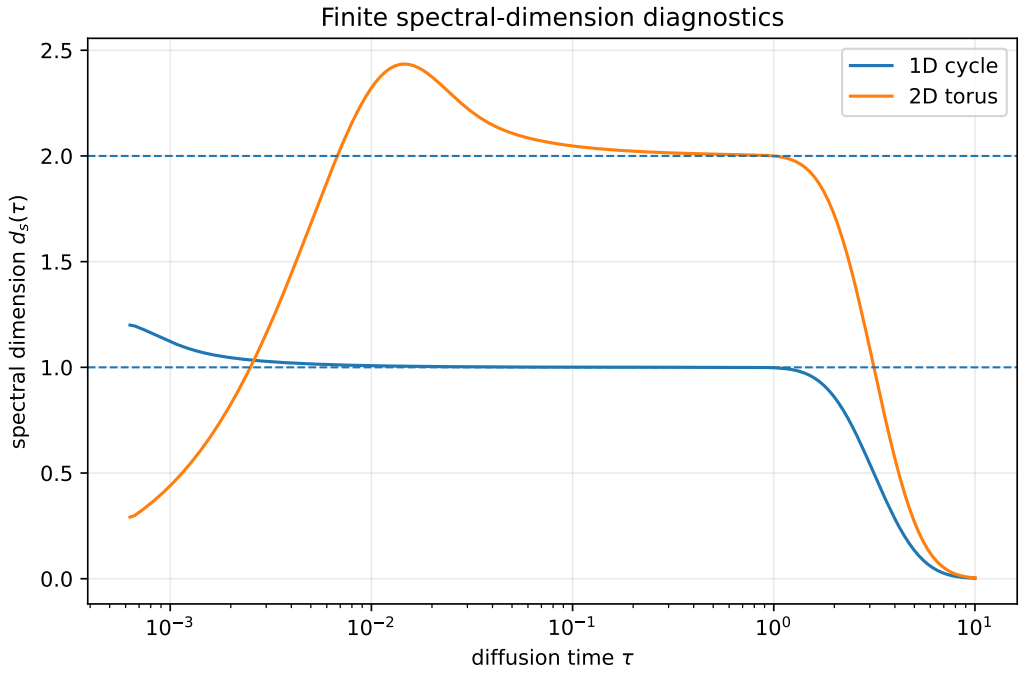


Figure 21. The curves show intermediate windows of spectral dimension for a finite cycle and a finite two-dimensional torus. Departures in the ultraviolet and infrared reflect the finite size of the models rather than additional dimensions.

I.12 Constraint packets and the quantum-spacetime boundary

At one finite level, let $\widehat{C}_A$ be a finite family of matrix constraints, with fixed scalar structure coefficients, and let Π^{phys} be the orthogonal projector onto their exact common kernel. If the classical constraint algebra has structure coefficients $f_{AB}^{\ C}$, define the anomaly operator

$$\boxed{\mathfrak{A}_{AB} = [\widehat{C}_A, \widehat{C}_B] - i \sum_C f_{AB}^{\ C} \widehat{C}_C.}$$

Its physical packet is

$$\Pi^{\mathrm{phys}} \mathfrak{A}_{AB} \Pi^{\mathrm{phys}}.$$

In this exact finite setting, $\widehat{C}_C \Pi^{\mathrm{phys}} = 0$ for every C. Associativity gives

$$\mathfrak{A}_{AB} \Pi^{\mathrm{phys}} = 0, \qquad \Pi^{\mathrm{phys}} \mathfrak{A}_{AB} \Pi^{\mathrm{phys}} = 0$$

automatically. This compression therefore cannot certify operator closure away from the physical range. A nonzero measured compression contradicts the exact-kernel assumptions or indicates an approximation or implementation error. For example, $C_1 = \mathrm{diag}(1, 0, 0)$ and $C_2 = E_{12} + E_{21}$ annihilate the same third coordinate, while their commutator $E_{12} - E_{21}$ is nonzero. With zero proposed structure coefficients, the anomaly is nonzero but its physical compression vanishes.

The closure target must be stated at the operator level, not inferred from that automatic compression. Unbounded constraints additionally require a specified common invariant domain. Neither such a domain theory nor gravitational structure functions are supplied by the finite check.

Conjecture I.12.1 (Anomaly-free refinement)**.** For a specified nontrivial quantum-geometric constraint model, there exists a coherent packet tower with nonzero physical spaces, compatible physical projectors and exact operator closure

$$\mathfrak{A}_{AB}^{(\ell)} = 0$$

at every finite level. The compatible physical compression then vanishes as a consequence, not as a substitute for closure.

The substantive research target is the operator condition. The earlier condition stated only in terms of compression was too weak. A choice of model, dynamics, and refinement maps is still needed before this program becomes a fully specified physical existence problem.

Conjecture I.12.2 (Uniform Feshbach control)**.** For the same specified tower, the self-energies from exact elimination of fine packets admit bounds uniform in cutoff and volume on a common spectral domain. Together with consistent identifications of the Hilbert spaces and a proved resolvent convergence criterion, they yield a nontrivial continuum limit in the strong resolvent sense. Uniform boundedness alone is not asserted to imply convergence.

Conjecture I.12.3 (Lorentzian reconstruction)**.** The Euclidean packet theory satisfies a positivity or reconstruction principle strong enough to produce a Lorentzian Hilbert space with causal propagation and positive physical norm.

Conjecture I.12.4 (Einstein infrared limit)**.** There exist semiclassical packet states $\Psi_{g,\ell}$ such that the effective action converges to

$$\frac{1}{16\pi G}\int \sqrt{-g}\,(R - 2\Lambda)\,d^4x$$

with controlled higher-order corrections.

Conjecture I.12.5 (Massless spin-two sector)**.** The continuum two-point function possesses a positive transverse-traceless massless spin-two pole, while all unphysical packet sectors are removed by the constraints.

The exact finite identities establish none of these physical conclusions, and no formal theorem of logical independence is claimed. Exact packet reconstruction provides a kinematic and computational advantage. It does not determine the physical action, prove existence of the continuum theory, or guarantee the limit of general relativity.

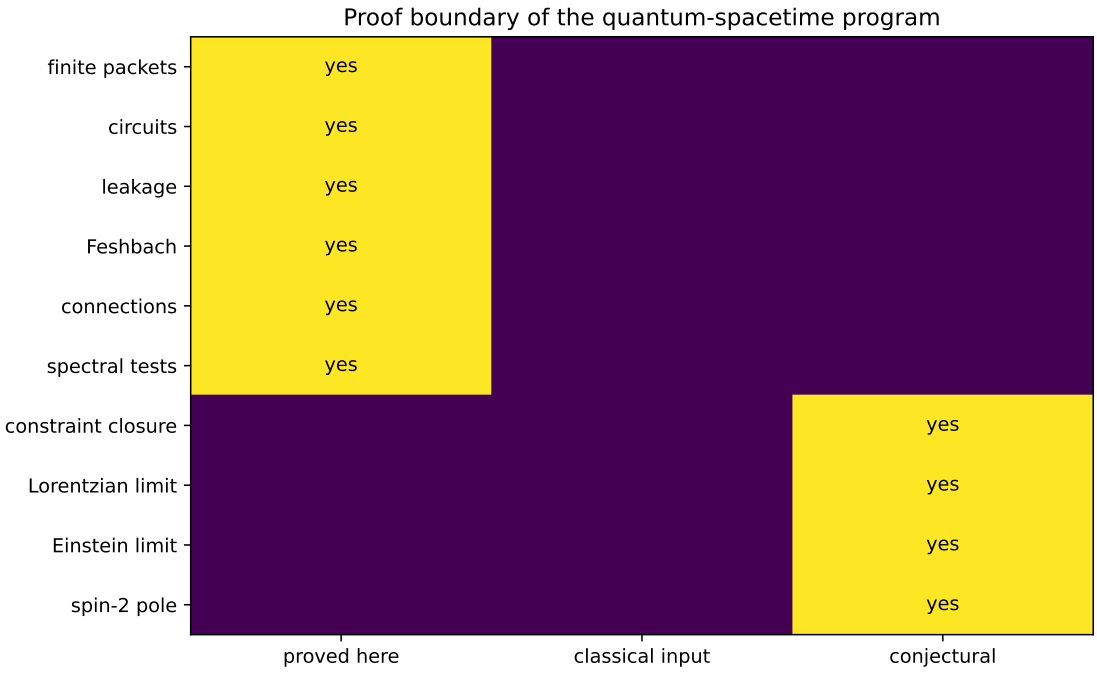


Figure 22. The proof boundary. Finite packet, circuit, leakage, Feshbach, connection, and spectral identities are established here. Constraint closure and the physical continuum claims remain conjectural.

I.13 Numerical certificates

The original manuscript reports CPU experiments and a suite of 22 tests. It makes no claim about GPU computation. The values below reproduce that historical report and have not been recomputed for this prose revision. These numerical observations are separate from the 323 declarations in the selected finite formal checkpoint of 6 September 2026. The recovered numerical source and raw records accompany the source corpus. A displayed floating-point residual of zero records the reported computation and does not independently prove equality in exact arithmetic.

The original reported count is

$$\boxed{22/22 \text{ historical numerical tests, not rerun here.}}$$

The 19 original figures are retained from the recovered numerical companion. The separate visual guide supplies a reading route through these constructions and the later strengthened results.

Table 1. Reported finite numerical checks, retained from the original manuscript and not rerun for this edition.

Certificate	Value
Bell-state residual	0
Three-qubit seed-orbit rank	$8/8$
Parity off-block norm	0
Circuit path reconstruction residual	0
Exact-symmetry maximum leakage	0
Maximum leakage-bound violation	0
Feshbach projected-resolvent residual	3.2291×10^{-17}
Bare-truncation projected-resolvent residual	1.3091×10^{-2}
Moving-frame residual with connection	1.0645×10^{-10}
Moving-frame residual without connection	7.0000×10^{-1}
Canonical packet-connection residual	0
Bloch-curvature residual	2.0803×10^{-11}
Kraus completeness residual	0
Output trace residual	0
Knill–Laflamme residual	0
Bit-flip recovery residual	1.0385×10^{-16}
Tensor parity-refinement residual	0
Circle low-mode convergence order	1.99936
One-dimensional spectral plateau	1.00062
Two-dimensional spectral plateau	2.03781
Minimum Euclidean-transfer eigenvalue	0.0767054
Transfer semigroup residual	0
Volume-packet reconstruction residual	0

I.15 Conclusion

The quantum realization of the seed calculus begins with a primitive state and a declared operator grammar. Symmetry projectors resolve the state and every operator into exact packets. In these coordinates, circuit products become sums over packet paths, and Hamiltonian symmetry appears as a diagonal block structure. When that symmetry is broken, the resulting transfer is measured by the leakage estimates.

Moving packets carry a canonical connection and curvature. Channels and measurements act on the corresponding operator packets, while the conditions for error correction become statements about compression to the code. Exact elimination retains the influence of hidden sectors through self-energy and memory.

The finite theory therefore provides a coherent language for

$$\boxed{\begin{array}{c}\text{seed reachability} + \text{symmetry resolution} + \text{circuit paths} \\ +\text{effective dynamics} + \text{geometric transport} + \text{constraint diagnostics}\end{array}}$$

A physical continuum theorem remains open. The next required results are anomaly-free refinement, uniform control of effective operators, Lorentzian reconstruction, the Einstein infrared limit, and a positive massless spin-two sector. Each requires its own hypotheses and proof. Agreement in a finite numerical model cannot replace those arguments.

Part II Strengthened quantum packet calculus and continuum towers

A route through this section

This part broadens the packet calculus while keeping its hypotheses explicit. Read each result with its assumptions about nonzero spaces, a common ambient space, self-adjointness, finite address sets, and trace class operators. Its bounded limits do not establish the five open physical continuum targets.

II.1 Introduction

Quantum mechanics repeatedly uses the same operation. A Hilbert space is split into sectors, an operator is resolved between those sectors, and the pieces are propagated or recombined. Symmetry sectors, eigenspaces, syndrome spaces, adiabatic subspaces, and retained model spaces are familiar examples. This article treats them as instances of one finite packet calculus.

The elementary coordinate object is a complete family of orthogonal projectors

$$P_a P_b = \delta_{ab} P_a, \qquad \sum_{a \in I} P_a = I.$$

Every vector has packet coordinates $P_a \psi$. Every operator has transfer blocks

$$A_{ba} = P_b A P_a.$$

These identities are simple. Their value appears when the same coordinates are used across representation theory, circuits, channels, error correction, effective dynamics, and geometric limits.

Quantum information and operator theory in finite dimensions provide the standard background [18, 27, 3]. Finite group projectors come from character theory [23, 9]. Moving spectral subspaces and geometric phase originate in the work of Kato, Berry, Wilczek, and Zee [12, 13, 2, 28]. Completely positive maps and quantum dynamical semigroups are treated in [24, 5, 15, 16]. Exact error correction is governed by the Knill Laflamme condition [14, 22, 1]. Projection methods and hidden state memory are linked by the Feshbach, Nakajima, and Zwanzig constructions [8, 17, 29, 4].

The first part begins with quantum seeds. A state is cyclic only relative to a declared observable algebra. For an algebra in multiplicity form, the local orbit dimension is controlled by the rank of a coefficient matrix. This recovers the relation between Schmidt rank and the dimension reached by local operations. The finite group section then constructs central isotypic projectors. Cyclic symmetry gives a sharper charge selection rule. An operator with charge q can move a state only from packet j to packet $j + q$.

A circuit is resolved by inserting the identity between successive gates. This produces a sum over packet paths. The target probability contains diagonal path terms and interference between distinct paths. Symmetry can remove entire path families before any matrix multiplication is performed. Unitarity gives exact row and column relations among the transfer blocks.

The moving packet section treats time dependent projectors. The canonical generator

$$K(t) = \sum_a \dot{P}_a(t) P_a(t)$$

is skew adjoint and transports every packet. In the moving frame, the physical Hamiltonian acquires the geometric term $-\mathrm{i}W(t)^*\dot{W}(t)$. The leakage estimate must account for the motion of the packet itself. The physical coupling QHP is therefore replaced by

$$Q(t)(H(t) - \mathrm{i}K(t))P(t).$$

This is the exact finite distinction between following a moving subspace and remaining in a fixed one.

Density matrices require separate packet labels for their output and input coordinates. The superoperators

$$\mathcal{P}_{ab}(X) = P_a X P_b$$

form a complete orthogonal packet system on Hilbert Schmidt operator space. Dephasing is the diagonal projection. Every channel has input and output superblocks, with the same composition law as ordinary matrix blocks. A covariant channel preserves the isotypic packets of the conjugation action. In the cyclic case these are coherence orders. The Choi matrix carries the equivalent symmetry under $U \otimes \overline{U}$.

Error correction is expressed through compression to a code. Let P be the code projector. The class of PAP modulo scalar multiples of P measures the obstruction to making A undetectable within the code. The Knill Laflamme criterion says that this obstruction vanishes for every product $E_a^* E_b$ from the error family. Diagonalizing the resulting positive coefficient matrix produces orthogonal syndrome packets and an explicit recovery on the error span.

The effective dynamics section returns to ordinary Hilbert space packets. Schur complementation gives the exact retained resolvent and a frequency dependent self energy. The same hidden block gives a causal memory kernel in time. For a self adjoint hidden Hamiltonian, the self energy has a fixed sign in the upper half plane, and the time kernel is positive definite. Uniform spectral separation gives direct bounds that can be carried through a refinement tower.

The geometric part develops two finite constructions. A strictly positive contraction gives a reflection positive Hankel kernel, and its logarithm reconstructs a nonnegative Hamiltonian. A finite Laplacian gives a heat trace from which the spectral dimension is defined at each diffusion scale. The article proves convergence from periodic lattices to the continuum torus at every fixed positive diffusion time. Poisson summation then determines the continuum dimension as diffusion time tends to zero.

Constraint closure needs a different obstruction. If C_a are self adjoint constraints and P_{phys} projects onto their common kernel, then

$$P_{\mathrm{phys}}[C_a, C_b]P_{\mathrm{phys}} = 0$$

holds automatically. This compression cannot test closure. The correct finite obstruction is the class of $[C_a, C_b]$ in the quotient of $\mathrm{End}(\mathcal{H})$ by the span of the constraints. Vanishing means that the constraint span is closed under commutators.

The last part gives two theorems for towers of bounded Hamiltonians. Exactly compatible finite Hamiltonians with a uniform norm bound define a bounded self adjoint operator on the Hilbert direct limit. When successive bounded self adjoint Hamiltonians on a common Hilbert space have norm summable differences, they converge to a bounded self adjoint limit. Their unitary evolutions, and their Euclidean

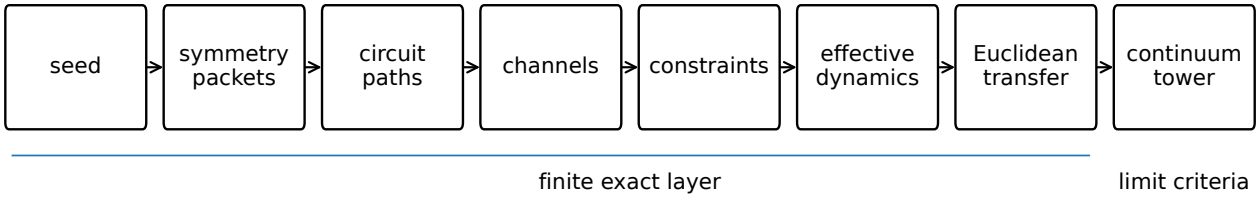


Figure 23. The finite mathematical layers developed in the article and the separate limit criteria needed at the continuum boundary.

Object	Packet coordinate	Exact structural condition
State	$P_a\psi$	completeness of the projector family
Operator	P_bAP_a	block multiplication
Circuit	intermediate packet path	insertion of complete resolutions
Density matrix	$P_a\rho P_b$	two sided operator packets
Channel	superoperator block	complete positivity and covariance when declared
Code	syndrome packet	scalar compression of error products
Effective model	Feshbach map	invertibility of the hidden resolvent
Euclidean model	positive transfer matrix	positivity and self adjointness
Constraint system	quotient obstruction	commutator closure modulo the constraint span
Continuum tower	direct or norm limit	compatibility plus explicit convergence

Table 2. The packet coordinates used in the article.

evolutions under the stated positivity assumption, converge uniformly on bounded time intervals. Reflection positivity and closure with fixed structure coefficients pass to the limit under the stated convergence assumptions.

These results do not construct an interacting continuum quantum field theory. They do not prove anomaly freedom on an unbounded common domain, Osterwalder Schrader reconstruction for a continuum measure, an Einstein infrared action, or a positive massless spin two sector. Each of those conclusions needs hypotheses absent from the finite calculations.

II.2 Quantum seeds and observable algebras

Definition II.2.1 (Finite quantum seed system)**.** A finite quantum seed system is a triple

$$(\mathcal{H}, \mathcal{A}, S),$$

where $\mathcal{H}$ is a finite dimensional Hilbert space, $\mathcal{A} \subseteq \mathrm{End}(\mathcal{H})$ is a unital star subalgebra, and $S \subseteq \mathcal{H}$ is a finite set. Its generated hull is

$$\mathcal{A}S = \mathrm{span}\{A\psi : A \in \mathcal{A},\ \psi \in S\}.$$

The seed set is cyclic when $\mathcal{A}S = \mathcal{H}$. The quantum seed rank is the least cardinality of a cyclic seed set.

The algebra is part of the data. A vector may be cyclic for $\mathrm{End}(\mathcal{H})$ and fail to be cyclic for a restricted observable or gate algebra.

Let

$$\mathcal{A} \cong \bigoplus_{r=1}^{s} (M_{d_r}(\mathbb{C}) \otimes I_{m_r})$$

act on

$$\mathcal{H} \cong \bigoplus_{r=1}^{s} (\mathbb{C}^{d_r} \otimes \mathbb{C}^{m_r}).$$

Assume $d_r, m_r \geq 1$ for each displayed block. For an empty block family, the seed rank and the displayed finite supremum are defined as zero. A vector in one block is identified with a d_r by m_r coefficient matrix.

Theorem II.2.2 (Orbit dimension of one seed). *For integers $d \geq 1$, $m \geq 0$, and the action of $M_d(\mathbb{C}) \otimes I_m$ on $\mathbb{C}^d \otimes \mathbb{C}^m$, let C_ψ be the coefficient matrix of ψ. Then*

$$\dim \mathrm{span}\{(A \otimes I_m)\psi : A \in M_d(\mathbb{C})\} = d \,\mathrm{rank}\, C_\psi.$$

The vector is cyclic exactly when $\mathrm{rank}\, C_\psi = m$.

Proof. Under the coefficient matrix identification, $(A \otimes I_m)\psi$ corresponds to AC_ψ. Every row of AC_ψ lies in the row space of C_ψ. Conversely, a matrix whose rows lie in that row space equals AC_ψ for a suitable A. There are d independent row choices in a space of dimension $\mathrm{rank}\, C_\psi$. The orbit dimension is therefore $d\,\mathrm{rank}\, C_\psi$. It equals dm exactly when C_ψ has full column rank. □

Theorem II.2.3 (Quantum seed rank). *For the displayed multiplicity decomposition,*

$$\mathrm{srank}_{\mathcal{A}}(\mathcal{H}) = \max_{1 \leq r \leq s} \left\lceil \frac{m_r}{d_r} \right\rceil.$$

Proof. A single seed contributes a row space of dimension at most d_r to the rth multiplicity factor. Hence k seeds cover at most kd_r multiplicity directions, which gives the lower bound.

Set

$$k = \max_{r} \left\lceil \frac{m_r}{d_r} \right\rceil.$$

For each r, partition a basis of $\mathbb{C}^{m_r}$ into at most k groups of size at most d_r. Choose the coefficient matrix of the jth seed so that its row space spans the jth group. The combined row spaces span every multiplicity factor. The preceding theorem then shows that the k seeds generate every summand. □

Corollary II.2.4 (Local orbit and Schmidt rank). *Let $\psi \in \mathcal{H}_A \otimes \mathcal{H}_B$, let $d_A = \dim \mathcal{H}_A \geq 1$, and let r be the Schmidt rank of ψ. Then*

$$\dim \mathrm{span}\{(A \otimes I_B)\psi : A \in \mathrm{End}(\mathcal{H}_A)\} = d_A r.$$

Local operators on A generate the whole bipartite Hilbert space exactly when the reduced state on B has full support.

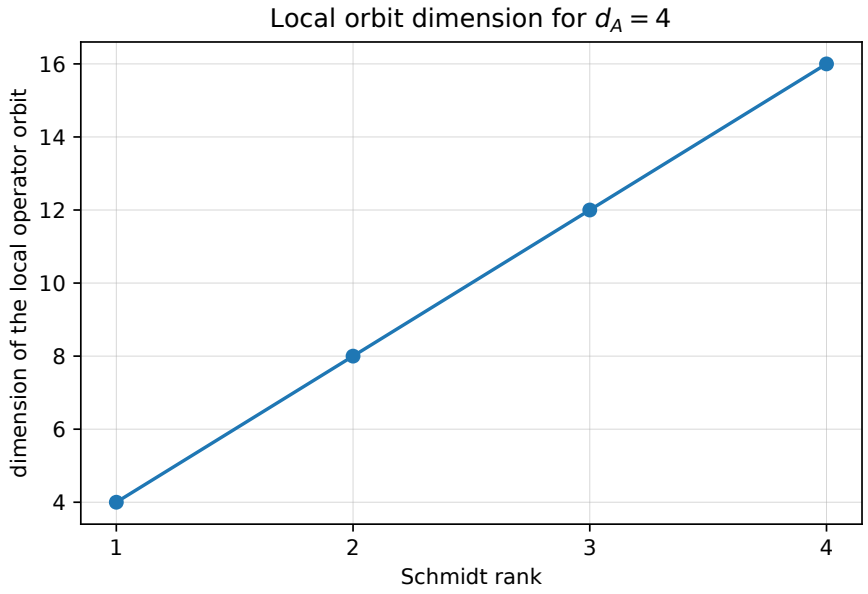


Figure 24. The dimension reached by all local operators is linear in Schmidt rank.

Proof. The Schmidt rank is the rank of the coefficient matrix in any product basis. Substituting that rank into theorem II.2.2 gives the stated orbit dimension. □

Proposition II.2.5 (Computational address orbit)**.** *For n qubits, let*

$$\psi_0 = |0\rangle^{\otimes n}$$

and let X_j be the Pauli X operator on the jth qubit. Then

$$\{X_1^{a_1} \cdots X_n^{a_n} \psi_0 : (a_1, \ldots, a_n) \in \{0,1\}^n\}$$

is the computational basis.

Proof. The addressed vector is $|a_1 \cdots a_n\rangle$. Distinct binary addresses produce the 2^n distinct basis vectors. □

Remark II.2.6. The seed rank records generation by a declared algebra. It does not measure circuit depth, locality cost, control complexity, or physical reachability under a restricted time dependent Hamiltonian.

II.3 Symmetry packets and selection rules

Let G be a finite group and let

$$U : G \longrightarrow \mathcal{U}(\mathcal{H})$$

be a unitary representation. Write $\widehat{G}$ for the set of irreducible unitary representations. For $\lambda \in \widehat{G}$, let d_λ and χ_λ denote its dimension and character.

Theorem II.3.1 (Finite group isotypic projectors)**.** *The operators*

$$P_\lambda = \frac{d_\lambda}{|G|} \sum_{g \in G} \overline{\chi_\lambda(g)} U(g)$$

are orthogonal projectors. They satisfy

$$P_\lambda P_\mu = \delta_{\lambda\mu} P_\lambda, \qquad \sum_{\lambda \in \widehat{G}} P_\lambda = I_{\mathcal{H}}.$$

The range of P_λ is the λ isotypic component of $\mathcal{H}$.

Proof. Complete reducibility gives a unitary decomposition

$$\mathcal{H} \cong \bigoplus_{\mu \in \widehat{G}} V_\mu \otimes M_\mu, \qquad U(g) \cong \bigoplus_{\mu} \pi_\mu(g) \otimes I_{M_\mu}.$$

On the μ summand, the displayed average is central in the irreducible representation π_μ, so it is a scalar by Schur's lemma. Taking its trace and applying character orthogonality shows that the scalar is one when $\mu = \lambda$ and zero otherwise. The asserted identities follow on the direct sum. □

The central projectors separate irreducible types but do not choose coordinates inside the representation factor. Matrix units provide that finer resolution.

Theorem II.3.2 (Representation matrix units)**.** *Fix an irreducible unitary representation $\pi_\lambda : G \to U(d_\lambda)$ and an orthonormal basis of its representation space. Define*

$$E^\lambda_{ij} = \frac{d_\lambda}{|G|} \sum_{g \in G} \left[\pi_\lambda(g^{-1})\right]_{ji} U(g).$$

Then

$$E^\lambda_{ij} E^\mu_{k\ell} = \delta_{\lambda\mu} \delta_{jk} E^\lambda_{i\ell}, \qquad \left(E^\lambda_{ij}\right)^* = E^\lambda_{ji},$$

and

$$P_\lambda = \sum_{i=1}^{d_\lambda} E^\lambda_{ii}.$$

Proof. Apply the matrix coefficient form of Schur orthogonality to the two group averages. It gives the matrix unit multiplication law. Unitarity gives the adjoint relation after replacing g by g^{-1}. Summing the diagonal coefficients gives the character average in theorem II.3.1. □

II.3.1 Cyclic charge packets

Let $N \geq 1$ be an integer, S unitary with $S^N = I$, and $\omega = \mathrm{e}^{2\pi \mathrm{i}/N}$.

Corollary II.3.3 (Cyclic charge projectors)**.** *The operators*

$$P_j = \frac{1}{N} \sum_{r=0}^{N-1} \omega^{-jr} S^r, \qquad j \in \mathbb{Z}/N\mathbb{Z},$$

form a complete orthogonal packet system and satisfy

$$SP_j = \omega^j P_j.$$

Proof. Apply theorem II.3.1 to the cyclic group. Its irreducible representations are the one dimensional characters $r \mapsto \omega^{jr}$. □

Definition II.3.4 (Operator charge)**.** An operator $A \in \mathrm{End}(\mathcal{H})$ has cyclic charge $q \in \mathbb{Z}/N\mathbb{Z}$ when

$$SAS^* = \omega^q A.$$

Theorem II.3.5 (Charge selection rule)**.** *If A has charge q, then*

$$P_k A P_j = 0$$

unless $k = j + q$ in $\mathbb{Z}/N\mathbb{Z}$. In fact,

$$AP_j = P_{j+q} A P_j.$$

Proof. For $x \in P_j\mathcal{H}$,

$$S(Ax) = (SAS^*)Sx = \omega^{q+j} Ax.$$

Thus $Ax \in P_{j+q}\mathcal{H}$. The block statement follows. □

Corollary II.3.6 (Charge addition)**.** *If A and B have charges q and r, then AB has charge $q + r$. The adjoint A^* has charge $-q$.*

Proof. Conjugation by S is a star automorphism. Applying it to AB adds the two charges, while applying it to A^* changes the sign of the charge. □

II.3.2 Tensor refinement

Suppose the ath tensor factor carries a cyclic packet family

$$(P_j^{(a)})_{j \in \mathbb{Z}/N\mathbb{Z}}.$$

The fine tensor packets are

$$P_{\boldsymbol{j}}^{\mathrm{fine}} = P_{j_1}^{(1)} \otimes \cdots \otimes P_{j_m}^{(m)}.$$

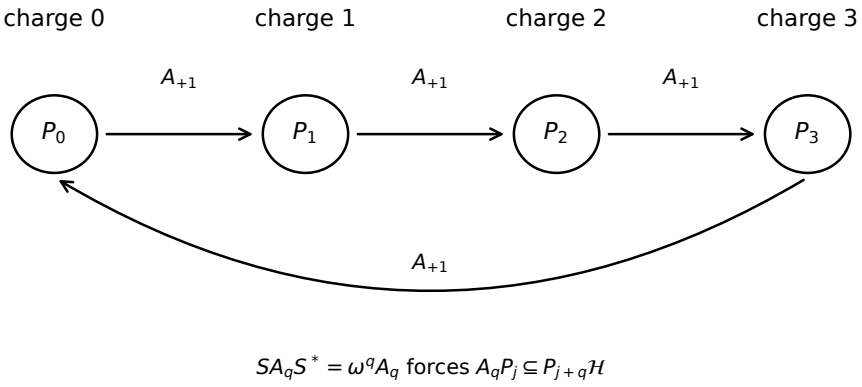


Figure 25. An operator of charge one moves each cyclic packet to the next packet and has no other transfer blocks.

Theorem II.3.7 (Tensor charge refinement)**.** *For $r \in \mathbb{Z}/N\mathbb{Z}$, define*

$$P_r^{\text{total}} = \sum_{j_1+\cdots+j_m=r} P_{j_1}^{(1)} \otimes \cdots \otimes P_{j_m}^{(m)}.$$

Then the P_r^{total} form a complete orthogonal packet system. Every total charge packet is the exact sum of its fine tensor descendants.

Proof. The fine tensor projectors are mutually orthogonal and sum to the identity. The total residue classes partition the fine address set. Summing the fine projectors over each class gives the result. □

Corollary II.3.8 (Tensor selection rule)**.** *If A_a has local charge q_a, then*

$$A_1 \otimes \cdots \otimes A_m$$

has total charge $q_1 + \cdots + q_m$.

Proof. Conjugate the tensor product by the total cyclic symmetry and multiply the local phase factors. □

Remark II.3.9. For a nonabelian group, tensor products are refined by irreducible fusion multiplicities rather than residue addition. The central isotypic projectors remain exact, but a complete tensor refinement also requires a choice of Clebsch Gordan intertwiners.

II.4 Quantum circuits as packet paths

Let

$$U = U_m U_{m-1} \cdots U_1$$

be a finite circuit with $m \geq 1$, and let $(P_a)_{a \in I}$ be a complete orthogonal packet family. For the empty circuit, $U = I$ and its transfer block is $P_b P_a = \delta_{ba} P_a$, whose endpoint sum reconstructs I.

Theorem II.4.1 (Exact circuit path expansion). *For source packet a_0 and target packet a_m,*

$$P_{a_m} U P_{a_0} = \sum_{a_1, \ldots, a_{m-1}} P_{a_m} U_m P_{a_{m-1}} \cdots P_{a_1} U_1 P_{a_0}.$$

Summing over a_0 and a_m reconstructs U.

Proof. Insert $I = \sum_a P_a$ between every adjacent pair of gates and distribute the finite sums. Completeness at the two endpoints gives the full operator. □

For a packet path

$$\gamma = (a_0, a_1, \ldots, a_m),$$

write

$$U_\gamma = P_{a_m} U_m P_{a_{m-1}} \cdots P_{a_1} U_1 P_{a_0}.$$

Theorem II.4.2 (Packet unitarity identities). *If U is unitary and $U_{ba} = P_b U P_a$, then*

$$\sum_b U_{ba}^* U_{bc} = \delta_{ac} P_a$$

and

$$\sum_a U_{ba} U_{da}^* = \delta_{bd} P_b.$$

Proof. Use completeness and unitarity:

$$\sum_b U_{ba}^* U_{bc} = P_a U^* \left(\sum_b P_b \right) U P_c = P_a P_c.$$

Summing instead over the source packets and using unitarity in the reverse order gives the second identity. □

Corollary II.4.3 (Probability conservation from one packet). *If $\psi \in P_a \mathcal{H}$, then*

$$\sum_b \|P_b U \psi\|^2 = \|\psi\|^2.$$

Proof. Take the inner product of the first identity in theorem II.4.2 with ψ and set $c = a$. □

Theorem II.4.4 (Path interference formula)**.** *Fix a source vector $\psi \in P_{a_0}\mathcal{H}$ and a target packet b. Let Γ_b be the set of packet paths from a_0 to b, and set*

$$\eta_\gamma = U_\gamma \psi.$$

Choose any total order on this finite path set. Then

$$\|P_b U\psi\|^2 = \sum_{\gamma\in\Gamma_b} \|\eta_\gamma\|^2 + 2\,\mathrm{Re} \sum_{\substack{\gamma,\gamma'\in\Gamma_b \\ \gamma<\gamma'}} \langle \eta_\gamma, \eta_{\gamma'} \rangle .$$

Consequently,

$$\|P_b U\psi\| \le \sum_{\gamma\in\Gamma_b} \|\eta_\gamma\| .$$

If the path outputs are pairwise orthogonal, the target probability is the sum of the path probabilities.

Proof. The path expansion gives

$$P_b U\psi = \sum_{\gamma\in\Gamma_b} \eta_\gamma.$$

Expanding the squared norm and grouping conjugate cross terms gives the interference formula. The triangle inequality gives the norm bound. When the path outputs are orthogonal, every cross term vanishes and only the individual path probabilities remain. □

Proposition II.4.5 (Charge pruning of circuit paths)**.** *Suppose every gate has a finite charge decomposition*

$$U_r = \sum_q U_r^{(q)}, \qquad S U_r^{(q)} S^* = \omega^q U_r^{(q)}.$$

A term with gate charges $q_1, \dots, q_m$ can contribute from source charge a_0 only to target charge

$$a_m = a_0 + q_1 + \cdots + q_m.$$

Every packet path violating one of the intermediate charge updates vanishes.

Proof. Apply theorem II.3.5 after each gate component. The packet address is forced at every step. □

Example II.4.6 (Bell circuit)**.** Starting from $|00\rangle$, apply a Hadamard gate to the first qubit and then a controlled NOT gate. The final state is

$$\frac{|00\rangle + |11\rangle}{\sqrt{2}}.$$

It lies in the even parity packet. The intermediate state has one even and one odd computational contribution, so the final even amplitude is reconstructed by more than one packet path.

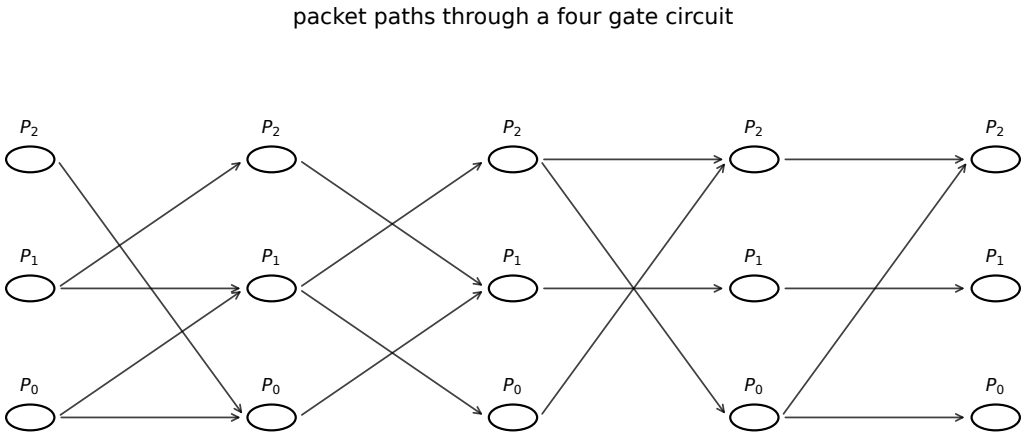


Figure 26. A circuit block is the coherent sum of its allowed packet paths. Selection rules remove forbidden paths before amplitudes are evaluated.

II.5 Symmetry resolved dynamics and leakage

Let $H = H^*$ and let $(P_a)_{a \in I}$ be a complete orthogonal packet system.

Theorem II.5.1 (Exact invariant packets)**.** *The following conditions are equivalent:*

1. *The Hamiltonian commutes with each projector:* $[H, P_a] = 0$ *for every* a.
2. *Transfer blocks between distinct packets vanish:* $P_b H P_a = 0$ *whenever* $a \neq b$.
3. *Every packet* $P_a \mathcal{H}$ *is invariant under* $\mathrm{e}^{-\mathrm{i}tH}$ *for every real* t.

When they hold,

$$H = \sum_a P_a H P_a$$

and

$$\mathrm{e}^{-\mathrm{i}tH} = \sum_a P_a \mathrm{e}^{-\mathrm{i}tH} P_a.$$

Proof. Commutation is equivalent to vanishing of every off diagonal block. The same block decomposition passes to polynomials in H, then to the exponential by norm convergence. Invariance of every packet implies invariance under both $\mathrm{e}^{-\mathrm{i}tH}$ and its adjoint. Differentiation at $t = 0$ gives commutation with H. □

Fix one packet projector P and set $Q = I - P$.

Lemma II.5.2 (Off diagonal norm)**.** *For self adjoint* H,

$$\|[H, P]\| = \|QHP\| = \|PHQ\|.$$

Proof. Relative to $P\mathcal{H} \oplus Q\mathcal{H}$,

$$[H, P] = \begin{pmatrix} 0 & -PHQ \\ QHP & 0 \end{pmatrix}.$$

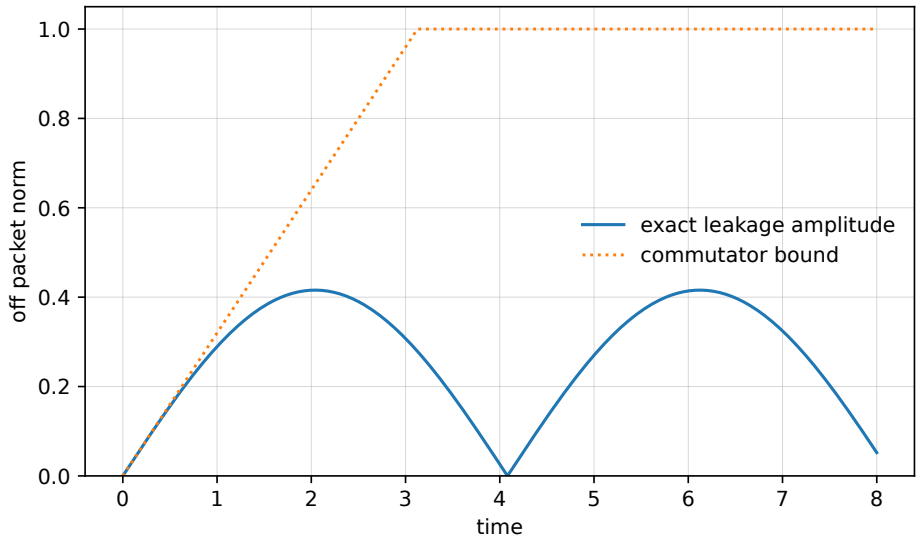


Figure 27. Exact transition amplitude in a two packet model and the linear commutator bound.

Its square has diagonal blocks $-PHQHP$ and $-QHPHQ$. The norm is therefore the largest singular value of QHP. □

Theorem II.5.3 (Fixed packet leakage). *For every real t,*

$$\left\|Q\mathrm{e}^{-\mathrm{i}tH}P\right\| \leq |t|\,\|QHP\| = |t|\,\|[H,P]\|\,.$$

Proof. Let

$$H_{\mathrm{d}} = PHP + QHQ, \qquad H_{\mathrm{o}} = PHQ + QHP.$$

The propagator generated by H_{d} preserves $P\mathcal{H}$ and $Q\mathcal{H}$. Duhamel's formula relative to H_{d} gives

$$Q\mathrm{e}^{-\mathrm{i}tH}P = -\mathrm{i}\int_0^t Q\mathrm{e}^{-\mathrm{i}(t-s)H}H_{\mathrm{o}}\mathrm{e}^{-\mathrm{i}sH_{\mathrm{d}}}P\,\mathrm{d}s.$$

Since $H_{\mathrm{o}}P = QHP$ and both propagators are unitary, the norm is at most $|t|\,\|QHP\|$. Use lemma II.5.2 for the last equality. □

Corollary II.5.4 (Leakage probability). *If $\psi \in P\mathcal{H}$ is a unit vector, then*

$$\left\|Q\mathrm{e}^{-\mathrm{i}tH}\psi\right\|^2 \leq t^2\,\|QHP\|^2\,.$$

Proof. Apply theorem II.5.3 to the unit vector, then square the resulting nonnegative bound. □

II.6 Moving packets and geometric transport

Let $(P_a(t))_{a\in I}$ be a twice continuously differentiable family of complete orthogonal packet systems on a finite dimensional Hilbert space.

Theorem II.6.1 (Canonical packet connection). *Define*

$$K(t) = \sum_a \dot{P}_a(t) P_a(t).$$

Then

$$K(t)^* = -K(t)$$

and

$$[K(t), P_a(t)] = \dot{P}_a(t)$$

for every a.

Proof. Differentiating $P_a^2 = P_a$ gives

$$\dot{P}_a P_a + P_a \dot{P}_a = \dot{P}_a.$$

Summing over a and using $\sum_a \dot{P}_a = 0$ yields

$$\sum_a P_a \dot{P}_a = -\sum_a \dot{P}_a P_a.$$

This proves skew adjointness. For fixed b,

$$K P_b = \dot{P}_b P_b.$$

Differentiating $P_b P_a = 0$ for $a \neq b$ gives

$$P_b \dot{P}_a = -\dot{P}_b P_a.$$

Hence

$$P_b K = -\dot{P}_b (I - P_b).$$

Subtracting gives $[K, P_b] = \dot{P}_b$. □

Theorem II.6.2 (Exact Kato transport). *Let $W(t)$ solve*

$$\dot{W}(t) = K(t) W(t), \qquad W(0) = I.$$

Then $W(t)$ is unitary and

$$P_a(t) W(t) = W(t) P_a(0)$$

for every packet a.

Proof. Skew adjointness gives

$$\frac{\mathrm{d}}{\mathrm{d}t} W(t)^* W(t) = 0.$$

Thus $W(t)$ is unitary. Next,

$$\frac{\mathrm{d}}{\mathrm{d}t}\left(W(t)^* P_a(t) W(t)\right) = W(t)^*\left(\dot{P}_a - [K, P_a]\right) W(t) = 0.$$

The expression equals $P_a(0)$ at $t = 0$, which proves the intertwining identity. □

Theorem II.6.3 (Moving frame Hamiltonian). *Let $U(t)$ solve*

$$\mathrm{i}\dot{U}(t) = H(t)U(t), \qquad U(0) = I,$$

where $H(t) = H(t)^*$ is continuous on the compact time interval under consideration. Set

$$V(t) = W(t)^* U(t).$$

Then

$$\mathrm{i}\dot{V}(t) = H_{\mathrm{mov}}(t)V(t),$$

where

$$H_{\mathrm{mov}}(t) = W(t)^* H(t) W(t) - \mathrm{i}W(t)^*\dot{W}(t) = W(t)^*(H(t) - \mathrm{i}K(t))W(t).$$

The moving frame Hamiltonian is self adjoint.

Proof. Differentiate $V = W^*U$. Since $\dot{W} = KW$ and $K^* = -K$,

$$\dot{W}^* = -W^*K.$$

Substitution gives the equation. The first term in H_{mov} is self adjoint. The operator $-\mathrm{i}W^*\dot{W}$ is self adjoint because $W^*\dot{W}$ is skew adjoint. □

Theorem II.6.4 (Moving packet leakage). *Fix a packet $P(t) = P_a(t)$ and put $Q(t) = I - P(t)$. For $0 \le t \le T$,*

$$\|Q(t)U(t)P(0)\| \le \int_0^t \left\|Q(s)(H(s) - \mathrm{i}K(s))P(s)\right\| \,\mathrm{d}s.$$

In particular, the physical evolution follows the moving packet exactly on $[0, T]$ when the displayed off packet block vanishes for every time in that interval.

Proof. In the Kato frame, $P(0)$ is fixed and

$$Q(t)U(t)P(0) = W(t)Q(0)V(t)P(0).$$

Apply the time dependent version of the Duhamel argument in theorem II.5.3 to $H_{\mathrm{mov}}(t)$. The off diagonal block is

$$Q(0)H_{\mathrm{mov}}(s)P(0) = W(s)^* Q(s)(H(s) - \mathrm{i}K(s))P(s)W(s).$$

Unitary conjugation preserves the norm. □

The exact coupling test therefore includes the geometric term. Even if the Hamiltonian is diagonal in the packet decomposition at every fixed time, its evolution can fail to follow a packet whose range rotates.

II.6.1 Discrete packet transport

Let (P_a) and (Q_a) be two complete packet systems with the same index set. Define

$$S(\mathcal{Q},\mathcal{P}) = \sum_a Q_a P_a.$$

Theorem II.6.5 (Direct packet rotation). *Assume*

$$\|S(\mathcal{Q},\mathcal{P}) - I\| < 1.$$

Then $S(\mathcal{Q},\mathcal{P})$ is invertible. Its unitary polar factor

$$\mathcal{U}(\mathcal{Q},\mathcal{P}) = S(S^*S)^{-1/2}$$

satisfies

$$Q_a \mathcal{U}(\mathcal{Q},\mathcal{P}) = \mathcal{U}(\mathcal{Q},\mathcal{P}) P_a$$

for every a.

Proof. The norm condition gives invertibility by the Neumann series. The identity

$$Q_a S = S P_a = Q_a P_a$$

shows that S^*S commutes with every P_a. Its inverse square root also commutes with every P_a. Hence

$$Q_a \mathcal{U} = Q_a S (S^*S)^{-1/2} = S P_a (S^*S)^{-1/2} = \mathcal{U} P_a.$$

The polar factor is unitary because S is invertible. □

Theorem II.6.6 (Convergence of short packet rotations). *Let $(P_a(t))$ be twice continuously differentiable on $[0,T]$. For a partition*

$$0 = t_0 < t_1 < \cdots < t_n = T,$$

let

$$W_\pi = \mathcal{U}(\mathcal{P}(t_n),\mathcal{P}(t_{n-1})) \cdots \mathcal{U}(\mathcal{P}(t_1),\mathcal{P}(t_0)).$$

For sufficiently fine partitions the factors are defined, and

$$\|W_\pi - W(T)\| \le C_T\, |\pi|$$

for a constant depending on the packet path but not on the partition. Here the size of the partition is measured by its mesh, which is the length of its largest subinterval.

Proof. Taylor expansion gives

$$S(\mathcal{P}(t+h),\mathcal{P}(t)) = I + hK(t) + O(h^2)$$

uniformly on $[0,T]$. Since $K(t)^* = -K(t)$,

$$S^*S = I + O(h^2),$$

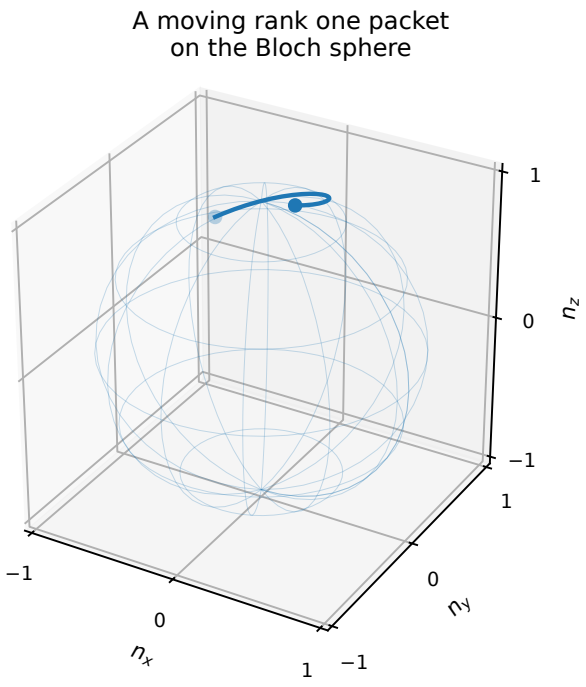


Figure 28. A moving rank one packet on the Bloch sphere. The Kato evolution transports the range without choosing a phase convention for its eigenvector.

so the polar factor satisfies

$$\mathcal{U}(\mathcal{P}(t+h), \mathcal{P}(t)) = I + hK(t) + O(h^2).$$

This gives a first order approximation to $\dot{W} = KW$ over a single time step. A telescoping product estimate over the partition gives a total error bounded by a constant times $\sum_j (t_{j+1} - t_j)^2$, which is at most $T\,|\pi|$. □

II.6.2 Local frames and curvature

Let $P(x)$ be a smooth rank r orthogonal projector over a parameter manifold. Choose a local isometry

$$V(x) : \mathbb{C}^r \longrightarrow \mathcal{H}, \qquad V(x)V(x)^* = P(x).$$

Theorem II.6.7 (Nonabelian packet connection)**.** *The one form with matrix values*

$$\mathcal{A} = V^* \,\mathrm{d}V$$

is skew adjoint. Under a frame change $V' = VG$, where $G(x) \in U(r)$,

$$\mathcal{A}' = G^* \mathcal{A} G + G^* \,\mathrm{d}G.$$

Its curvature

$$\mathcal{F} = \mathrm{d}\mathcal{A} + \mathcal{A} \wedge \mathcal{A}$$

satisfies

$$\mathcal{F} = V^* (\,\mathrm{d}P \wedge \,\mathrm{d}P) V.$$

Proof. Differentiate $V^*V = I$ to obtain $\mathcal{A}^* = -\mathcal{A}$. The gauge transformation law follows by differentiating VG. Since $P = VV^*$ and $(I - P)\,\mathrm{d}V = \,\mathrm{d}P\,V$, direct expansion gives

$$\mathrm{d}\mathcal{A} + \mathcal{A} \wedge \mathcal{A} = \,\mathrm{d}V^* (I - P) \wedge \,\mathrm{d}V = V^* (\,\mathrm{d}P \wedge \,\mathrm{d}P) V.$$

□

Corollary II.6.8 (Bloch sphere curvature)**.** *Let*

$$P(\theta, \phi) = \frac{1}{2} \left(I + \boldsymbol{n}(\theta, \phi) \cdot \boldsymbol{\sigma} \right),$$

where

$$\boldsymbol{n} = (\sin\theta \cos\phi, \sin\theta \sin\phi, \cos\theta).$$

With the convention

$$\mathcal{F}_{\theta\phi} = -\mathrm{i} \,\mathrm{Tr}(P[\partial_\theta P, \partial_\phi P]),$$

one has

$$\mathcal{F}_{\theta\phi} = \frac{1}{2} \sin\theta$$

and

$$\frac{1}{2\pi} \int_0^{2\pi} \int_0^{\pi} \mathcal{F}_{\theta\phi} \,\mathrm{d}\theta \,\mathrm{d}\phi = 1.$$

Proof. The Pauli identity

$$(\boldsymbol{a} \cdot \boldsymbol{\sigma})(\boldsymbol{b} \cdot \boldsymbol{\sigma}) = (\boldsymbol{a} \cdot \boldsymbol{b}) I + \mathrm{i} (\boldsymbol{a} \times \boldsymbol{b}) \cdot \boldsymbol{\sigma}$$

gives

$$-\mathrm{i} \,\mathrm{Tr}(P[\partial_\theta P, \partial_\phi P]) = \frac{1}{2} \boldsymbol{n} \cdot (\partial_\theta \boldsymbol{n} \times \partial_\phi \boldsymbol{n}) = \frac{1}{2} \sin\theta.$$

Integrating the displayed curvature over the sphere and applying the stated normalization gives one. □

II.7 Operator packets, measurements, and quantum channels

Density matrices and observables carry both an input packet and an output packet. Equip $\mathrm{End}(\mathcal{H})$ with the Hilbert Schmidt inner product

$$\langle X, Y\rangle_{\mathrm{HS}} = \mathrm{Tr}(X^* Y).$$

Definition II.7.1 (Two sided operator packet)**.** For a complete orthogonal family (P_a), define

$$\mathcal{P}_{ab}(X) = P_a X P_b.$$

The range

$$\mathcal{B}_{ab} = P_a \,\mathrm{End}(\mathcal{H}) P_b$$

is the operator packet with output address a and input address b.

Theorem II.7.2 (Complete operator packet system)**.** *The superoperators $(\mathcal{P}_{ab})_{a,b\in I}$ are mutually orthogonal projections on Hilbert Schmidt operator space. They satisfy*

$$X = \sum_{a,b} P_a X P_b$$

and

$$\|X\|_{\mathrm{HS}}^2 = \sum_{a,b} \|P_a X P_b\|_{\mathrm{HS}}^2 .$$

Proof. Idempotence and completeness follow from the projector identities. For Hilbert Schmidt orthogonality,

$$\begin{aligned}\langle P_a X P_b, P_c Y P_d\rangle_{\mathrm{HS}} &= \mathrm{Tr}(P_b X^* P_a P_c Y P_d) \\ &= \delta_{ac}\delta_{bd}\,\mathrm{Tr}(P_b X^* P_a Y P_b).\end{aligned}$$

Since the packets are orthogonal and sum to the original operator, their squared norms add to its squared norm. □

Definition II.7.3 (Packet dephasing)**.** The packet dephasing map is

$$\mathcal{D}_{\mathcal{P}}(X) = \sum_a P_a X P_a.$$

Theorem II.7.4 (Dephasing as conditional expectation)**.** *The map $\mathcal{D}_{\mathcal{P}}$ is completely positive, trace preserving, unital, and idempotent. It is the Hilbert Schmidt orthogonal projection onto the block diagonal algebra*

$$\mathcal{A}_{\mathcal{P}} = \{X : [X, P_a] = 0 \text{ for every } a\}.$$

In particular,

$$\|\mathcal{D}_{\mathcal{P}}(X)\|_{\mathrm{HS}} \le \|X\|_{\mathrm{HS}} .$$

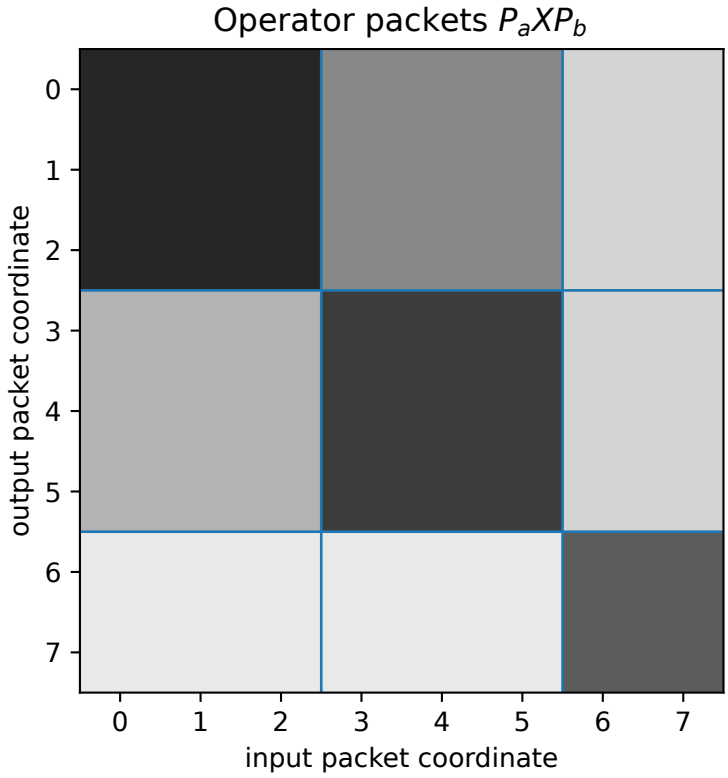


Figure 29. A density matrix or observable carries two packet addresses. Diagonal packets contain populations and internal observables. Off diagonal packets contain coherences.

Proof. The projectors P_a form a Kraus family because $\sum_a P_a^* P_a = I$. Thus the map is completely positive and trace preserving. It is unital for the same reason. Orthogonality and idempotence follow from theorem II.7.2. Its range is the sum of the diagonal operator packets. This is exactly the commutant of the projector family. □

Corollary II.7.5 (Block diagonal measurement invariance)**.** *Let (E_k) be a positive operator valued measurement, and suppose*

$$E_k = \mathcal{D}_{\mathcal{P}}(E_k)$$

for every k. Then every density matrix ρ satisfies

$$\mathrm{Tr}(E_k \rho) = \mathrm{Tr}(E_k \mathcal{D}_{\mathcal{P}}(\rho)).$$

Proof. Since $\mathcal{D}_{\mathcal{P}}$ is self adjoint for the Hilbert Schmidt inner product,

$$\mathrm{Tr}(E_k \rho) = \mathrm{Tr}(\mathcal{D}_{\mathcal{P}}(E_k)\rho) = \mathrm{Tr}(E_k \mathcal{D}_{\mathcal{P}}(\rho)).$$

□

II.7.1 Channel superblocks

Let $\Phi : \mathrm{End}(\mathcal{H}_X) \to \mathrm{End}(\mathcal{H}_Y)$ be linear. Choose packet systems (P_a) on $\mathcal{H}_X$ and (Q_c) on $\mathcal{H}_Y$. Define

$$\Phi_{cd,ab} = \mathcal{Q}_{cd}\Phi\mathcal{P}_{ab}.$$

Theorem II.7.6 (Exact channel block calculus)**.** *Every linear map has the exact reconstruction*

$$\Phi = \sum_{a,b,c,d} \Phi_{cd,ab}.$$

If $\Psi : \mathrm{End}(\mathcal{H}_Y) \to \mathrm{End}(\mathcal{H}_Z)$*, then*

$$(\Psi\Phi)_{ef,ab} = \sum_{c,d} \Psi_{ef,cd}\Phi_{cd,ab}.$$

Proof. Insert the complete operator packet resolutions before and after Φ. For composition, insert the middle resolution between Ψ and Φ and collect the output and input packets. □

Standard Fact II.7.7 (Finite Kraus and Choi criteria)**.** A linear map $\Phi : M_n(\mathbb{C}) \to M_m(\mathbb{C})$ is completely positive exactly when it has a Kraus representation

$$\Phi(X) = \sum_r K_r X K_r^*.$$

It is trace preserving exactly when

$$\sum_r K_r^* K_r = I.$$

Equivalently, its Choi matrix

$$J(\Phi) = \sum_{i,j} \Phi(|i\rangle\langle j|) \otimes |i\rangle\langle j|$$

is positive, and trace preservation is

$$\mathrm{Tr}_{\mathrm{out}}\, J(\Phi) = I_{\mathrm{in}}.$$

These finite criteria are classical [24, 5, 15, 27].

II.7.2 Covariance and coherence order

Let S be unitary and $N \geq 1$ an integer with $S^N = I$, and define the conjugation action

$$\mathrm{Ad}_S(X) = SXS^*.$$

Theorem II.7.8 (Coherence order projectors)**.** *For $q \in \mathbb{Z}/N\mathbb{Z}$, define*

$$\mathcal{L}_q(X) = \frac{1}{N}\sum_{r=0}^{N-1} \omega^{-qr} S^r X S^{-r}.$$

Then the $\mathcal{L}_q$ form a complete orthogonal packet system on Hilbert Schmidt operator space. Their ranges are the operators satisfying

$$SXS^* = \omega^q X.$$

If P_j are the state charge projectors, then

$$\operatorname{Ran} \mathcal{L}_q = \bigoplus_j P_{j+q} \operatorname{End}(\mathcal{H}) P_j.$$

Proof. Apply the cyclic character projector formula to the unitary representation Ad_S on operator space. The last identity follows from theorem II.3.5 applied to each operator packet. □

Theorem II.7.9 (Covariant channels preserve coherence order)**.** *Suppose*

$$\Phi(SXS^*) = S\Phi(X)S^*$$

for every X. Then

$$\Phi\mathcal{L}_q = \mathcal{L}_q\Phi$$

for every q. Thus Φ cannot mix distinct coherence orders.

Proof. The covariance identity says that Φ commutes with every power of Ad_S. It therefore commutes with each finite character average $\mathcal{L}_q$. □

Theorem II.7.10 (Choi symmetry criterion)**.** *Let $U : G \to \mathcal{U}(\mathcal{H})$ be a finite group representation. A channel Φ is covariant,*

$$\Phi(U(g)XU(g)^*) = U(g)\Phi(X)U(g)^*,$$

if and only if

$$(U(g) \otimes \overline{U(g)}) J(\Phi) (U(g)^* \otimes U(g)^{\mathsf{T}}) = J(\Phi)$$

for every $g \in G$.

Proof. Let

$$\Omega = \sum_i |i\rangle \otimes |i\rangle .$$

Then

$$J(\Phi) = (\Phi \otimes \mathrm{id})(|\Omega\rangle \langle\Omega|).$$

The vector Ω is invariant under $U \otimes \overline{U}$. Covariance therefore implies the displayed Choi invariance. Conversely, the displayed transformation is the Choi matrix of

$$\mathrm{Ad}_{U(g)} \circ \Phi \circ \mathrm{Ad}_{U(g)^*} .$$

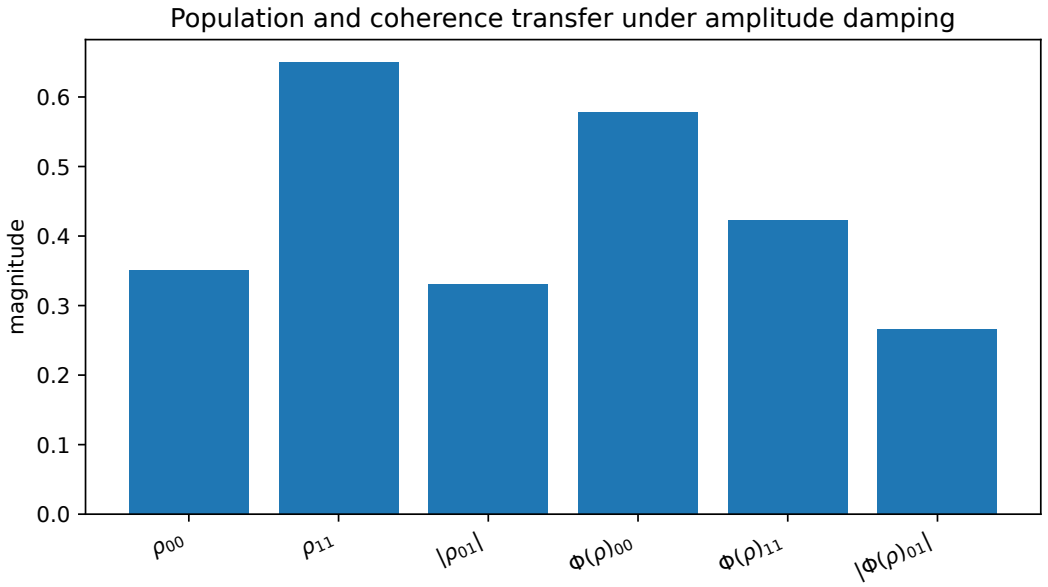


Figure 30. Amplitude damping transfers population and contracts the coherence packet.

The Choi correspondence is injective, so invariance implies that this map equals Φ, which is covariance. □

Corollary II.7.11 (Choi packet decomposition)**.** *The Choi matrix of a covariant channel is block diagonal with respect to the isotypic decomposition of $U \otimes \overline{U}$.*

Proof. Apply theorem II.3.1 to the representation $U \otimes \overline{U}$ and use theorem II.7.10. □

Example II.7.12 (Amplitude damping)**.** For $0 \leq \gamma \leq 1$, let

$$K_0 = \begin{pmatrix} 1 & 0 \\ 0 & \sqrt{1-\gamma} \end{pmatrix}, \qquad K_1 = \begin{pmatrix} 0 & \sqrt{\gamma} \\ 0 & 0 \end{pmatrix}.$$

The channel

$$\Phi_\gamma(\rho) = K_0 \rho K_0^* + K_1 \rho K_1^*$$

is trace preserving. It sends the off diagonal packet $|0\rangle\langle 1|$ to $\sqrt{1-\gamma}\,|0\rangle\langle 1|$, while the excited population transfers partly into the ground population.

II.7.3 Quantum dynamical semigroups

Standard Fact II.7.13 (Finite Lindblad generator)**.** A norm continuous semigroup of completely positive trace preserving maps on a finite matrix algebra, in the Schrödinger picture, has a generator of the form

$$\mathcal{G}(X) = -\mathrm{i}[H, X] + \sum_r \left(L_r X L_r^* - \frac{1}{2} L_r^* L_r X - \frac{1}{2} X L_r^* L_r \right),$$

where $H = H^*$. Conversely, every operator of this form generates a completely positive trace preserving semigroup [16].

Theorem II.7.14 (Charge preservation by a Lindblad generator)**.** *Let S be unitary and $N \geq 1$ an integer with $S^N = I$. Assume*

$$SHS^* = H$$

and, for every jump operator, there is a charge q_r such that

$$SL_rS^* = \omega^{q_r} L_r.$$

Then the Lindblad generator $\mathcal{G}$ preserves every coherence order:

$$\mathcal{G}\mathcal{L}_p = \mathcal{L}_p\mathcal{G}.$$

The quantum dynamical semigroup $\mathrm{e}^{t\mathcal{G}}$ has the same property.

Proof. Let X have coherence order p. The Hamiltonian commutator has order p because H has charge zero. The jump term $L_rXL_r^*$ has charge

$$q_r + p - q_r = p.$$

Also $L_r^*L_r$ has charge zero, so both anticommutator terms have charge p. Thus $\mathcal{G}$ preserves $\operatorname{Ran}\mathcal{L}_p$. The exponential series then shows that $\mathrm{e}^{t\mathcal{G}}$ preserves the same packets. □

Corollary II.7.15 (Independent coherence evolution)**.** *Under the hypotheses of theorem II.7.14, each coherence component of an initial operator evolves within its own order. In particular, a density matrix in the zero order sector remains in that sector.*

Proof. Decompose the initial operator by theorem II.7.8 and apply the invariant packet statement to each component. □

Preservation of coherence order does not by itself give a closed classical Markov chain for the packet populations. Such scalar population equations require additional isotropy within each packet.

II.8 Quantum error correction as a compression obstruction

Let P be the orthogonal projector onto a code space

$$\mathcal{C} = P\mathcal{H}, \qquad k = \dim \mathcal{C} \geq 1.$$

The compression of $A \in \operatorname{End}(\mathcal{H})$ to the code is $PAP \in \operatorname{End}(\mathcal{C})$. The zero code has only the zero supported operator and no normalized code state. Part III treats that branch in the mathematical completion.

Definition II.8.1 (Code compression obstruction)**.** Let

$$q_P : \mathrm{End}(\mathcal{C}) \longrightarrow \mathrm{End}(\mathcal{C})/(\mathbb{C}I_{\mathcal{C}})$$

be the quotient map. Define

$$\mathrm{Ob}_P(A) = q_P(PAP).$$

Equivalently, one may use the traceless representative

$$\mathfrak{o}_P(A) = PAP - \frac{\mathrm{Tr}(PAP)}{k}P.$$

The class vanishes exactly when A acts as a scalar after compression to the code. Such an operator cannot distinguish normalized code vectors by expectation value.

Exact correction of an error span means that one completely positive trace preserving recovery $\mathcal{R}$ satisfies $\mathcal{R}(F\rho F^*) = q_F\rho$ for every F in that span and every code-supported matrix ρ, with a nonnegative scalar q_F depending on F but not on the logical input. For every normalized channel with Kraus operators in the same span, the same recovery restores the code input with total scalar one. Individual unnormalized errors are not required to have unit recovery weight.

Theorem II.8.2 (Knill Laflamme as obstruction vanishing)**.** *Let $E_1, \dots, E_r$ be an error family. The code $\mathcal{C}$ corrects their linear span exactly if and only if*

$$\mathrm{Ob}_P(E_a^* E_b) = 0$$

for all a, b. Equivalently, there is a matrix $c = (c_{ab})$ such that

$$PE_a^* E_b P = c_{ab} P$$

for all a, b.

Proof. The equivalence between the quotient statement and the scalar compression identity is immediate from the definition. The latter identity is the finite Knill Laflamme criterion [14, 22]. □

The next result turns the scalar compression identities into a family of orthogonal syndrome packets. Those packets provide the coordinates used by the recovery map.

Theorem II.8.3 (Orthogonal syndrome construction)**.** *Assume the Knill Laflamme identities. Then the coefficient matrix c is positive semidefinite. Choose a unitary matrix W such that*

$$WcW^* = \operatorname{diag}(\lambda_1, \dots, \lambda_r), \qquad \lambda_j \geq 0,$$

and define

$$F_j = \sum_a \overline{W_{ja}} E_a.$$

For every j with $\lambda_j > 0$, the operator

$$V_j = \lambda_j^{-1/2} F_j P$$

is an isometry from the code into $\mathcal{H}$. Its range projector

$$Q_j = V_j V_j^*$$

is a syndrome packet, and the nonzero Q_j are pairwise orthogonal.

Proof. For $z \in \mathbb{C}^r$, let $F_z = \sum_a z_a E_a$. Then

$$P F_z^* F_z P = (z^* c z) P \geq 0,$$

so $c \geq 0$. The unitary change of error coordinates gives

$$P F_j^* F_\ell P = \lambda_j \delta_{j\ell} P.$$

Thus

$$V_j^* V_\ell = \delta_{j\ell} P.$$

Each V_j is an isometry on $P\mathcal{H}$, and distinct ranges are orthogonal. Their range projectors are therefore pairwise orthogonal. □

Theorem II.8.4 (Exact recovery on the error span)**.** *Under the hypotheses of theorem II.8.3, define on the syndrome support*

$$Q = \sum_{\lambda_j > 0} Q_j$$

the completely positive map

$$\mathcal{R}_0(X) = \sum_{\lambda_j > 0} V_j^* Q_j X Q_j V_j.$$

It extends to a quantum channel $\mathcal{R}$ on $\operatorname{End}(\mathcal{H})$*. If*

$$\Phi(X) = \sum_a E_a X E_a^*$$

is trace preserving on code states, then

$$\mathcal{R}\Phi(\rho) = \rho$$

for every density matrix $\rho = P\rho P$.

Proof. The map $\mathcal{R}_0$ is completely positive. It is trace preserving on operators supported in $Q\mathcal{H}$ because

$$\mathrm{Tr}(V_j^* Q_j X Q_j V_j) = \mathrm{Tr}(Q_j X Q_j).$$

Fix a code state ρ_0 and write $Q^\perp = I - Q$. Then

$$\mathcal{R}(X) = \mathcal{R}_0(QXQ) + \mathrm{Tr}(Q^\perp X)\rho_0$$

is completely positive and trace preserving. It extends $\mathcal{R}_0$ on operators supported in $Q\mathcal{H}$.

Unitary mixing of a Kraus family does not change the channel, so

$$\Phi(\rho) = \sum_j F_j \rho F_j^* = \sum_{\lambda_j > 0} \lambda_j V_j \rho V_j^*.$$

Recovery gives

$$\mathcal{R}\Phi(\rho) = \left(\sum_j \lambda_j \right) \rho.$$

Trace preservation on a code state implies $\sum_j \lambda_j = 1$. □

Corollary II.8.5 (Syndrome measurement preserves logical information)**.** *For a channel trace preserving on code states as in the preceding theorem, the completed projective measurement consisting of $(Q_j)_{\lambda_j>0}$ and $I - \sum_{\lambda_j>0} Q_j$ identifies the orthogonal error syndrome without resolving the encoded state inside the code. The complement outcome has probability zero on the corrupted code state.*

Proof. On syndrome j, the encoded state is carried by the isometry V_j. The outcome probability is λ_j, independent of the normalized code state, while the postmeasurement state is $V_j \rho V_j^*$. □

Definition II.8.6 (Approximate Knill Laflamme defect)**.** For a finite error family, define the following defect. When the family is empty, assign the maximum the value zero.

$$\varepsilon_{\mathrm{KL}} = \max_{a,b} \inf_{c \in \mathbb{C}} \| P E_a^* E_b P - cP \|.$$

Proposition II.8.7 (Meaning of the approximate defect)**.** *For each pair (a, b), choose a minimizing scalar c_{ab}. For unit code vectors ψ, ϕ,*

$$|\langle E_a \psi, E_b \phi \rangle - c_{ab} \langle \psi, \phi \rangle| \le \varepsilon_{\mathrm{KL}}.$$

Thus $\varepsilon_{\mathrm{KL}}$ controls the deviation of error overlaps from their scalar code form.

Proof. The left side is

$$|\langle \psi, (P E_a^* E_b P - c_{ab} P)\phi \rangle|,$$

which is bounded by the operator norm. □

No recovery fidelity estimate is inferred from this norm alone. Approximate error correction requires a separate continuity theorem and a declared channel metric.

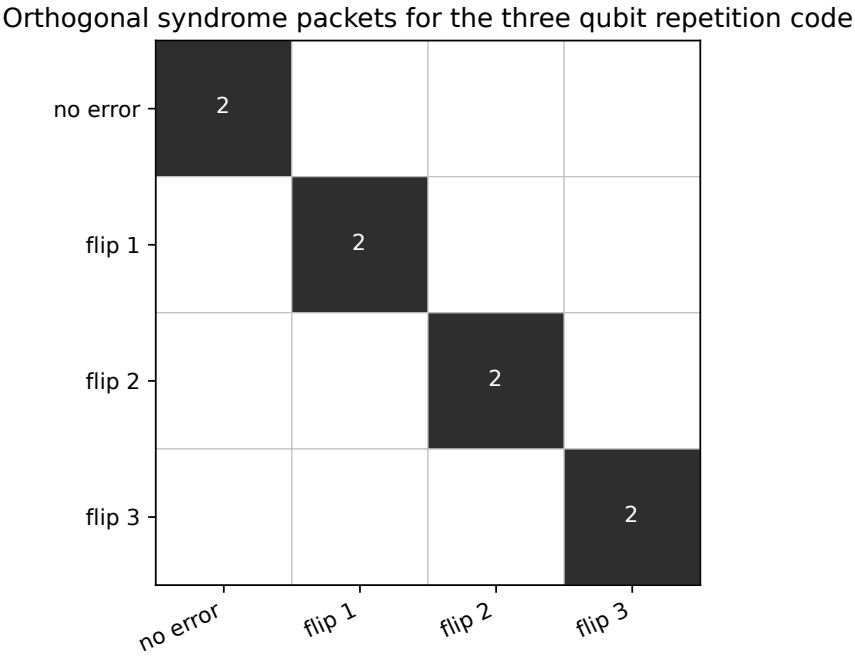


Figure 31. The syndrome packets of the three qubit repetition code. Each packet has dimension two and carries the full logical state.

Example II.8.8 (Three qubit repetition code)**.** Let

$$|0_L\rangle = |000\rangle\,, \qquad |1_L\rangle = |111\rangle\,,$$

and take the errors

$$I, \quad X \otimes I \otimes I, \quad I \otimes X \otimes I, \quad I \otimes I \otimes X.$$

Their images of the code are four pairwise orthogonal two dimensional syndrome packets whose sum is the full eight dimensional Hilbert space.

Standard Fact II.8.9 (Correctable observable algebras)**.** Let Φ be a finite completely positive trace preserving channel with Kraus operators (E_a). A finite dimensional unital star subalgebra $\mathcal{M} \subseteq P\,\mathrm{End}(\mathcal{H})P$ is correctable when a completely positive trace preserving recovery $\mathcal{R}$ satisfies $P(\Phi^* \circ \mathcal{R}^*)(X)P = X$ for every $X \in \mathcal{M}$, where stars on maps denote Heisenberg adjoints. This holds exactly when every compressed product $PE_a^*E_bP$ belongs to the commutant $\mathcal{M}'$ on the code. The scalar code criterion is the special case $\mathcal{M} = P\,\mathrm{End}(\mathcal{H})P$ [1].

II.9 Feshbach effective dynamics and hidden packet memory

Let P be an orthogonal projector, put $Q = I - P$, and write a self adjoint Hamiltonian as

$$H = \begin{pmatrix} A & B \\ B^{*} & D \end{pmatrix}$$

relative to $P\mathcal{H} \oplus Q\mathcal{H}$.

Definition II.9.1 (Feshbach map and self energy)**.** For $z \notin \operatorname{Spec} D$, define

$$\Sigma(z) = B(z - D)^{-1} B^{*}$$

and

$$F_{P}(z) = z - A - \Sigma(z).$$

Theorem II.9.2 (Exact projected resolvent)**.** *If $z \notin \operatorname{Spec} D$ and $F_{P}(z)$ is invertible, then*

$$P(z - H)^{-1} P = F_{P}(z)^{-1}$$

as an operator on $P\mathcal{H}$.

Proof. The lower right block of $z - H$ is $z - D$. Block Gaussian elimination gives

$$\begin{pmatrix} I & B(z-D)^{-1} \\ 0 & I \end{pmatrix} (z - H) \begin{pmatrix} I & 0 \\ (z-D)^{-1}B^{*} & I \end{pmatrix} = \begin{pmatrix} F_{P}(z) & 0 \\ 0 & z - D \end{pmatrix}.$$

Invert the factors. The retained resolvent is the block in the upper left corner of the resulting inverse. □

Theorem II.9.3 (Spectral equivalence)**.** *Let $z \notin \operatorname{Spec} D$. Then*

$$z \in \operatorname{Spec} H \quad \Longleftrightarrow \quad 0 \in \operatorname{Spec} F_{P}(z).$$

The map

$$x \longmapsto \begin{pmatrix} x \\ (z - D)^{-1} B^{*} x \end{pmatrix}$$

is an isomorphism from $\operatorname{Ker} F_{P}(z)$ *onto* $\operatorname{Ker}(z - H)$.

Proof. The equation $(z - H)(x, y)^{\mathsf{T}} = 0$ is

$$(z - A)x - By = 0, \qquad -B^{*}x + (z - D)y = 0.$$

The second equation gives $y = (z - D)^{-1} B^{*} x$. Substitution into the first gives $F_{P}(z)x = 0$. The construction is reversible. □

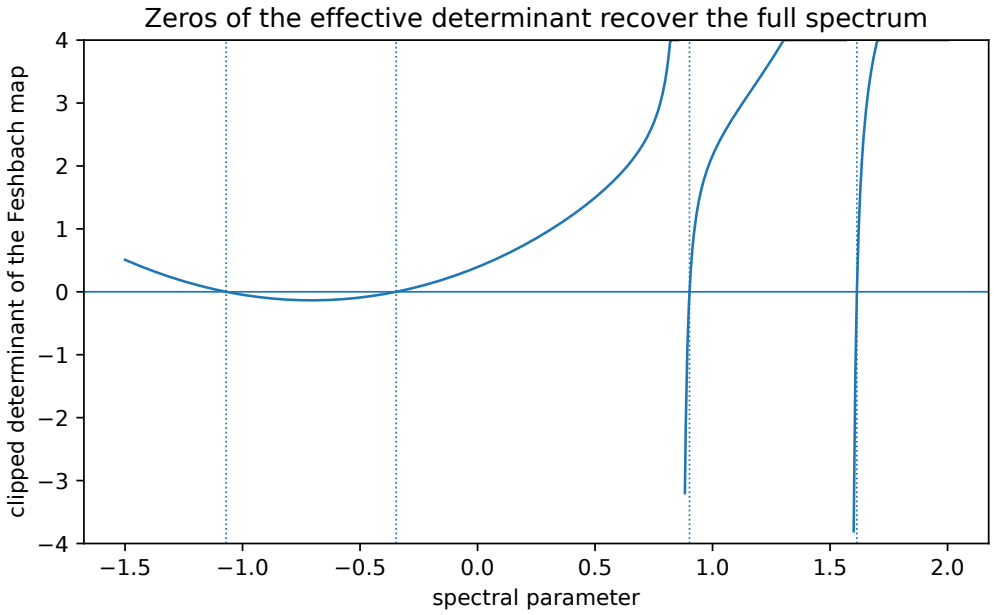


Figure 32. The zeros of the Feshbach determinant recover the eigenvalues of the full finite Hamiltonian away from the hidden spectrum.

Theorem II.9.4 (Upper half plane sign)**.** *If* $\operatorname{Im} z > 0$*, then*

$$\operatorname{Im} \Sigma(z) = -(\operatorname{Im} z) B (z - D)^{-1} (\overline{z} - D)^{-1} B^* \leq 0.$$

Thus $-\Sigma$ *is an operator valued Herglotz function.*

Proof. For $R(z) = (z - D)^{-1}$, the resolvent identity gives

$$R(z) - R(z)^* = (\overline{z} - z) R(z) R(z)^*.$$

Divide by 2i, then multiply the result on the left by B and on the right by B^*. □

Proposition II.9.5 (Uniform self energy bounds)**.** *Let*

$$\delta = \operatorname{dist}(z, \operatorname{Spec} D) > 0, \qquad g = \|B\|.$$

Then

$$\|\Sigma(z)\| \leq \frac{g^2}{\delta}$$

and

$$\|\Sigma'(z)\| \leq \frac{g^2}{\delta^2}.$$

For real E, E' *in an interval at distance at least* δ *from* $\operatorname{Spec} D$*,*

$$\|\Sigma(E) - \Sigma(E')\| \leq \frac{g^2}{\delta^2} |E - E'|.$$

Proof. The self adjoint resolvent satisfies

$$\left\|(z-D)^{-1}\right\| = \frac{1}{\operatorname{dist}(z, \operatorname{Spec} D)}.$$

Differentiate the resolvent to obtain

$$\Sigma'(z) = -B(z-D)^{-2}B^*.$$

Taking operator norms gives the first two estimates. Applying the derivative bound along the real interval gives the final mean value estimate. □

Proposition II.9.6 (Low energy expansion)**.** *Assume D is invertible and $|z|\left\|D^{-1}\right\| < 1$. Then*

$$\Sigma(z) = -\sum_{n=0}^{\infty} z^n B D^{-n-1} B^*$$

with norm convergence. In particular,

$$F_P(z) = z - A + BD^{-1}B^* + O(|z|\,\|B\|^2\left\|D^{-1}\right\|^2).$$

Proof. Write

$$(z-D)^{-1} = -D^{-1}(I - zD^{-1})^{-1} = -\sum_{n=0}^{\infty} z^n D^{-n-1}$$

and multiply on the left by B and on the right by B^*. □

Proposition II.9.7 (Bare truncation error identity)**.** *If both $F_P(z)$ and $z - A$ are invertible, then*

$$P(z-H)^{-1}P - (z-A)^{-1} = F_P(z)^{-1}\Sigma(z)(z-A)^{-1}.$$

Proof. Use the inverse difference identity

$$X^{-1} - Y^{-1} = X^{-1}(Y-X)Y^{-1}$$

with $X = F_P(z)$ and $Y = z - A$. □

II.9.1 Time memory

Write a Schrödinger state as $\psi = x + y$, where $x = P\psi$ and $y = Q\psi$.

Theorem II.9.8 (Exact retained memory equation)**.** *The retained coordinate satisfies*

$$\mathrm{i}\dot{x}(t) = Ax(t) + B\mathrm{e}^{-\mathrm{i}tD}y(0) - \mathrm{i}\int_0^t K(t-s)x(s)\,\mathrm{d}s,$$

where

$$K(t) = B\mathrm{e}^{-\mathrm{i}tD}B^*.$$

For $\operatorname{Re} s > 0$*,*

$$\int_0^\infty \mathrm{e}^{-st}K(t)\,\mathrm{d}t = B(s+\mathrm{i}D)^{-1}B^*.$$

Proof. The hidden equation is

$$\mathrm{i}\dot{y} = B^*x + Dy.$$

Variation of constants gives

$$y(t) = \mathrm{e}^{-\mathrm{i}tD}y(0) - \mathrm{i}\int_0^t \mathrm{e}^{-\mathrm{i}(t-s)D}B^*x(s)\,\mathrm{d}s.$$

Substitute into $\mathrm{i}\dot{x} = Ax + By$. The Laplace formula follows by diagonalizing D or integrating the norm convergent finite dimensional exponential. □

Theorem II.9.9 (Positive definite quantum memory)**.** *The kernel $K(t-s)$ is positive definite. For times $t_1, \dots, t_m$ and retained vectors $v_1, \dots, v_m$,*

$$\sum_{j,k=1}^m \left\langle v_j, K(t_j - t_k)v_k \right\rangle \geq 0.$$

Proof. Set

$$w = \sum_{k=1}^m \mathrm{e}^{\mathrm{i}t_k D}B^*v_k.$$

Then

$$\|w\|^2 = \sum_{j,k} \left\langle B^*v_j, \mathrm{e}^{-\mathrm{i}(t_j - t_k)D}B^*v_k \right\rangle = \sum_{j,k} \left\langle v_j, K(t_j - t_k)v_k \right\rangle.$$

□

Corollary II.9.10 (Finite oscillatory memory expansion)**.** *If*

$$D = \sum_r E_r Q_r$$

is the spectral decomposition of the hidden Hamiltonian, then

$$K(t) = \sum_r \mathrm{e}^{-\mathrm{i}tE_r}BQ_rB^*.$$

Every coefficient BQ_rB^* is positive semidefinite.

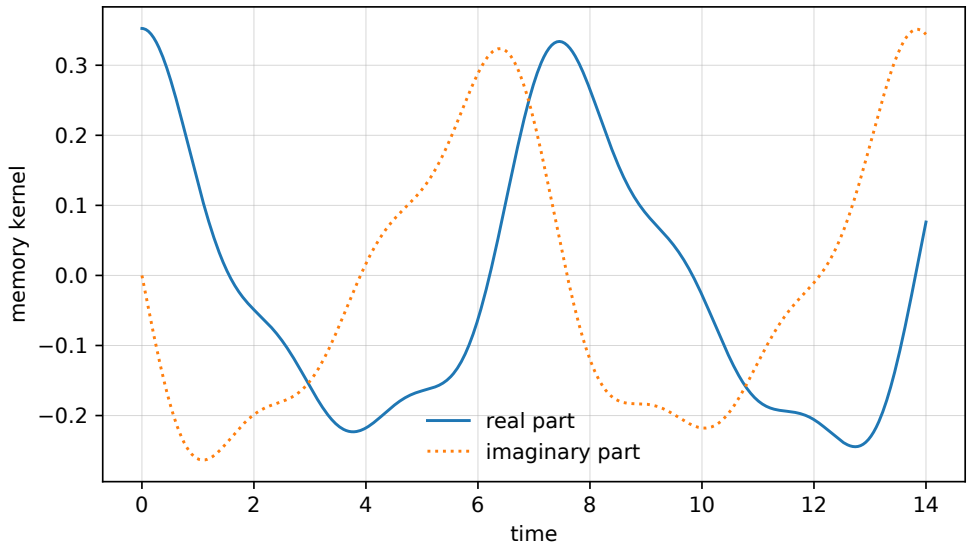


Figure 33. A finite hidden spectrum produces an oscillatory memory kernel. The retained dynamics therefore depend on the history of the retained state.

Proof. Inserting the spectral decomposition into the exponential gives the stated sum. The spectral projectors are positive semidefinite, so multiplication by the coupling and its adjoint preserves positivity of each coefficient. □

Theorem II.9.11 (Exact local closure criterion). *Assume $y(0) = 0$. The retained equation is local and equal to*

$$\mathrm{i}\dot{x} = Ax$$

for every retained initial state exactly when $B = 0$. Equivalently, exact local closure holds exactly when the retained and hidden packets reduce H.

Proof. If $B = 0$, the retained and hidden equations decouple. Conversely, suppose that every solution with $y(0) = 0$ satisfies $x(t) = \mathrm{e}^{-\mathrm{i}tA}x(0)$. The full block equation gives

$$\ddot{x}(0) = -(A^2 + BB^*)x(0),$$

while the declared local equation gives

$$\ddot{x}(0) = -A^2x(0).$$

Since this holds for every retained initial vector, $BB^* = 0$. Hence $B = 0$. □

II.9.2 Stability across models

Theorem II.9.12 (Stability of the self energy)**.** *Let $D = D^*$ and $\widetilde{D} = \widetilde{D}^*$ act on one fixed hidden Hilbert space, and let $B, \widetilde{B}$ map that hidden space to one fixed retained Hilbert space. Define*

$$\Sigma(z) = B(z - D)^{-1}B^*, \qquad \widetilde{\Sigma}(z) = \widetilde{B}(z - \widetilde{D})^{-1}\widetilde{B}^*.$$

Assume

$$\|B\|, \left\|\widetilde{B}\right\| \le g$$

and

$$\operatorname{dist}(z, \operatorname{Spec} D), \operatorname{dist}(z, \operatorname{Spec} \widetilde{D}) \ge \delta > 0.$$

Then

$$\left\|\Sigma(z) - \widetilde{\Sigma}(z)\right\| \le \frac{2g}{\delta}\left\|B - \widetilde{B}\right\| + \frac{g^2}{\delta^2}\left\|D - \widetilde{D}\right\|.$$

Proof. Add and subtract $\widetilde{B}(z - D)^{-1}B^*$ and $\widetilde{B}(z - D)^{-1}\widetilde{B}^*$. The first two differences give the coupling term. For the last, use

$$(z - D)^{-1} - (z - \widetilde{D})^{-1} = (z - D)^{-1}(D - \widetilde{D})(z - \widetilde{D})^{-1}.$$

Apply the resolvent bounds. □

Corollary II.9.13 (Uniform Feshbach control)**.** *For a family represented on fixed retained and hidden Hilbert spaces, with self adjoint hidden Hamiltonians, a common hidden spectral separation δ, and a common coupling bound g, the self energies are uniformly bounded and uniformly Lipschitz on the declared spectral region. If the couplings and hidden Hamiltonians converge in norm, then the self energies converge uniformly there.*

Proof. The common gap and coupling bounds allow proposition II.9.5 and theorem II.9.12 to be applied uniformly across the family. □

This result identifies hypotheses that make Feshbach control uniform in the cutoff. Whether a chosen geometric refinement tower satisfies those hypotheses remains a separate question.

II.10 Euclidean transfer and finite reflection positivity

Let $H = H^*$ on a nonzero finite dimensional Hilbert space and let

$$E_0 = \min \operatorname{Spec} H.$$

For a lattice time step $a > 0$, define

$$T = \mathrm{e}^{-a(H - E_0 I)}.$$

Theorem II.10.1 (Finite Euclidean transfer). *The operator T is positive definite, self adjoint, and contractive. Its spectrum lies in $(0, 1]$, and*

$$T^n = \mathrm{e}^{-na(H - E_0 I)}$$

for every $n \in \mathbb{N}$.

Proof. Diagonalize H. Each eigenvalue of T is

$$\mathrm{e}^{-a(E_j - E_0)}$$

and therefore lies in $(0, 1]$. The power law follows from the functional calculus. □

Theorem II.10.2 (Hamiltonian reconstruction from transfer). *Let T be positive definite, self adjoint, and contractive. Then*

$$H_T = -a^{-1} \log T$$

is a nonnegative self adjoint operator and

$$T^n = \mathrm{e}^{-naH_T}.$$

It is the unique nonnegative self adjoint operator with $T = \mathrm{e}^{-aH_T}$.

Proof. Apply the real logarithm to the positive spectrum of T. The spectral calculus gives existence and the power identity. Injectivity of the scalar exponential on $[0, \infty)$ gives uniqueness. □

Theorem II.10.3 (Finite reflection positivity). *For vectors $v_1, \dots, v_m \in \mathcal{H}$ and nonnegative integers $n_1, \dots, n_m$, the matrix*

$$G_{jk} = \left\langle v_j, T^{n_j + n_k} v_k \right\rangle$$

is positive semidefinite. Equivalently,

$$\sum_{j,k} \overline{c_j} c_k \left\langle v_j, T^{n_j + n_k} v_k \right\rangle \geq 0$$

for every $c \in \mathbb{C}^m$.

Proof. Since T is positive and self adjoint,

$$\left\langle v_j, T^{n_j + n_k} v_k \right\rangle = \left\langle T^{n_j} v_j, T^{n_k} v_k \right\rangle.$$

The quadratic form is the squared norm of

$$\sum_k c_k T^{n_k} v_k.$$

□

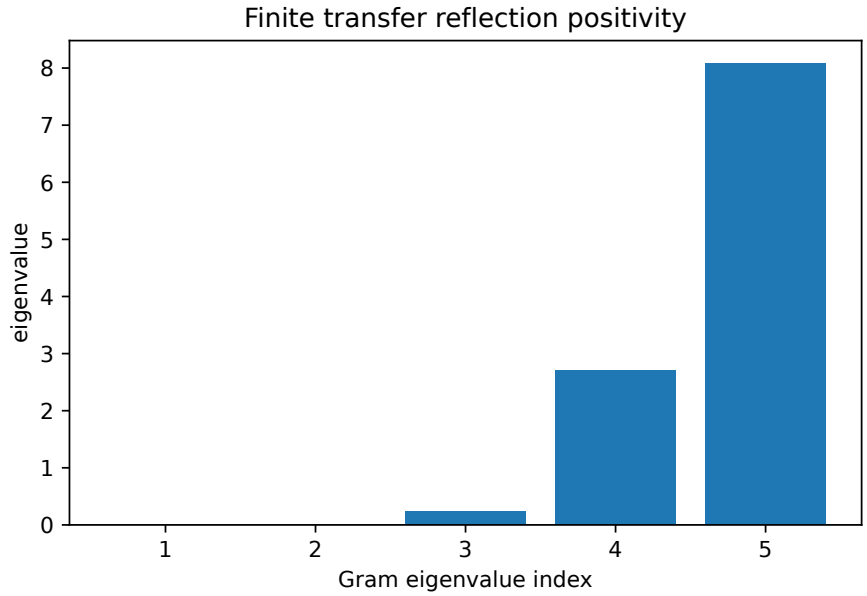


Figure 34. Eigenvalues of a finite reflection positive Gram matrix. Small numerical negative values would signal either roundoff or failure of the transfer assumptions.

Corollary II.10.4 (Reflection positive correlators)**.** *Fix a vector Ω and operators $A_1, \dots, A_m$. The matrix*

$$C_{jk} = \langle A_j \Omega, T^{n_j + n_k} A_k \Omega \rangle$$

is positive semidefinite.

Proof. Apply theorem II.10.3 with $v_j = A_j \Omega$. □

Proposition II.10.5 (Ground packet convergence)**.** *Let P_0 be the spectral projector of H at E_0, and let*

$$\Delta = \min\{E_j - E_0 : E_j > E_0\}.$$

If an excited eigenvalue exists, then

$$\|T^n - P_0\| = \mathrm{e}^{-na\Delta}.$$

Proof. In the spectral decomposition, $T^n - P_0$ has eigenvalues zero on the ground space and $\mathrm{e}^{-na(E_j - E_0)}$ on the excited eigenspaces. The largest is $\mathrm{e}^{-na\Delta}$. □

Proposition II.10.6 (Symmetry resolved transfer)**.** *If $[H, P_a] = 0$ for a complete packet family, then*

$$T = \sum_a P_a T P_a$$

and each reflection positive Gram matrix decomposes as the sum of its packet Gram matrices.

Proof. The functional calculus preserves commutation. Decompose every vector into packet components and use orthogonality. □

Finite reflection positivity is a necessary structural property of transfer data. It is not by itself the continuum Osterwalder Schrader theorem, which also requires a suitable algebra of Euclidean fields, covariance, regularity, clustering, and a controlled continuum limit [19, 20, 10].

II.11 Finite spectral geometry and diffusion dimension

A finite spectral datum consists of a finite dimensional Hilbert space, a nonnegative self adjoint operator L, and any declared packet family. One may take $L = D^2$ for a finite Dirac type operator or a graph Laplacian. Related geometric viewpoints appear in [6, 26].

Definition II.11.1 (Heat trace and spectral dimension)**.** Let the eigenvalues of L be $\lambda_1, \dots, \lambda_N$, with at least one zero eigenvalue. Define

$$Z_L(t) = \mathrm{Tr}(\mathrm{e}^{-tL})$$

and

$$d_L(t) = -2\frac{\mathrm{d}\log Z_L(t)}{\mathrm{d}\log t} = 2t\frac{\mathrm{Tr}(L\mathrm{e}^{-tL})}{\mathrm{Tr}(\mathrm{e}^{-tL})}.$$

Proposition II.11.2 (Finite scale limits)**.** *For every finite nonnegative L with nontrivial kernel,*

$$\lim_{t\downarrow 0} d_L(t) = 0$$

and

$$\lim_{t\to\infty} d_L(t) = 0.$$

For every $t > 0$,

$$0 \le d_L(t) \le 2t\,\|L\|\,.$$

Proof. The formula in definition II.11.1 is twice t times a weighted average of the eigenvalues. This gives the bound and the limit at zero. At large time, the denominator converges to $\dim \mathrm{Ker}\, L$, while every positive eigenvalue contribution in the numerator decays exponentially. □

Thus a finite system cannot have a nonzero spectral dimension at the extreme ultraviolet or infrared ends. A geometric dimension can appear only in a refinement window.

Proposition II.11.3 (Heat packet decomposition)**.** *If $[L, P_a] = 0$ for every packet, then*

$$Z_L(t) = \sum_a Z_{L,a}(t), \qquad Z_{L,a}(t) = \mathrm{Tr}(P_a\mathrm{e}^{-tL}).$$

The global spectral dimension is the average of the packet dimensions weighted by their heat traces:

$$d_L(t) = \sum_{a: Z_{L,a}(t)>0} \frac{Z_{L,a}(t)}{Z_L(t)} d_{L,a}(t),$$

where

$$d_{L,a}(t) = 2t\frac{\mathrm{Tr}(P_aL\mathrm{e}^{-tL})}{Z_{L,a}(t)}$$

for nonempty packet heat traces.

Proof. Commutation gives a block diagonal heat operator. Add the traces and the corresponding first spectral moments, then divide by the total heat trace. □

II.11.1 Periodic lattices

Let $N \geq 2$ and let $\Lambda_N = (\mathbb{Z}/N\mathbb{Z})^d$ be the unit flat torus grid with spacing $1/N$. The standard periodic difference Laplacian has eigenvalues

$$\lambda_N(k) = 4N^2 \sum_{j=1}^{d} \sin^2\left(\frac{\pi k_j}{N}\right),$$

where k runs through centered residue representatives. This is the standard periodic finite difference Laplacian [25].

Theorem II.11.4 (Low mode dispersion in dimension d)**.** *For every centered mode k,*

$$0 \leq 4\pi^2 |k|^2 - \lambda_N(k) \leq \frac{4\pi^4}{3N^2} \sum_{j=1}^{d} k_j^4.$$

Proof. For $x \in [0, \pi/2]$,

$$\sin x \leq x$$

and

$$\sin x \geq x - \frac{x^3}{6}.$$

Thus

$$0 \leq x^2 - \sin^2 x \leq \frac{x^4}{3}.$$

Apply this with $x = \pi |k_j| / N$, multiply by $4N^2$, and sum over j. □

Theorem II.11.5 (Fixed time heat trace convergence)**.** *For every $t > 0$,*

$$\sum_{k \in \Lambda_N^*} \mathrm{e}^{-t\lambda_N(k)} \longrightarrow \sum_{k \in \mathbb{Z}^d} \mathrm{e}^{-4\pi^2 t |k|^2}$$

as $N \to \infty$. The first spectral moments also converge:

$$\sum_{k \in \Lambda_N^*} \lambda_N(k) \mathrm{e}^{-t\lambda_N(k)} \longrightarrow \sum_{k \in \mathbb{Z}^d} 4\pi^2 |k|^2 \mathrm{e}^{-4\pi^2 t |k|^2}.$$

Consequently, the discrete spectral dimensions converge to the continuum torus spectral dimension at every fixed positive time.

Proof. For a fixed integer mode, theorem II.11.4 gives

$$\lambda_N(k) \longrightarrow 4\pi^2 |k|^2.$$

For centered modes, the inequality

$$\sin x \geq \frac{2x}{\pi}, \qquad 0 \leq x \leq \frac{\pi}{2},$$

gives

$$\lambda_N(k) \geq 16 \left|k\right|^2.$$

Also $\lambda_N(k) \leq 4\pi^2 \left|k\right|^2$. Extend the discrete summands by zero outside the centered residue box. The heat trace terms are dominated by

$$\mathrm{e}^{-16t|k|^2},$$

and the moment terms by

$$4\pi^2 \left|k\right|^2 \mathrm{e}^{-16t|k|^2}.$$

Both dominating sequences are summable on $\mathbb{Z}^d$. Dominated convergence proves the two limits. Their quotient gives spectral dimension convergence. □

Standard Fact II.11.6 (Theta transformation)**.** The continuum flat torus heat trace satisfies

$$Z_d(t) = \sum_{k \in \mathbb{Z}^d} \mathrm{e}^{-4\pi^2 t|k|^2} = (4\pi t)^{-d/2} \sum_{n \in \mathbb{Z}^d} \mathrm{e}^{-|n|^2/(4t)}.$$

This is the Poisson summation formula for a Gaussian.

Theorem II.11.7 (Continuum torus small time dimension)**.** *Let*

$$d_{\text{torus}}(t) = -2 \frac{\mathrm{d} \log Z_d(t)}{\mathrm{d} \log t}.$$

Then

$$d_{\text{torus}}(t) = d + O\left(t^{-1} \mathrm{e}^{-1/(4t)}\right)$$

as $t \downarrow 0$.

Proof. By standard fact II.11.6,

$$Z_d(t) = (4\pi t)^{-d/2}(1 + R(t)),$$

where

$$R(t) = \sum_{n \neq 0} \mathrm{e}^{-|n|^2/(4t)} = O(\mathrm{e}^{-1/(4t)}).$$

Differentiation gives

$$tR'(t) = O\left(t^{-1} \mathrm{e}^{-1/(4t)}\right).$$

Substituting this estimate into the logarithmic derivative gives the stated small time expansion. □

Corollary II.11.8 (Rigorous intermediate dimension window)**.** *For every* $\varepsilon > 0$*, there is a diffusion time* $t_\varepsilon > 0$ *and an integer* N_ε *such that*

$$\left|d_{L_N}(t_\varepsilon) - d\right| < \varepsilon$$

for every $N \geq N_\varepsilon$.

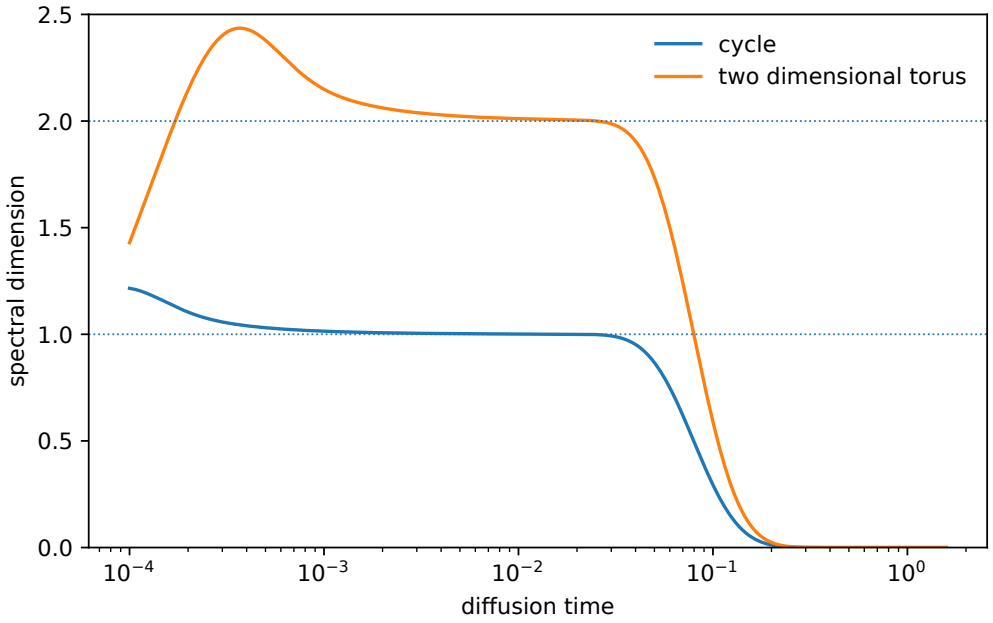


Figure 35. Finite periodic lattices show an intermediate dimension window. The ultraviolet and infrared limits return to zero because the state space is finite.

Proof. Choose t_ε so that theorem II.11.7 is within $\varepsilon/2$ of d. Then apply theorem II.11.5 to choose N_ε so that the discrete spectral dimension is within $\varepsilon/2$ of the continuum value. □

The order of limits matters. Taking $t \downarrow 0$ at fixed N gives zero. Taking $N \to \infty$ at fixed positive t, then taking $t \downarrow 0$, gives the continuum dimension.

II.12 Constraint closure and anomaly packets

Let $C_1, \dots, C_m$ be self adjoint constraint operators on a finite dimensional Hilbert space. The distinction between constraint action and constraint closure is standard in constrained Hamiltonian theory [7, 11]. Write

$$\mathfrak{c} = \operatorname{span}_{\mathbb{C}}\{C_1, \dots, C_m\} \subseteq \operatorname{End}(\mathcal{H}).$$

Definition II.12.1 (Universal closure obstruction)**.** Let

$$q_{\mathfrak{c}} : \operatorname{End}(\mathcal{H}) \longrightarrow \operatorname{End}(\mathcal{H})/\mathfrak{c}$$

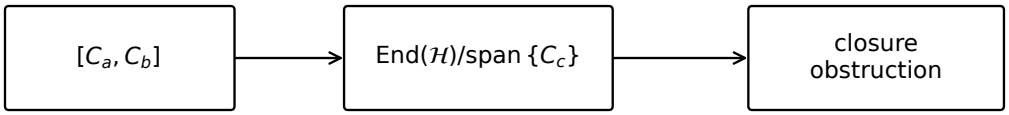
be the quotient map. Define

$$\mathrm{Ob}^{\mathrm{cl}}_{ab} = q_{\mathfrak{c}}([C_a, C_b]).$$

Theorem II.12.2 (Finite constraint closure criterion)**.** *The constraint span* $\mathfrak{c}$ *is closed under commutators exactly when*

$$\mathrm{Ob}^{\mathrm{cl}}_{ab} = 0$$

for all a, b*.*



Compression to the physical kernel is not a closure test for self adjoint constraints.

Figure 36. The closure obstruction lives in a quotient by the constraint span. Physical compression is automatic for self adjoint constraints and cannot replace this quotient.

Proof. The quotient class vanishes exactly when $[C_a, C_b] \in \mathfrak{c}$. This holds for every pair exactly when $\mathfrak{c}$ is a Lie algebra under the commutator. □

If structure coefficients ${f_{ab}}^c$ are prescribed, define the fixed structure anomaly

$$\mathfrak{A}_{ab} = [C_a, C_b] - \mathrm{i} \sum_c {f_{ab}}^c C_c.$$

Exact realization of the prescribed algebra is the stronger condition $\mathfrak{A}_{ab} = 0$.

Proposition II.12.3 (Physical compression is not a closure test)**.** *Let*

$$\mathcal{H}_{\text{phys}} = \bigcap_a \operatorname{Ker} C_a$$

and let P_{phys} be its orthogonal projector. Then

$$P_{\text{phys}}[C_a, C_b]P_{\text{phys}} = 0$$

for every pair a, b, whether or not the constraint span closes.

Proof. Self adjointness and $C_a P_{\text{phys}} = 0$ give $P_{\text{phys}} C_a = 0$. Both terms in the compressed commutator therefore vanish. □

The quotient in definition II.12.1 is needed because closure concerns the operator algebra. Compression to physical states tests only the action on the common kernel, where the constraints already vanish.

Theorem II.12.4 (Invariance of the physical space)**.** *Let $H = H^*$. Suppose*

$$[H, C_a] = \sum_c {b_a}^c C_c$$

for every a. Then H preserves $\mathcal{H}_{\text{phys}}$, and so does $\mathrm{e}^{-\mathrm{i}tH}$ for every real t.

Proof. For $\psi \in \mathcal{H}_{\text{phys}}$,

$$C_a H\psi = HC_a\psi - [H, C_a]\psi = 0.$$

Thus $H\psi \in \mathcal{H}_{\text{phys}}$. The exponential preserves every invariant finite dimensional subspace. □

II.12.1 Constraint refinement

Let $(\mathcal{H}_\ell, C_{\ell,a})$ and $(\mathcal{H}_{\ell+1}, C_{\ell+1,a})$ be two levels, and let

$$R_\ell : \mathcal{H}_\ell \longrightarrow \mathcal{H}_{\ell+1}$$

be an isometry.

Theorem II.12.5 (Exact constraint transport)**.** *Assume*

$$C_{\ell+1,a} R_\ell = R_\ell C_{\ell,a}$$

for every a. Then

$$[C_{\ell+1,a}, C_{\ell+1,b}] R_\ell = R_\ell [C_{\ell,a}, C_{\ell,b}].$$

If the same structure coefficients are used at both levels, then

$$\mathfrak{A}_{\ell+1,ab} R_\ell = R_\ell \mathfrak{A}_{\ell,ab}.$$

The isometry maps coarse physical states into fine physical states.

Proof. Apply the intertwining identity twice to each product in the commutator. The anomaly identity follows by subtracting the same linear combination of constraints. If $C_{\ell,a}\psi = 0$, then

$$C_{\ell+1,a} R_\ell \psi = R_\ell C_{\ell,a}\psi = 0.$$

□

Proposition II.12.6 (Approximate constraint transport)**.** *Assume*

$$\|C_{\ell+1,a} R_\ell - R_\ell C_{\ell,a}\| \le \varepsilon_a$$

and

$$\|C_{\ell,a}\|, \|C_{\ell+1,a}\| \le M.$$

Then a coarse physical unit vector ψ satisfies

$$\|C_{\ell+1,a} R_\ell \psi\| \le \varepsilon_a.$$

Also,

$$\begin{aligned}\|[C_{\ell+1,a}, C_{\ell+1,b}] R_\ell - R_\ell [C_{\ell,a}, C_{\ell,b}]\| \\ \le 2M(\varepsilon_a + \varepsilon_b).\end{aligned}$$

Proof. The first claim follows by applying the intertwining defect to ψ. Write

$$E_a = C_{\ell+1,a} R_\ell - R_\ell C_{\ell,a}.$$

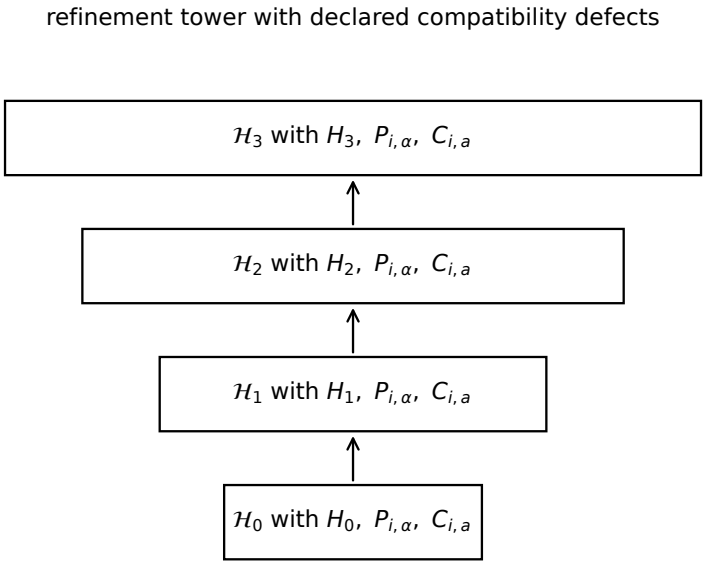


Figure 37. A refinement tower carries Hamiltonians, packets, constraints, and transfer data. Each family has its own compatibility defect.

Expanding the two commutators gives four error terms:

$$E_a C_{\ell,b}, \quad C_{\ell+1,a} E_b, \quad -E_b C_{\ell,a}, \quad -C_{\ell+1,b} E_a.$$

The triangle inequality and the stated bounds on the constraints and defects give the claimed estimate. □

Approximate transport controls finite violations. It does not turn a nonzero anomaly into an exact continuum algebra without a limit theorem and a common operator domain.

II.13 Quantum refinement towers

Definition II.13.1 (Finite quantum refinement tower)**.** A finite quantum refinement tower consists of Hilbert spaces $\mathcal{H}_\ell$, isometries

$$R_\ell : \mathcal{H}_\ell \longrightarrow \mathcal{H}_{\ell+1},$$

self adjoint Hamiltonians H_ℓ, packet projectors $P_{\ell,a}$, constraints $C_{\ell,r}$, and positive transfer operators T_ℓ. Exact compatibility means that every declared object intertwines with R_ℓ. Approximate compatibility is recorded by the corresponding operator norm defects.

II.13.1 Exact bounded direct limits

Let $\mathcal{H}_\infty$ be the Hilbert direct limit of the isometric system, and let

$$\iota_\ell : \mathcal{H}_\ell \longrightarrow \mathcal{H}_\infty$$

be the canonical isometries.

Theorem II.13.2 (Bounded Hamiltonian direct limit)**.** *Assume*

$$H_{\ell+1} R_\ell = R_\ell H_\ell$$

and

$$\sup_\ell \|H_\ell\| < \infty.$$

Then there is a unique bounded self adjoint operator H_∞ on $\mathcal{H}_\infty$ such that

$$H_\infty \iota_\ell = \iota_\ell H_\ell$$

for every ℓ. It satisfies

$$\mathrm{e}^{-\mathrm{i}tH_\infty} \iota_\ell = \iota_\ell \mathrm{e}^{-\mathrm{i}tH_\ell}$$

and

$$\mathrm{e}^{-tH_\infty} \iota_\ell = \iota_\ell \mathrm{e}^{-tH_\ell}$$

when the Hamiltonians are nonnegative.

Proof. Define H_∞ on the algebraic union of the embedded levels by

$$H_\infty \iota_\ell x = \iota_\ell H_\ell x.$$

Compatibility makes the definition independent of the chosen level. The uniform norm bound makes the operator bounded on the dense union, so it extends uniquely to the completion. It is symmetric because every H_ℓ is self adjoint. A bounded symmetric operator defined on the whole Hilbert space is self adjoint. The functional calculus intertwining follows first for polynomials and then for exponentials by uniform convergence. □

Theorem II.13.3 (Exact packet direct limit)**.** *Assume the packet families have one fixed finite address set at every level and each packet address a is compatible in the sense*

$$P_{\ell+1,a} R_\ell = R_\ell P_{\ell,a}.$$

Then there is an orthogonal projector $P_{\infty,a}$ on $\mathcal{H}_\infty$ satisfying

$$P_{\infty,a} \iota_\ell = \iota_\ell P_{\ell,a}.$$

Finite completeness and orthogonality pass to the direct limit.

Proof. Use the same construction as in theorem II.13.2. Every projector has norm at most one, so no additional boundedness assumption is needed. The projector identities hold on the dense algebraic union and hence on the completion. □

II.13.2 Norm summable approximation

The next theorem places all approximating Hamiltonians on a common Hilbert space. It applies to bounded effective Hamiltonians. An unbounded field Hamiltonian requires a different convergence argument.

Theorem II.13.4 (Norm summable Hamiltonian tower)**.** *Let (H_n) be bounded self adjoint operators on one Hilbert space and assume*

$$\sum_{n=0}^{\infty} \|H_{n+1} - H_n\| < \infty.$$

Then H_n converges in norm to a bounded self adjoint operator H. For every $T > 0$,

$$\sup_{|t|\le T} \left\| \mathrm{e}^{-\mathrm{i}tH_n} - \mathrm{e}^{-\mathrm{i}tH} \right\| \le T \, \|H_n - H\| .$$

If every $H_n \ge 0$, then

$$\sup_{0\le t\le T} \left\| \mathrm{e}^{-tH_n} - \mathrm{e}^{-tH} \right\| \le T \, \|H_n - H\| .$$

Proof. The summability condition makes (H_n) Cauchy in operator norm. The limit is self adjoint. Duhamel's identity gives

$$\mathrm{e}^{-\mathrm{i}tH_n} - \mathrm{e}^{-\mathrm{i}tH} = -\mathrm{i} \int_0^t \mathrm{e}^{-\mathrm{i}(t-s)H_n} (H_n - H) \mathrm{e}^{-\mathrm{i}sH} \, \mathrm{d}s.$$

Both unitary factors have norm one, which gives the first estimate. The same argument gives the Euclidean estimate because the semigroups generated by nonnegative Hamiltonians are contractions. □

Corollary II.13.5 (Limit of packet leakage)**.** *Let P_n be orthogonal projectors and H_n bounded self adjoint operators on one Hilbert space, with $P_n \to P$ and $H_n \to H$ in norm. Then for every bounded time interval,*

$$(I - P_n)\mathrm{e}^{-\mathrm{i}tH_n} P_n \longrightarrow (I - P)\mathrm{e}^{-\mathrm{i}tH} P$$

uniformly in time.

Proof. Add and subtract terms so that one factor changes at a time. The projector terms converge uniformly because $P_n \to P$ in norm. Duhamel's identity gives

$$\sup_{|t|\le T} \left\| \mathrm{e}^{-\mathrm{i}tH_n} - \mathrm{e}^{-\mathrm{i}tH} \right\| \le T \, \|H_n - H\| ,$$

which proves uniform convergence of the middle factor. □

Theorem II.13.6 (Reflection positivity is closed under limits)**.** *Suppose $C_n(j,k)$ are reflection positive kernels on $\mathbb{N}$, meaning every finite matrix*

$$(C_n(j_r, j_s))_{r,s}$$

is positive semidefinite. If

$$C_n(j,k) \longrightarrow C(j,k)$$

for every pair, then C is reflection positive.

Proof. For a fixed finite set of times and coefficients, the corresponding quadratic forms are nonnegative and converge to the quadratic form of C. The limit is nonnegative. □

Theorem II.13.7 (Constraint closure under norm convergence)**.** *Let $C_{n,a} \to C_a$ in norm for every a, and fix structure coefficients ${f_{ab}}^c$. If*

$$\left\| [C_{n,a}, C_{n,b}] - \mathrm{i} \sum_c {f_{ab}}^c C_{n,c} \right\| \longrightarrow 0,$$

then

$$[C_a, C_b] = \mathrm{i} \sum_c {f_{ab}}^c C_c.$$

Proof. Operator multiplication and the commutator are continuous in operator norm. Pass to the limit in the anomaly identity. □

Theorem II.13.8 (Heat trace convergence from trace norm)**.** *Let L_n, L be nonnegative self adjoint operators on one Hilbert space. For a fixed $t > 0$, assume their heat operators are trace class and that*

$$\mathrm{e}^{-tL_n} \longrightarrow \mathrm{e}^{-tL}$$

in trace norm. Then

$$\mathrm{Tr}(\mathrm{e}^{-tL_n}) \longrightarrow \mathrm{Tr}(\mathrm{e}^{-tL}).$$

If also the heat moment operators are trace class and

$$L_n \mathrm{e}^{-tL_n} \longrightarrow L\mathrm{e}^{-tL}$$

in trace norm and the limiting heat trace is nonzero, then the spectral dimensions defined by the heat moment ratio converge at that time.

Proof. The trace is continuous in trace norm. Apply this to the heat operators and to the first heat moments, then take the quotient in definition II.11.1. □

Remark II.13.9. The theorems above produce bounded continuum Hamiltonians. A physically useful continuum Hamiltonian is often unbounded. Its construction generally requires strong resolvent convergence, convergence of closed quadratic forms, or another method that controls operator domains [13, 21]. None of those conclusions follows from finite matrix convergence without additional hypotheses.

II.14 Continuum milestones and exact boundary

The finite theorems establish exact identities and criteria for bounded limits. Passing from a finite transfer model to a continuum theory still requires several separate arguments. This section states those remaining mathematical tasks.

Definition II.14.1 (Anomaly free continuum constraint system)**.** A continuum constraint system consists of a Hilbert space, a common invariant dense domain $\mathcal{D}$, and operators C_a on $\mathcal{D}$. It is anomaly free for prescribed structure coefficients when

$$[C_a, C_b]\psi = \mathrm{i}\sum_c f_{ab}{}^c C_c \psi$$

for every $\psi \in \mathcal{D}$, and when the associated gauge evolution is defined on the physical quotient or physical subspace.

Norm closure of bounded finite constraints, as in theorem II.13.7, is one special case. It does not treat unbounded constraints, changing domains, structure functions, or renormalized operator products.

Definition II.14.2 (Reflection positive Euclidean limit)**.** A reflection positive Euclidean limit requires a limiting algebra of observables, Euclidean time translations, a reflection operation, and correlation functions whose reflected quadratic forms are nonnegative. A field theoretic reconstruction also requires the regularity and covariance assumptions needed to construct a Hilbert space, a vacuum, and a self adjoint time translation generator.

Theorem II.13.6 shows that positivity of each fixed finite Gram matrix survives pointwise convergence. It does not prove existence, locality, clustering, or the remaining Osterwalder Schrader axioms.

Definition II.14.3 (Einstein infrared criterion)**.** A quantum geometric tower meets an Einstein infrared criterion only if an effective action is controlled at long wavelengths and has an expansion whose leading geometric terms take the form

$$\Gamma_{\mathrm{eff}}[g] = \int \sqrt{|g|}\left(\Lambda + \frac{1}{16\pi G}R + \text{controlled higher order terms}\right)\mathrm{d}^d x.$$

Here the volume coefficient includes the sign and normalization written explicitly in the cosmological term in Part I. The expansion must respect the limiting gauge identities and must include an estimate for the omitted terms on the declared infrared regime.

A spectral dimension close to four does not imply this criterion. A heat trace records eigenvalue growth. It does not determine the tensor structure, gauge identities, sign, or interaction coefficients of an effective action.

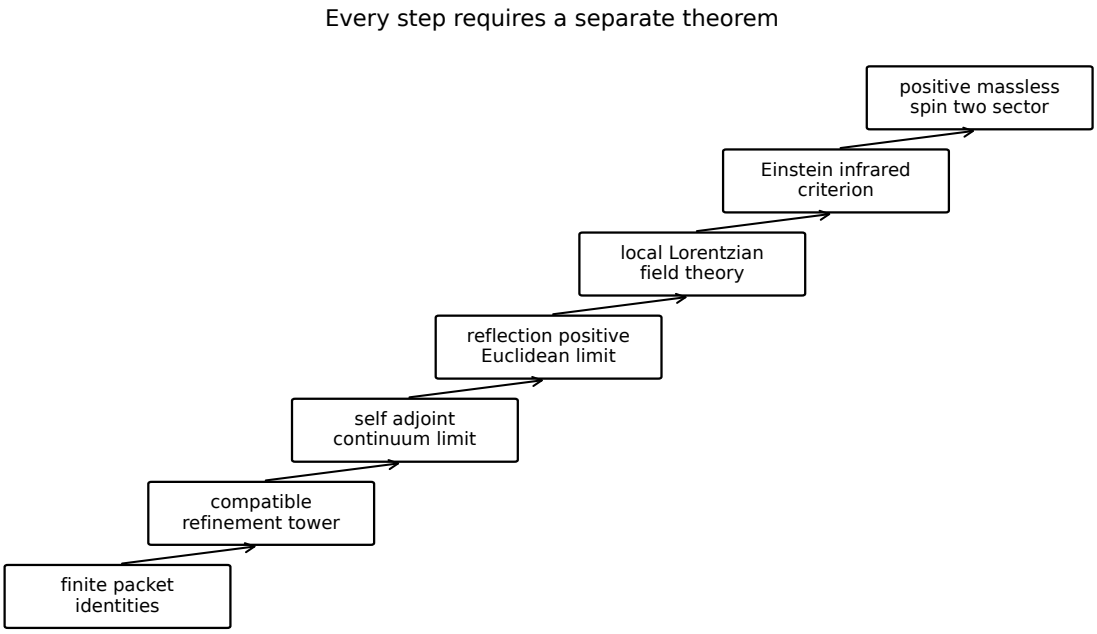


Figure 38. The finite identities occupy the first step. Every later step needs a separate convergence or reconstruction theorem.

Definition II.14.4 (Massless spin two criterion)**.** A positive massless spin two sector requires a physical two point function or resolvent with a massless pole in the transverse traceless sector, positive residue on physical states, absence of negative norm modes, and compatibility with the limiting gauge constraints. Interactions must preserve the constraint structure.

A low energy eigenvalue, a spectral dimension plateau, or a finite rank two tensor packet does not establish a massless spin two particle.

II.15 Conclusion

A complete packet family gives one coordinate language for finite quantum structure. Group characters produce symmetry packets. Charged operators obey exact selection rules. Circuits become coherent sums over packet paths. The canonical moving connection separates geometric transport from physical mixing. Density matrices and channels use two sided packets, while channel covariance becomes block preservation on operator space and symmetry of the Choi matrix.

Compression to a code gives a natural error correction obstruction. Its vanishing is the Knill Laflamme condition. Diagonalizing the resulting coefficient matrix produces orthogonal syndrome packets and an exact recovery on the error span. Schur Feshbach elimination gives an equally exact description of hidden Hamiltonian packets. Their frequency response is the self energy, and their time response is a positive definite memory kernel.

Positive Euclidean transfer gives finite reflection positivity. Periodic lattice heat traces converge to the continuum torus at every fixed positive diffusion time, and the continuum small time spectral dimension is recovered after the refinement limit. Constraint closure is measured by a quotient of operator space, not by compression to the physical kernel.

Milestone	Finite result available here	Missing continuum input
Symmetry and constraints	exact packets and quotient obstruction	common unbounded domain and renormalized closure
Effective dynamics	exact Feshbach map and uniform gap bounds	cutoff independent spectral separation and locality
Euclidean transfer	positive finite transfer and finite reflection positivity	convergent Euclidean fields and reconstruction axioms
Spectral dimension	lattice heat trace convergence	relation to a physical metric and interacting observables
Lorentzian theory	bounded unitary direct limits	unbounded generator, causality, locality, and field algebra
Einstein regime	a definition of the required expansion	derivation and error control for the effective action
Spin two sector	a precise spectral criterion	positive physical pole and interaction consistency

Table 3. What the finite results establish and what remains outside the article.

The theorems for bounded towers show how exact compatibility and summable differences in operator norm produce limiting quantum evolutions. Their hypotheses also mark the scope of the argument. Unbounded field Hamiltonians, continuum gauge constraints, reflection positive field measures, the Einstein infrared action, and a massless spin two sector each require additional theorems. The finite packet calculus gives a common framework in which those questions can be stated and studied, while leaving their physical resolution open.

Part III Mathematical proof completions and retained derivations

A route through this section

The six supplements retain the substantive algebra and geometry of the formal completion. The final supplement constructs local range-bundle charts, their overlaps, and a fiber-valued connection. Three earlier derivations follow because they offer a distinct route through the same finite mathematics.

III.1 Exact packets and arbitrary circuit length

Let R be a unital ring, not necessarily commutative, and let I be a finite address set. An exact packet family consists of elements $P_a \in R$ satisfying

$$P_a P_b = \begin{cases} P_a, & a = b, \\ 0, & a \neq b, \end{cases} \qquad \sum_{a \in I} P_a = 1.$$

Adjoint conditions are added when needed. For an operator U, define the transfer corner

$$U_{ba} = P_b U P_a.$$

The target index comes first. Completeness and distributivity give

$$\sum_{b,a} U_{ba} = U, \qquad (UV)_{ba} = \sum_c U_{bc} V_{ca}.$$

The second identity uses $P_c^2 = P_c$ when adjacent transfer corners are multiplied.

III.1.1 Circuit paths: source Theorem 4.1

For $U = U_m \cdots U_1$, the checked result is

$$P_{a_m} U P_{a_0} = \sum_{a_1, \ldots, a_{m-1}} P_{a_m} U_m P_{a_{m-1}} \cdots P_{a_1} U_1 P_{a_0}.$$

The Lean implementation defines a recursive path sum and proves the identity by induction over an arbitrary finite gate list. It is not restricted to a fixed circuit depth. The empty list has circuit operator 1 and path value $P_b P_a$. Summing the source and target indices reconstructs the full circuit.

III.1.2 Adjoint conservation: source Theorem 4.2

Assume a star operation with $P_a^* = P_a$. Then

$$(U_{ba})^* = P_a U^* P_b.$$

The two checked conservation laws are

$$U^*U = 1 \quad \Longrightarrow \quad \sum_b (U_{ba})^* U_{bc} = \delta_{ac} P_a,$$
$$UU^* = 1 \quad \Longrightarrow \quad \sum_a U_{ba} (U_{da})^* = \delta_{bd} P_b.$$

For the first law, expand each corner, collapse P_b^2 and sum:

$$\sum_b P_a U^* P_b U P_c = P_a U^* \left(\sum_b P_b \right) U P_c = P_a P_c.$$

The second law follows by the analogous calculation and has its own formal proof. For complex matrices, the adjoint is the conjugate transpose. The order of the operator products is preserved throughout.

III.2 Symmetry and measurement

III.2.1 Exact symmetry: source Theorem 5.1

If $HP_a = P_a H$ for every packet, then

$$P_b H P_a = 0 \quad (b \neq a), \qquad H = \sum_a P_a H P_a.$$

In a complex Banach algebra, commutation also propagates to the actual exponential:

$$e^{zH} P_a = P_a e^{zH} \qquad (z \in \mathbb{C}).$$

Consequently,

$$e^{zH} = \sum_a P_a e^{zH} P_a, \qquad P_b e^{zH} P_a = 0 \quad (b \neq a).$$

Taking $z = -it$ gives evolution in real time. The Lean proof applies the exponential commutation theorem directly, so invariance of the packets is a proved consequence of commutation. Self-adjointness of H is not needed for the algebraic reducing property, so this result applies more broadly than the Hermitian specialization in the paper.

This result describes exact symmetry. The quantitative leakage estimate when symmetry is broken appears in Theorem 5.2 and requires the separate Duhamel and norm arguments developed later.

III.2.2 Measurements: source Theorem 7.1

For finite complex matrices, define packet dephasing by

$$\mathcal{D}_P(X) = \sum_a P_a X P_a.$$

The code proves idempotence and trace duality:

$$\mathcal{D}_P(\mathcal{D}_P(X)) = \mathcal{D}_P(X), \qquad \operatorname{tr}(\mathcal{D}_P(E)\rho) = \operatorname{tr}(E\mathcal{D}_P(\rho)).$$

Trace duality follows term by term from cyclicity:

$$\operatorname{tr}(P_a E P_a \rho) = \operatorname{tr}(E P_a \rho P_a).$$

Therefore an effect that is diagonal in the packets, $\mathcal{D}_P(E) = E$, satisfies

$$\boxed{\operatorname{tr}(E\rho) = \operatorname{tr}(E\mathcal{D}_P(\rho)).}$$

The proof holds for arbitrary finite complex matrices E and ρ. Density matrices and positive measurement effects are valid specializations rather than assumptions needed for this trace identity. Taking $E = 1$ also gives trace preservation of packet dephasing.

The full theorem for Kraus channels and the Knill–Laflamme recovery criterion require further arguments about positivity, auxiliary systems, and recovery maps. The trace identity above supplies only the measurement statement.

III.3 Corrected Feshbach resolvent

Write a finite complex matrix in retained and eliminated coordinates:

$$H = \begin{pmatrix} A & B \\ C & D \end{pmatrix}, \qquad zI - H = \begin{pmatrix} zI_P - A & -B \\ -C & zI_Q - D \end{pmatrix}.$$

Set

$$D_z = zI_Q - D, \qquad S_z = zI_P - A - BD_z^{-1}C.$$

The effective Hamiltonian is $H_{\text{eff}}(z) = A + BD_z^{-1}C$, so $S_z = zI_P - H_{\text{eff}}(z)$.

III.3.1 Correct statement: source Theorem 9.1

Assume both D_z and $zI - H$ are invertible. Then S_z is invertible and

$$\boxed{\left((zI - H)^{-1}\right)_{PP} = S_z^{-1}.}$$

The left side is the submatrix of the full inverse on the retained coordinates. This matches the paper's compressed operator when written in an orthonormal basis of the retained subspace. The proof is valid for arbitrary complex blocks of compatible sizes and does not require Hermiticity.

The checked invertibility criterion is

$$D_z \text{ invertible} \quad \Longrightarrow \quad (zI - H \text{ invertible} \iff S_z \text{ invertible}).$$

Thus one may equivalently assume invertibility of D_z and S_z.

Why the original assumption is insufficient. Take $z = 0$ and $H = \operatorname{diag}(0, -1)$, retaining the first coordinate. Then

$$D_z = 1, \qquad zI - H = \begin{pmatrix} 0 & 0 \\ 0 & 1 \end{pmatrix}.$$

The eliminated block is invertible, but the full matrix is singular. Hence the original hypothesis does not ensure the existence of its stated resolvent. The Lean counterexample proves invertibility of the scalar 1 and noninvertibility of this full 2×2 matrix.

III.3.2 Provenance and limits

The proof of the general block inverse was reused from the checked fifth block of Paper VI and compiled in the Paper VII namespace for the archived formal checkpoint. That formal development also added the counterexample above. The retained checkpoint is dated 6 September 2026. This edition revises the exposition without claiming a new Schur identity or a fresh Lean compilation.

The memory equation in the time domain in Section 9.2, resolvent control uniform in the cutoff, and continuum limits require arguments beyond this finite inverse identity. The source amendment makes the two invertibility assumptions explicit without changing the intended effective Hamiltonian.

III.4 Dispersion with an explicit spacing condition

The grid eigenvalue in source Theorem 11.1 is

$$\lambda_{k,h} = \frac{4}{h^2} \sin^2\left(\frac{kh}{2}\right).$$

The original low-mode condition is $0 \le kh/2 \le 1$. A nonzero spacing is also required for the quotient to have its intended meaning. For a physical grid, one normally takes $h > 0$.

III.4.1 Checked stronger statement

For every $k, h \in \mathbb{R}$ with $h \neq 0$,

$$\boxed{0 \le k^2 - \lambda_{k,h} \le \frac{k^4 h^2}{12}.}$$

The code proves this without the low-mode restriction. The bound may be loose away from the low-mode regime, but it remains valid.

The proof begins with an estimate valid for every real argument:

$$0 \le x^2 - \sin^2 x \le \frac{x^4}{3}.$$

The lower bound follows from $|\sin x| \le |x|$. For the upper bound, use

$$|x - \sin x| \le \frac{|x|^3}{6}, \qquad |x + \sin x| \le 2|x|.$$

Factoring the difference of squares gives

$$0 \le x^2 - \sin^2 x = |x - \sin x|\,|x + \sin x| \le \frac{x^4}{3}.$$

With $x = kh/2$ and $h \neq 0$,

$$k^2 - \lambda_{k,h} = \frac{4}{h^2}\left(x^2 - \sin^2 x\right),$$
$$\frac{4}{h^2}\frac{x^4}{3} = \frac{k^4 h^2}{12}.$$

Every algebraic transformation and inequality in the active source was accepted by Lean.

III.4.2 What this does not establish

This is an exact deterministic error bound for the displayed dispersion relation. The original paper's numerical convergence experiment and spectral dimension measurements provide a different kind of evidence and were not rerun during this prose revision. The bound alone does not select a physical spacetime geometry.

III.5 A constraint diagnostic that vanishes automatically

Section 12 defines the physical projector using the exact common kernel of the constraints. In finite dimensions this gives $C_a P = 0$ for every a. Absorb the factor i and any structure coefficient into f_c, and write

$$\mathcal{A}_{ab} = C_a C_b - C_b C_a - \sum_c f_c C_c.$$

Proposition III.5.1 (Exact common-kernel compression)**.** *If $C_c P = 0$ for every c, then*

$$\mathcal{A}_{ab} P = 0, \qquad P \mathcal{A}_{ab} P = 0.$$

No idempotence or adjoint property of P is needed for this implication.

Proof. Associativity gives

$$\mathcal{A}_{ab} P = C_a(C_b P) - C_b(C_a P) - \sum_c f_c (C_c P) = 0.$$

Left multiplication by P gives the second identity. □

III.5.1 Compressed vanishing without operator closure

Over the rationals, take

$$P = \begin{pmatrix} 1 & 0 & 0 \\ 0 & 0 & 0 \\ 0 & 0 & 0 \end{pmatrix}, \quad X = \begin{pmatrix} 0 & 0 & 0 \\ 0 & 0 & 1 \\ 0 & 1 & 0 \end{pmatrix}, \quad Z = \begin{pmatrix} 0 & 0 & 0 \\ 0 & 1 & 0 \\ 0 & 0 & -1 \end{pmatrix}.$$

These displayed matrices are symmetric. The code checks that $P^2 = P$, $P \neq 0$ and $XP = ZP = 0$, but

$$[X, Z] = \begin{pmatrix} 0 & 0 & 0 \\ 0 & 0 & -2 \\ 0 & 2 & 0 \end{pmatrix} \neq 0, \qquad P[X, Z]P = 0.$$

The commutator therefore violates the closure relation with zero structure coefficients outside the physical range, even though its physical compression vanishes exactly.

III.5.2 Interpretation for the paper

Vanishing of the compressed anomaly is automatic for the exact finite common kernel. It therefore cannot by itself certify full operator closure. A nonzero computed compression would instead contradict those exact assumptions or expose an approximation or implementation defect.

Existence of a nontrivial compatible refinement tower and the broader continuum program remain separate questions. A stronger closure claim must test more than this compression, and unbounded constraints need their operator domains specified. This audit is additional to the six checked source items and is not counted as a seventh original theorem.

III.6 One seed for the computational basis

Manuscript item 2.4. `ComputationalSeed.lean` 14 declarations

For $n \geq 0$, let

$$A_n = (\mathbb{Z}/2\mathbb{Z})^{\{0,\ldots,n-1\}}, \qquad V_n = \{v : A_n \to \mathbb{C}\}.$$

For an address $a \in A_n$, define the standard coordinate vector

$$|a\rangle\,(x) = \begin{cases} 1 & x = a, \\ 0 & x \neq a. \end{cases}$$

The seed is $\psi_0 = |0\rangle$. Define a translation operator by

$$(T_a v)(x) = v(x - a).$$

At position j, the local Pauli X is $X_j = T_{e_j}$, where e_j has a single nonzero binary coordinate. The formal circuit uses the identity when $a_j = 0$ and X_j when $a_j = 1$.

Supplementary statement. For every binary address a,

$$W_a = \prod_{j=0}^{n-1} X_j^{a_j} = T_a, \qquad W_a \psi_0 = |a\rangle\,.$$

The family $(W_a\psi_0)_{a\in A_n}$ is linearly independent, spans V_n, and has exactly 2^n elements. It is the standard computational basis.

Proof. Composition gives $T_aT_b = T_{a+b}$, and direct evaluation gives $T_a|b\rangle = |a+b\rangle$. Every binary address satisfies $a + a = 0$, so each translation is an involution. In particular, the local operator changes precisely the addressed bit:

$$X_j|a\rangle = \big|a \text{ with coordinate } j \text{ replaced by } a_j + 1\big\rangle .$$

The selected factor at j equals translation by the address supported at j with value a_j. Induction on a list proves that the product of translations is translation by their sum. Each of these addresses contributes one coordinate, and their sum is a. Thus $W_a = T_a$ and $W_a\psi_0 = |a\rangle$.

Lean identifies the resulting family with `Pi.basisFun` over $\mathbb{C}$. Its standard basis theorems supply linear independence and full span. The finite function-space cardinality gives $|A_n| = 2^n$. □

Formal scope. The proof constructs the sequence of gates that produces each addressed state and then identifies the resulting family with the standard coordinate basis. It includes the empty circuit for $n = 0$. Orthogonality belongs to the usual computational basis interpretation. The formal endpoint records the basis identification, together with separate explicit theorems for span and linear independence.

III.7 Tensor and polyphase refinement

Manuscript item 3.2. `TensorRefinement.lean` 11 declarations

Let F be an arbitrary finite set of factors and let D_i be a finite coordinate index for factor i. For matrix families A_i, define the coordinate tensor product on the product index space by

$$\mathsf{T}(A)(x, y) = \prod_{i\in F} A_i(x_i, y_i).$$

The proof first establishes the laws for multiplication, identity, adjoints, and finite sums. These laws apply to any finite number of factors with the stated finite coordinate sets.

Suppose $N > 0$ and each factor has a complete orthogonal self-adjoint projector family $(P_j^{(i)})_{j\in\mathbb{Z}/N\mathbb{Z}}$. For a fine address $a : F \to \mathbb{Z}/N\mathbb{Z}$, set

$$Q_a = \mathsf{T}(i \mapsto P_{a_i}^{(i)}), \qquad C_r = \sum_{\sum_i a_i = r} Q_a.$$

Supplementary statement. The fine and coarse families are complete orthogonal self-adjoint projector systems. In particular,

$$C_rC_s = \delta_{rs}C_r, \qquad \sum_r C_r = I, \qquad C_r^* = C_r.$$

Each coarse projector is exactly the displayed sum of its fine descendants.

Proof. Expanding the finite product of sums gives

$$\mathsf{T}(A)\mathsf{T}(B) = \mathsf{T}(i \mapsto A_iB_i).$$

Consequently, if two fine addresses differ in any coordinate, the corresponding product contains a zero factor. If the addresses agree, the product is the same fine projector. The adjoint passes through

the finite coordinate product, so $Q_a^* = Q_a$. Summing over all address functions and using the same expansion yields

$$\sum_a Q_a = \mathsf{T}\left(i \mapsto \sum_j P_j^{(i)}\right) = I.$$

A separate algebraic regrouping theorem applies to any finite orthogonal family and any address map into a finite set. In the double sum for $C_r C_s$, orthogonality removes all terms with different fine addresses. A surviving address can lie in both classes only when $r = s$. Completeness follows by summing each fine projector exactly once. Adjoint preservation follows term by term. Specializing the address map to total residue proves the claim. □

Formal scope. Residue grouping is proved for every positive modulus and arbitrary finite factor dimensions. It assumes the supplied local projector laws. Constructing those local projectors from cyclic characters, as in item 3.1, requires the separate proof in the next supplement.

III.8 Differentiated moving coordinates

Manuscript item 6.1. `MovingFrames.lean` 9 declarations

Fix a real time t and a finite complex coordinate space. Let $U(s)$ be a unitary matrix curve, differentiable entrywise at t, and let $\psi(s)$ be differentiable componentwise at t. Write $\dot{U}$ and $\dot{\psi}$ for those derivatives. Suppose

$$i\dot{\psi} = H\psi(t).$$

Only the value of the Hamiltonian at the chosen time is needed. No derivative of H is assumed.

Supplementary statement. The explicitly defined coordinate curve

$$y(s) = U(s)^*\psi(s)$$

is differentiable at t, with

$$\dot{y} = \dot{U}^*\psi(t) + U(t)^*\dot{\psi}.$$

It satisfies

$$\boxed{i\dot{y} = H_{\text{eff}}y(t), \qquad H_{\text{eff}} = U(t)^*HU(t) - iU(t)^*\dot{U}.}$$

The connection term $-iU(t)^*\dot{U}$ is Hermitian. If $H^* = H$, then $H_{\text{eff}}^* = H_{\text{eff}}$.

Proof. Applying the product rule entry by entry proves the differentiation formulas for matrix products and for matrices acting on vectors. Since the parameter is real, conjugation commutes with differentiation, giving the stated derivative of U^* and hence of y.

Differentiate $U^*U = I$ using those rules and uniqueness of derivatives:

$$\dot{U}^*U + U^*\dot{U} = 0.$$

Thus $(U^*\dot{U})^* = -U^*\dot{U}$, so multiplication by $-i$ produces a Hermitian matrix.

The identity $UU^* = I$ gives $\psi = Uy$ for the constructed coordinate curve. Differentiating and inserting the original equation yields

$$i\dot{U}y + iU\dot{y} = HUy.$$

Multiplying by U^* and using $U^*U = I$ gives the transformed equation, with the negative sign on the connection term. Finally, conjugation by U preserves Hermiticity of H, and the sum of the two Hermitian terms is Hermitian. □

Formal scope. The main certificate constructs y and its derivative rather than assuming a separate derivative witness for the desired answer. Both unitary identities are explicit. The proofs are pointwise and apply at any time where the stated hypotheses hold. They do not assert existence of a global solution to an evolution equation.

III.9 The canonical packet connection

Manuscript item 6.3. `CanonicalConnection.lean` 9 declarations

Let $P_a(s)$ be a finite family in a normed real algebra with a continuous compatible adjoint. Assume actual derivatives $D_a = \dot{P}_a(t)$ exist and, for all parameter values under consideration,

$$P_a P_b = \delta_{ab} P_a, \qquad \sum_a P_a = I, \qquad P_a^* = P_a.$$

In the supplied Lean theorem, the curves are defined on $\mathbb{R}$ and the projector laws hold at every real parameter. The algebraic formulation applies to matrices and bounded operators whenever they satisfy the stated typeclass hypotheses.

Supplementary statement. Define $C = \sum_a D_a P_a(t)$. Then

$$\boxed{C = \frac{1}{2}\sum_a [D_a, P_a(t)], \qquad C^* = -C,}$$

and, for every b,

$$\boxed{[C, P_b(t)] = D_b.}$$

Proof. The derivative product rule and uniqueness of derivatives give

$$D_a P_b + P_a D_b = \delta_{ab} D_a.$$

Differentiating completeness and adjoint invariance gives

$$\sum_a D_a = 0, \qquad D_a^* = D_a.$$

These are proved derivative consequences, not additional axioms supplied in place of differentiation.

On the diagonal, $D_a P_a + P_a D_a = D_a$. Summing shows

$$\sum_a P_a D_a = -\sum_a D_a P_a = -C.$$

This proves the formula involving half the sum of commutators, together with $C^* = -C$.

Orthogonality directly yields $C P_b = D_b P_b$. For the left product, multiply the differentiated identity for (b, a) on the right by P_a and sum over a. Completeness reduces the result to

$$D_b + P_b C = D_b P_b.$$

Subtracting this equation from the identity for multiplication on the right gives $CP_b - P_bC = D_b$. □

Formal scope. The proof derives the differentiated identities before using their algebraic consequences, so the role of the derivative hypotheses remains explicit. It establishes the canonical connection identity for one parameter. The range bundle over a parameter manifold, the exterior differential calculus, and the curvature theorem of item 6.4 are developed in the later supplements.

III.10 Finite Kraus channels and full amplification

Manuscript item 7.2. `KrausChannels.lean` 7 declarations

For a finite family of complex matrices K_a, define

$$\Phi(\rho) = \sum_a K_a \rho K_a^*.$$

The formalization constructs this as a complex-linear map and proves the following properties directly in the finite matrix representation.

Supplementary statement. The map Φ is completely positive. If

$$\sum_a K_a^* K_a = I,$$

then $\operatorname{tr}\Phi(\rho) = \operatorname{tr}\rho$ for every matrix ρ. In particular, positive semidefinite matrices of trace one are mapped to positive semidefinite matrices of trace one.

Proof. Matrix multiplication distributes across addition and scalar multiplication, which gives complex linearity. If $\rho \succeq 0$, each term $K_a \rho K_a^*$ is positive semidefinite, hence so is their finite sum.

To prove complete positivity rather than positivity alone, let J be an arbitrary finite auxiliary index set. For a matrix X indexed by $J \times n$, define its blockwise amplification by

$$[\Phi^{(J)}(X)]_{(i,u),(j,v)} = \Phi\big(X_{(i,\cdot),(j,\cdot)}\big)_{u,v}.$$

The explicit index calculation proves the identity

$$\boxed{\Phi^{(J)}(X) = \sum_a (I_J \otimes K_a) X (I_J \otimes K_a)^*.}$$

The displayed identity identifies the defined amplification with tensoring by the identity, which is the operation needed for complete positivity. Every summand on the right is positive when X is positive, and this holds for every finite J.

Finally, cyclicity and linearity of the trace give

$$\begin{aligned}\operatorname{tr}\Phi(\rho) &= \sum_a \operatorname{tr}(K_a \rho K_a^*) \\ &= \operatorname{tr}\left(\left(\sum_a K_a^* K_a\right)\rho\right) = \operatorname{tr}\rho.\end{aligned}$$

Positivity together with trace preservation gives the stated conclusion for density matrices. □

Formal scope. Complete positivity is proved for every finite auxiliary dimension. Normalization is required only for trace preservation and the conclusion about density matrices. The converse representation theorem for arbitrary completely positive maps lies outside this argument.

III.11 Actual orbits and sharp seed counts

Let $C \in M_{d\times m}(\mathbb{C})$ be the coefficient matrix of one seed. Define its orbit by actual matrix multiplication:

$$\mathcal{O}(C) = \{AC : A \in M_d(\mathbb{C})\}.$$

This set is already a linear subspace. The source proves that it equals the linear span of the orbit before computing its dimension.

A matrix X belongs to $\mathcal{O}(C)$ exactly when each of its rows belongs to $\mathrm{Row}(C)$. One direction follows by expanding AC. For the converse, choose the coefficients producing each row separately and place them in the corresponding row of A. An explicit linear equivalence therefore gives

$$\mathcal{O}(C) \simeq \mathrm{Row}(C)^d, \qquad \boxed{\dim_{\mathbb{C}} \mathcal{O}(C) = d\ \mathrm{rank}\, C.}$$

If $d > 0$, equality with the full $d \times m$ coefficient space is equivalent to $\mathrm{rank}\, C = m$. Consequently a cyclic seed requires $m \le d$. The assumption that there is at least one row is essential for canceling the factor d.

III.11.1 Several seeds: both necessity and construction

Continue under the assumption above that the number of rows is positive. For seeds $C_1, \dots, C_k$, generation means the concrete statement

$$\forall X \in M_{d\times m}(\mathbb{C}), \quad \exists A_1, \dots, A_k \in M_d(\mathbb{C}) : \quad X = \sum_{a=1}^{k} A_a C_a.$$

Stack the C_a vertically into a $kd \times m$ matrix D. The source identifies the action on the stacked matrix and proves the equivalence

$$\text{the seeds generate} \quad \Longleftrightarrow \quad \mathrm{rank}\, D = m.$$

Thus $m \le kd$ is necessary. It is sufficient as well: embed the m coordinate columns into kd coordinate positions to obtain a matrix D of full column rank, then split its rows back into k seeds. This construction proves that generating matrices with the required dimensions exist.

III.11.2 Simultaneous generation in a direct sum

For the stipulated block representation

$$\mathcal{A} = \bigoplus_i (M_{d_i}(\mathbb{C}) \otimes I_{m_i}), \qquad d_i > 0,$$

the proof establishes that k seeds generate all blocks simultaneously exactly when $m_i \le kd_i$ for every i. It follows that

$$\boxed{\mathrm{srank}_{\mathcal{A}}(\mathcal{H}) = \max_i \left\lceil \frac{m_i}{d_i} \right\rceil.}$$

The final Lean proposition is an `IsLeast` statement over the set of feasible seed counts. It proves both attainment and minimality. For an empty block family the finite supremum is defined as 0, matching the zero module.

III.12 Schmidt rank and the reduced state

Use coordinates ψ_{ij} in the standard product basis and let $C_{ij} = \psi_{ij}$. An explicit linear equivalence identifies the state vector on the product index set with its coefficient matrix. The implementation checks the actual Kronecker action:

$$\operatorname{coeff}((A \otimes I_B)\psi) = AC.$$

It also proves that the transported matrix orbit equals the span of the state vectors obtained by this Kronecker action. The dimension formula therefore applies to the physical local action on the state space.

III.12.1 An independent definition of Schmidt rank

The source defines Schmidt rank as the least number of summands that are product vectors. A decomposition of length s is the concrete equality

$$C_{ij} = \sum_{a=1}^{s} u_a(i) v_a(j).$$

It factors $C = UV$ through an s-dimensional intermediate space, so $\operatorname{rank} C \le s$. Conversely, choose a basis of the row space of C. Expanding each row in this basis constructs a decomposition with exactly $\operatorname{rank} C$ product terms. Thus

$$\boxed{r(\psi) = \operatorname{rank} C.}$$

The definition uses a least natural number, and the equality with matrix rank is a theorem. This argument establishes the minimum number of product terms. It does not construct an orthonormal Schmidt decomposition or prove a new theorem on singular value decomposition.

The matrix-orbit dimension and the coefficient equivalence now yield

$$\boxed{\dim_{\mathbb{C}} \operatorname{span}\{(A \otimes I_B)\psi : A \in M_{d_A}(\mathbb{C})\} = d_A r(\psi).}$$

III.12.2 The actual partial trace and its support

The reduced matrix is defined by tracing the addressed index of the density matrix of the pure state:

$$(\rho_B)_{j\ell} = \sum_i \psi_{ij} \overline{\psi_{i\ell}}.$$

For the coefficient convention used here, the exact Gram identity is

$$\rho_B = C^{\mathsf{T}} (C^{\mathsf{T}})^*, \qquad \operatorname{rank} \rho_B = \operatorname{rank} C = r(\psi).$$

The transpose is important. With this convention, writing C^*C instead would conjugate the reduced matrix. The Lean source checks the entrywise identity and positivity of the resulting matrix.

Full support is expressed as surjectivity of the reduced matrix's linear map. Assuming $d_A > 0$, the checked equivalence is

$$\boxed{\mathcal{O}_A(\psi) = \mathcal{H}_A \otimes \mathcal{H}_B \quad \Longleftrightarrow \quad \operatorname{Ran} \rho_B = \mathcal{H}_B.}$$

Normalization of ψ is unnecessary for these dimension and support statements. The zero state has rank 0 because its decomposition needs no product terms.

III.13 Constructed cyclic character projectors

Let $N > 0$ and let S be a unitary complex matrix with $S^N = I$. The implementation uses the standard additive character of $\mathbb{Z}/N\mathbb{Z}$ and proves its expression through a root of unity:

$$\omega = \exp(2\pi i/N), \qquad \chi(r) = \omega^{\operatorname{val}(r)}.$$

Here $\operatorname{val}(r)$ is the canonical representative in $\{0, \dots, N-1\}$. The representation is constructed as

$$\rho(r) = S^{\operatorname{val}(r)}.$$

Reduction of exponents modulo N is proved from $S^N = I$, giving $\rho(r+s) = \rho(r)\rho(s)$ and $\rho(0) = I$. The final matrix theorem derives the representation law and character orthogonality from the stated inputs.

III.13.1 Exact coefficient formula

The packet definition is a finite sum over residue classes:

$$P_j = \frac{1}{N} \sum_{r \in \mathbb{Z}/N\mathbb{Z}} \chi(-rj)\rho(r).$$

The source proves

$$\chi(-rj) = \left(\omega^{\operatorname{val}(r)\operatorname{val}(j)}\right)^{-1},$$

so this is precisely the manuscript's N-term Fourier projector formula, with canonical representatives.

III.13.2 Algebraic identities

Primitivity of the standard character yields the checked finite sum

$$\sum_r \chi(tr) = \begin{cases} N, & t = 0, \\ 0, & t \neq 0. \end{cases}$$

Reindexing finite sums then gives

$$\boxed{P_j P_k = \delta_{jk} P_j, \qquad \sum_j P_j = I, \qquad S P_j = \omega^j P_j.}$$

Multiplicativity and completeness are first proved for a general representation in a complex algebra, then instantiated with the actual powers of S. This organization makes the algebra of finite sums reusable while preserving the final hypotheses.

III.13.3 Orthogonality of the projectors

Unitarity supplies $\rho(r)^* = \rho(-r)$, while the character obeys $\overline{\chi(r)} = \chi(-r)$. Reindexing $r \mapsto -r$ proves $P_j^* = P_j$. The final concrete matrix theorem includes Hermiticity together with multiplication, completeness, and eigenaction. Together these identities establish orthogonal spectral packets.

The proof includes the degenerate modulus $N = 1$: finite order then forces $S = I$ and the sole projector is I. It does not need an artificial assumption $N > 1$.

III.14 The actual Euclidean transfer exponential

Let H be a Hermitian matrix on a nonzero complex state space of finite dimension. The source defines

$$T_e(t) = \exp(-t(H - eI))$$

using Lean's exponential defined by a power series. The proof then relates this defined operator to its spectral expansion.

III.14.1 Connecting power series and spectral calculus

The shifted generator is proved Hermitian. The implementation then identifies the actual matrix exponential with continuous functional calculus:

$$\boxed{T_e(t) = f_t(H), \qquad f_t(x) = e^{-t(x-e)}.}$$

The formal proof uses composition, scalar multiplication, subtraction, and the established agreement between the exponential in functional calculus and the exponential defined by a power series. Spectral mapping is consequently available for the operator that was actually defined:

$$\operatorname{Spec}_{\mathbb{R}} T_e(t) = \{e^{-t(x-e)} : x \in \operatorname{Spec}_{\mathbb{R}} H\}.$$

Hermiticity also identifies the full complex spectrum with the image of these real eigenvalues. A separate checked theorem states the interval containing the complex spectrum explicitly.

III.14.2 The minimum eigenvalue

The ground energy is the minimum of the finite, nonempty eigenvalue set. The proof establishes both

$$E_0 \in \operatorname{Spec}_{\mathbb{R}} H, \qquad E_0 \le x \quad (x \in \operatorname{Spec}_{\mathbb{R}} H).$$

The assumption that the state space is nonzero is recorded in the theorem because the minimum of an empty spectrum is not defined by the manuscript's formula.

III.14.3 Positivity, semigroup composition, and the interval

Every eigenvalue of $T_e(t)$ is strictly positive, for arbitrary real e, t, since the real exponential is positive. For $e = E_0$ and $t \geq 0$ it is also at most one. Therefore

$$\boxed{T_{E_0}(t) > 0, \qquad \operatorname{Spec} T_{E_0}(t) \subseteq (0, 1].}$$

The two scalar multiples of $H - eI$ commute, so the exponential defined by the power series obeys

$$\boxed{T_e(t+s) = T_e(t)T_e(s), \qquad T_e(0) = I.}$$

The semigroup identity is proved for all real t, s. Nonnegative time is needed for the upper spectral bound, not for the composition identity or strict positivity.

These results concern operators on a finite dimensional space. Continuum transfer limits, gravitational path integrals, and physical spacetime models require further structure. The numerical figures retain their earlier computation records and were not recomputed during this prose revision.

III.15 Quantitative leakage from the actual exponential

Let A be a unital complex C-star algebra, let $H = H^*$, and let $P = P^* = P^2$. Put $Q = 1 - P$. The checked statement is

$$\boxed{\|Q \exp(-itH)P\| \leq |t| \, \|HP - PH\| \qquad (t \in \mathbb{R}).}$$

The matrix specialization uses the operator norm on the Hilbert space, implemented by `Matrix.Norms.L2Operator`. It is not an entrywise norm or the row-sum operator norm. The theorem includes the zero projector and empty matrix index type. The theorem also applies at time zero.

III.15.1 Deriving the estimate by differentiation

For a skew-adjoint generator G, define the actual conjugation path

$$T_P(t) = \exp(tG)P\exp(-tG).$$

The formalization derives its derivative from the exponential power series and the product rule:

$$T_P'(t) = \exp(tG)(GP - PG)\exp(-tG).$$

Both exponential factors are proved unitary. Left and right multiplication by a unitary preserve the C-star norm. Therefore

$$\|T_P'(t)\| = \|GP - PG\|, \qquad \|T_P(t) - T_P(s)\| \leq |t - s| \, \|GP - PG\|.$$

The second inequality follows from the mean value inequality in normed spaces and covers either ordering of s and t. It is not a finite-difference estimate or a numerical time discretization.

Multiplication by $\exp(tG)$ gives

$$(T_P(t) - P)\exp(tG) = \exp(tG)P - P\exp(tG).$$

For every orthogonal projector, $\|P\| \le 1$ and $\|1 - P\| \le 1$. The exact corner identity

$$(1 - P)UP = (1 - P)(UP - PU)P$$

then bounds leakage by the exponential commutator. Taking $G = -iH$ gives the stated theorem because $\|[G, P]\| = \|[H, P]\|$.

III.15.2 Checked consequences

Unitarity also gives the capped estimate

$$\|Q \exp(-itH)P\| \le \min\{1,\ |t|\,\|[H, P]\|\}.$$

If $H = H_0 + V$, both summands are self-adjoint, and $[H_0, P] = 0$, then

$$\|Q \exp(-it(H_0 + V))P\| \le 2|t|\,\|V\|.$$

The latter uses $\|[V, P]\| \le 2\|V\|$. Its constant is not claimed to be optimal. Exact commutation gives zero leakage. The work does not include unbounded generators or time-dependent Hamiltonians.

III.16 Actual projected differentiation and curvature

Let E, F be real normed spaces. Let $P : E \to \mathcal{L}(F, F)$ be differentiable with $P(x)^2 = P(x)$ for every x. Let $s : E \to F$ be C^2 with $P(x)s(x) = s(x)$, and let $X, Y : E \to E$ be differentiable vector fields. The checked connection is the actual expression

$$\nabla_X s(x) = P(x)\, Ds(x)[X(x)].$$

It is proved to preserve the range condition. It is linear in the vector field direction and obeys the scalar Leibniz rule

$$\nabla_X(cs) = Dc[X]\, s + c\nabla_X s$$

for differentiable real scalar functions c. No differentiated projector identities are inserted as hypotheses in the main curvature theorem.

III.16.1 Differentiated projector and section identities

Differentiating $P^2 = P$ and $Ps = s$ produces

$$\begin{aligned} DP[v]P + PDP[v] &= DP[v], \\ PDP[v]P &= 0, \\ Ds[v] &= DP[v]s + PDs[v]. \end{aligned}$$

The zero sandwich follows algebraically from the first identity. All products preserve their noncommutative order.

III.16.2 Retaining the bracket of vector fields

Define the actual curvature action by

$$R_P(X,Y)s = \nabla_X \nabla_Y s - \nabla_Y \nabla_X s - \nabla_{[X,Y]} s.$$

The source uses the Lie bracket defined through Fréchet derivatives. Symmetry of second derivatives is supplied by the C^2 hypothesis, not postulated separately. Expanding the connection gives

$$R_P(X,Y)s = P(DP[X]Ds[Y] - DP[Y]Ds[X]).$$

Substituting the section identity and removing the zero sandwich terms proves

$$\boxed{R_P(X,Y)s = P(DP[X]DP[Y] - DP[Y]DP[X])Ps.}$$

Thus the coefficient is precisely $P(\,\mathrm{d}P \wedge \mathrm{d}P)P$ with the convention $(\,\mathrm{d}P \wedge \mathrm{d}P)(v,w) = DP[v]DP[w] - DP[w]DP[v]$.

III.16.3 Tensor properties and the remaining global boundary

The coefficient is proved bilinear, alternating, and supported on the range on both sides. The chain rule proves the pullback identity

$$F_{P\circ f}(x)(v,w) = F_P(f(x))(Df(x)v, Df(x)w).$$

The main theorem has global regularity hypotheses on normed parameter spaces. The pullback identity alone does not supply localization, smooth local trivializations, or gluing. The final supplement constructs the global range bundle and proves that the local connections glue.

III.17 A constructive and total syndrome recovery

Let P be an orthogonal code projector. The input certificate consists of a finite family V_a satisfying

$$V_a P = V_a, \qquad V_a^* V_b = \delta_{ab} P.$$

These hypotheses state that the operators are partial isometries with orthogonal syndromes. The next supplement derives such a family from arbitrary Knill–Laflamme Gram data.

III.17.1 Constructing the recovery on the whole ambient space

Define the syndrome projectors and their complement by

$$S_a = V_a V_a^*, \qquad S = \sum_a S_a, \qquad Q = 1 - S.$$

The source proves self-adjointness, $S_a S_b = \delta_{ab} S_a$, $S^2 = S$, and $Q^2 = Q = Q^*$. It also proves $QV_a = 0$ and $V_a^* Q = 0$.

The recovery is not left undefined outside the syndrome subspaces. Its explicit Kraus operators are $R_a = V_a^*$ together with $R_{\text{extra}} = Q$, giving

$$\mathcal{R}(\rho) = \sum_a V_a^* \rho V_a + Q\rho Q.$$

They satisfy exact completeness:

$$\sum_a R_a^* R_a + R_{\text{extra}}^* R_{\text{extra}} = \sum_a V_a V_a^* + Q = S + Q = I.$$

For finite complex matrices, trace preservation and complete positivity at every finite auxiliary dimension are proved for this actual map. The amplified map is identified with the Kraus family $I_J \otimes R_a$, including the complement term. Positivity is not merely checked on a single matrix size.

III.17.2 Exact correction, including coherent errors

For every operator supported on the code, $P\rho P = \rho$, the central identity is

$$\boxed{\mathcal{R}(V_a \rho V_b^*) = \delta_{ab}\rho.}$$

Consequently normalized mixtures satisfy

$$\mathcal{R}\left(\sum_a p_a V_a \rho V_a^*\right) = \rho \quad \text{when} \quad \sum_a p_a = 1.$$

The identity is algebraic and is proved for complex weights. Physical mixtures use the nonnegative real case. For a coherent error $E_z = \sum_a z_a V_a$, the calculation of the cross terms yields

$$\mathcal{R}(E_z \rho E_z^*) = \left(\sum_a z_a \overline{z_a}\right) \rho.$$

Thus the same map also corrects normalized coherent superpositions. This construction supplies the recovery stage used in the full Knill–Laflamme proof that follows.

III.18 The precise finite channel statement

Let $\mathcal{H} = \mathbb{C}^n$ be a finite coordinate space and let $P = P^* = P^2$. A matrix is code supported when $P\rho P = \rho$. For a finite family of square matrices E_a, put

$$\mathcal{N}_E(\rho) = \sum_a E_a \rho E_a^*.$$

The input channel normalization is the actual matrix identity

$$\sum_a E_a^* E_a = I.$$

A finite Kraus recovery has the form $\mathcal{R}(\sigma) = \sum_r R_r \sigma R_r^*$, with $\sum_r R_r^* R_r = I$. This representation, together with the checked amplification results, provides complete positivity and trace preservation on the entire ambient matrix space.

III.18.1 Necessary and sufficient conditions

Under the stated normalization, the following equivalence is proved:

$$\boxed{\begin{array}{c}\exists\,\mathcal{R}\text{ of the above finite Kraus form,}\\ \mathcal{RN}_{E}(\rho)=\rho\quad\text{for every }\rho\succeq 0,\ \operatorname{Tr}\rho=1,\ P\rho P=\rho\end{array}}\quad\Longleftrightarrow\quad\boxed{\begin{array}{c}\exists C\succeq 0,\\ PE_a^*E_bP=C_{ab}P\quad\text{for all } a,b.\end{array}}$$

The statement applies throughout the code space. The formalization separately proves equivalence with correction of *every* complex matrix supported on the code. It also proves preservation with arbitrary finite reference systems, as detailed in the discussion of density matrices and reference systems below.

III.18.2 Including degenerate cases

The matrix C need not be positive definite. The proof includes zero eigenvalues, redundant error operators, an empty set of positive eigenvalues, and the zero projector. If $P=0$, the only supported matrix is zero and no trace-one code density matrix exists. The proofs handle that case separately rather than dividing by the code rank or by $\operatorname{Tr}P$.

For an unnormalized error family, the correct statement is generally

$$\mathcal{RN}_{E}(\rho)=\operatorname{Tr}(C)\rho,$$

not unconditional equality to ρ. Normalization forces $\operatorname{Tr}C=1$ on a nonzero code. The discussion of coherent errors below treats unrestricted error families and shows when the same decoder works throughout their span.

III.19 From Gram data to an actual total recovery

Assume $C\succeq 0$ and $PE_a^*E_bP=C_{ab}P$. First restrict the error operators to the code, $F_a=E_aP$. The finite Hermitian spectral theorem supplies a unitary U such that

$$U^*CU=\operatorname{diag}(\lambda_r),\qquad \lambda_r\geq 0.$$

Define the transformed errors by an actual finite sum,

$$B_r=\sum_a U_{ar}F_a.$$

The formal module proves the identities

$$B_rP=B_r,\qquad B_r^*B_s=\delta_{rs}\lambda_rP,\qquad \sum_r B_r\rho B_r^*=\sum_a F_a\rho F_a^*.$$

For ρ supported on the code, the restricted and unrestricted error sums are equal. Thus the unitary change of error coordinates preserves the actual channel on the code.

III.19.1 Null directions are removed by proof

If $\lambda_r = 0$, then $B_r^* B_r = 0$. Positivity of the ordinary complex matrix inner product gives $B_r = 0$. This is the checked declaration `DiagonalErrors.zero_weight_error`. The normalized syndrome operators are defined only on

$$A_+ = \{r : \lambda_r > 0\}, \qquad V_r = \lambda_r^{-1/2} B_r.$$

Consequently no inverse square root at a null eigenvalue is needed. Lean proves

$$V_r P = V_r, \qquad V_r^* V_s = \delta_{rs} P.$$

The previous block's recovery is now instantiated from these derived syndromes, rather than from an assumed orthogonal error family.

III.19.2 A channel on the whole ambient space

Put $Q = I - \sum_{r \in A_+} V_r V_r^*$. The recovery is

$$\boxed{\mathcal{R}(\sigma) = \sum_{r \in A_+} V_r^* \sigma V_r + Q \sigma Q.}$$

The complement is an orthogonal projector and

$$\sum_{r \in A_+} V_r V_r^* + Q^* Q = I.$$

Hence the recovery is trace preserving. Its finite Kraus form also proves positivity after amplification by the identity on every finite auxiliary space. The complement term matters: the map is defined as a channel even outside the syndrome ranges.

Finally the checked calculation gives $\mathcal{R}\mathcal{N}_E(\rho) = \sum_r \lambda_r \rho = \mathrm{Tr}(C)\rho$. Under normalization of the input channel and $P \neq 0$, summing the diagonal Gram identities gives $\mathrm{Tr}(C)P = P$, hence $\mathrm{Tr}\, C = 1$. The proof for the zero code does not use this cancellation.

III.20 Deriving the Gram matrix from recovery

Suppose a finite recovery that preserves trace corrects every operator supported on the code. To derive the Knill–Laflamme condition without assuming a syndrome decomposition, the proof expands the composite channel into the finite Kraus family

$$A_{ra} = R_r E_a P.$$

For every ambient matrix ρ, correction on the code implies

$$\sum_{r,a} A_{ra} \rho A_{ra}^* = P \rho P.$$

This equality on all matrices follows by applying correction to the sandwich supported on the code, $P\rho P$, using the projector identities.

III.20.1 Rank-one rigidity of the corrected channel

The module tests the map equality on actual matrix units and flattens each A_{ra} into a row. If X is the matrix of those rows and p is the vector of entries of P, the resulting Gram identity is

$$X^*X = \overline{p}\,p^{\mathsf{T}}.$$

The checked rank-one Gram lemma proves that every row of X is proportional to p. For nonzero p, a nonzero coordinate is selected and a test vector supported on two coordinates is placed in the null space of the Gram matrix. The implication $X^*Xv = 0 \Rightarrow Xv = 0$ then gives the required proportionality. When $p = 0$, the Gram identity forces $X = 0$ directly.

Applied to the corrected Kraus family, this yields scalars z_{ra} with

$$R_r E_a P = z_{ra} P.$$

The essential declarations are `rank_one_gram_rigidity`, `kraus_rank_one_rigidity` and `corrected_kraus_family`. No rank-one Choi characterization is inserted as an axiom or as the desired conclusion in hypothesis form.

III.20.2 Trace-preserving recovery supplies the original Gram data

Let $Z_{ra} = z_{ra}$. The recovery normalization gives

$$\begin{aligned} PE_a^*E_bP &= PE_a^*\Big(\sum_r R_r^*R_r\Big)E_bP \\ &= \sum_r (R_rE_aP)^*(R_rE_bP) \\ &= \Big(\sum_r \overline{z_{ra}}z_{rb}\Big)P = (Z^*Z)_{ab}P. \end{aligned}$$

Thus $C = Z^*Z$ is positive semidefinite and satisfies the required compressed identities. The theorem `gram_of_recovery` implements this calculation with the original error and recovery matrices.

A second rigidity argument handles a nonnegative scalar multiple of the identity code map. It uses $\sqrt{t}\,P$ as the rank-one map generator and includes $t = 0$. That argument proves necessity for unnormalized error families, which need not define channels.

III.21 Density matrices, all operators and finite references

The necessity argument is stated for all operators, so it must be connected to correction of physical density matrices. The proof establishes this connection explicitly for complex linear maps on finite matrices.

III.21.1 Normalization is not an extra assumption

A nonzero positive semidefinite matrix has strictly positive real trace. If a complex-linear map fixes every normalized code density matrix, apply that hypothesis to

$$\frac{\rho}{\operatorname{Tr}\rho}$$

for each nonzero positive code-supported ρ. Linearity then gives equality on ρ itself. The zero matrix is handled separately. The source proves that the trace is real and nonzero, then justifies cancellation of the scalar. These steps establish that normalization is valid.

III.21.2 Complex polarization reaches the whole operator space

Write $q(x) = xx^*$. The module proves the exact identity

$$4xy^* = q(x+y) - q(x-y) + i(q(x+iy) - q(x-iy)).$$

Agreement on all positive pure outer products therefore implies agreement on every outer product. Actual matrix units then span the full matrix space. Applying this argument to the sandwich by P proves equality on every code-supported operator, including non-Hermitian ones.

The result `density_corrects_iff_operators` establishes the equivalence for the actual composite Kraus maps. It does not replace the set of density matrices by an assumed basis of logical states.

III.21.3 An arbitrary finite reference system

For any finite reference index set A, the amplified channel is defined using the actual Kronecker Kraus operators,

$$\widetilde{\mathcal{N}}_E(\rho) = \sum_a (I_A \otimes E_a)\rho(I_A \otimes E_a)^*.$$

Its reference blocks are proved equal to the original channel applied blockwise. If

$$(I_A \otimes P)\rho(I_A \otimes P) = \rho,$$

then every reference block is code supported. Applying the checked correction theorem for operators to those blocks gives

$$\boxed{\widetilde{\mathcal{R}}\,\widetilde{\mathcal{N}}_E(\rho) = \rho.}$$

This includes entangled density matrices supported on the combined reference and code space. In fact, the identity holds for every jointly supported matrix and every finite reference dimension.

The declaration `recovery_with_reference` proves the equality. The finite Kraus amplification separately establishes complete positivity of the recovery, which is needed to preserve states in the presence of a reference system.

III.22 Coherent combinations and normalization

A correction proof for only one selected Kraus presentation is weaker than a proof that one decoder works throughout the error span. The formal module connects the constructed spectral recovery back to the original error operators.

III.22.1 Cross terms for the original errors

For arbitrary positive Gram data, the same recovery satisfies

$$\boxed{\mathcal{R}(E_a \rho E_b^*) = C_{ba}\rho \qquad (P\rho P = \rho).}$$

The index order ba is intentional: the defining Gram relation is $PE_a^*E_bP = C_{ab}P$. The proof first derives scalar corrected Kraus composites for the constructed recovery and then uses its trace-preserving completeness to identify the original Gram entries.

For $E(c) = \sum_a c_a E_a$, finite-sum expansion gives

$$\mathcal{R}(E(c)\rho E(c)^*) = \left(\sum_{a,b} c_a \overline{c_b} C_{ba}\right)\rho = (c^*Cc)\rho.$$

The formula with a double sum is the literal checked conclusion. The final notation as a quadratic form follows by renaming finite indices. It is not restricted to orthogonal errors or real coefficients.

III.22.2 Every normalized channel in the same span

Suppose $F_j = \sum_a c_{ja} E_a$ and $\sum_j F_j^* F_j = I$. The decoder is *not* reconstructed for the F_j. Summing the coherent identities gives a scalar multiple $q\rho$. Trace preservation of both the F channel and the recovery forces $q = 1$ on a nonzero code. The proof uses positivity of P to justify cancellation of its trace and handles $P = 0$ separately. Therefore

$$\boxed{\mathcal{R}\Big(\sum_j F_j \rho F_j^*\Big) = \rho.}$$

This is `Data.recovery_span_channel`, a quantified statement over arbitrary finite F families and their complex coefficients.

III.22.3 The equivalence for unnormalized error families

For arbitrary finite E, define exact family recovery to mean that a finite trace-preserving Kraus recovery and a single $t \geq 0$ exist such that

$$\mathcal{R}\mathcal{N}_E(\rho) = t\rho \quad \text{for every code-supported } \rho.$$

Then `error_family_correctable_iff_gram` proves that this condition is equivalent to the existence of $C \succeq 0$ satisfying the Gram identities. Sufficiency chooses $t = \operatorname{Tr} C$. Necessity constructs C from the scaled rank-one rigidity argument.

The scale is essential. Zero errors can give $t = 0$ and cannot be inverted to a nonzero normalized state. An input with a larger total trace is not silently declared a channel. For normalized input channels, the separate channel theorem removes the scale exactly as described in the sufficiency argument above.

III.23 Exact examples, trust audit and remaining work

III.23.1 Singular, nonorthogonal errors are accepted

On a qubit with full code $P = I$, take

$$E_0 = \frac{3}{5}I, \qquad E_1 = \frac{4}{5}I, \qquad C = \begin{pmatrix} 9/25 & 12/25 \\ 12/25 & 16/25 \end{pmatrix}.$$

Lean checks the channel normalization, the Gram identities, positivity of C, $\det C = 0$, and the nonzero off-diagonal entry. It then applies the criterion for density matrices to prove correctability. The calculation is exact and uses rational complex entries.

III.23.2 A genuine channel can still be uncorrectable

For full qubit dephasing, $E_0 = \mathrm{diag}(1, 0)$ and $E_1 = \mathrm{diag}(0, 1)$, the Kraus normalization is checked. But $E_0^* E_0$ cannot be a scalar multiple of I, as its two diagonal entries differ. Necessity therefore proves that no finite recovery channel corrects the full code space. The case of the zero code is also checked independently.

III.24 The global projected connection

Let M be a smooth real manifold without boundary, F a complete normed real vector space and $P : M \to \mathrm{End}(F)$ a smooth family of bounded idempotents. For smooth range sections s, define

$$\nabla_X s = P\ \mathrm{d}s[X].$$

The proof begins by constructing the range bundle from P. Its local connection formulas glue, and the actual covariant commutator satisfies

$$\boxed{(\nabla_X \nabla_Y - \nabla_Y \nabla_X - \nabla_{[X,Y]})s = P(\,\mathrm{d}P[X]\,\mathrm{d}P[Y] - \,\mathrm{d}P[Y]\,\mathrm{d}P[X])P\,s.}$$

The derivative and Lie bracket are Mathlib's actual manifold operators. No global coordinate chart is assumed. The result requires idempotence, not an additional orthogonality hypothesis.

III.25 Local products constructed from the projector

The fiber over x is the actual fixed subspace

$$\mathcal{E}_x = \{v \in F : P(x)v = v\} = \mathrm{Ran}\, P(x).$$

The total space is the subset $\mathcal{E} = \{(x, v) : P(x)v = v\} \subseteq M \times F$, with the induced topology. The construction provides local homeomorphisms of this total space as well as the transition functions between them.

III.25.1 An invertible intertwiner near each anchor

For idempotents p, q, set

$$T(p,q) = pq + (I-p)(I-q).$$

Lean proves $T(p,p) = I$ and $pT(p,q) = T(p,q)q$. For an anchor $a \in M$, define

$$U_a = \{x : T(P(x), P(a)) \text{ is invertible}\}.$$

The invertible elements form an open subset of the algebra of bounded operators. Consequently U_a is open and contains a. The family (U_a) covers the whole base. Invertibility is *derived locally*, not assumed at every pair of points.

III.25.2 The mutually inverse local maps

Write $T_a(x) = T(P(x), P(a))$. For $x \in U_a$,

$$B_a(x) : \mathcal{E}_a \longrightarrow \mathcal{E}_x, \quad v \longmapsto T_a(x)v,$$

$$A_a(x) : \mathcal{E}_x \longrightarrow \mathcal{E}_a, \quad w \longmapsto P(a)T_a(x)^{-1}w.$$

The intertwining identity and its inverse counterpart show that the displayed targets are correct. Lean proves both inverse laws, continuity, linearity in the fiber and smooth dependence on the base. Thus

$$\mathcal{E}|_{U_a} \;\cong\; U_a \times \mathcal{E}_a$$

is a local product homeomorphism that preserves the base point.

III.25.3 Smooth overlap maps and rank

The coordinate transition is $g_{ab}(x) = A_b(x)B_a(x)$. It is smooth on $U_a \cap U_b$, agrees with the actual change between local homeomorphisms, and satisfies

$$g_{aa} = I, \qquad g_{bc}g_{ab} = g_{ac}.$$

A continuous linear equivalence between $\mathcal{E}_a$ and $\mathcal{E}_x$ also gives local constancy of fiber dimension. No single constant rank across disconnected components is assumed.

III.26 A connection on the constructed bundle

The global formula is defined using the actual manifold derivative:

$$\nabla_X s(x) = P(x)\, D_M s(x)[X(x)].$$

Here D_M is represented by `mvfderiv`. A second definition, `GlobalConnection.covariant`, has values in the actual fiber:

$$\nabla s(x) : T_x M \longrightarrow \mathcal{E}_x.$$

It is not only an ambient expression asserted to land in the range.

III.26.1 Connection axioms and smoothness

The formal proofs establish range preservation, additivity in the section, linearity over functions in the vector field argument, and the scalar Leibniz identity

$$\nabla_X(fs) = \mathrm{d}f[X]\, s + f\nabla_X s.$$

Smooth P, smooth sections and smooth vector fields give smooth covariant derivatives. Equality of section germs gives equality of covariant derivatives at the point, so the operation is local.

III.26.2 Smoothness of sections in bundle coordinates

Let $x \in U_a$. If $P(y)s(y) = s(y)$ in a neighborhood of x, then

$$s \text{ is smooth at } x \quad \Longleftrightarrow \quad (y \mapsto A_a(y)s(y)) \text{ is smooth at } x.$$

The range condition is only local. The proof uses the actual inverse local maps and equality of germs. It follows that smoothness in bundle coordinates does not depend on the chosen chart.

III.26.3 The local connection and its change of coordinates

For a coordinate function u valued in $\mathcal{E}_a$, define

$$\nabla_X^{(a)} u = A_a(P\, D_M(B_a u)[X]).$$

For every overlap point, Lean proves the operator identity

$$\boxed{\nabla_X^{(b)}(g_{ab}u) = g_{ab}\nabla_X^{(a)}u.}$$

This is proved for arbitrary local coordinate functions. It does not assume that u was obtained from a globally smooth section or that a smooth extension has been supplied. Together with the local smoothness criterion, this closes the gluing step left open in the fifth block.

III.27 From differentiated projectors to the two-form

The curvature is defined by the covariant commutator, including the *actual manifold Lie bracket*. It is not defined to equal the desired projector expression.

III.27.1 The flat ambient identity is proved in charts

For a smooth vector-valued function s, the proof identifies directional derivatives with the pullback into each extended chart. It then proves

$$D_M s([X,Y]) = D_M(D_M s[Y])[X] - D_M(D_M s[X])[Y].$$

This uses the chart pullback of the actual vector fields and the ordinary differential identity, then transfers the result back to the manifold. The auxiliary module works locally at a point, so the argument applies within arbitrary open chart domains.

III.27.2 Projector and section identities are derived

Differentiating $P^2 = P$ in a tangent direction v yields

$$(\,\mathrm{d}P[v])P + P\,\mathrm{d}P[v] = \mathrm{d}P[v], \qquad P\,\mathrm{d}P[v]P = 0.$$

Differentiating $Ps = s$ gives

$$\mathrm{d}s[v] = \mathrm{d}P[v]s + P\,\mathrm{d}s[v].$$

Both statements are consequences of actual derivative rules. They are not additional assumptions.

III.27.3 Cancellation of the second derivatives

The product rule and the identity for the ambient Lie bracket reduce curvature to

$$R^{\nabla}(X,Y)s = P\,\mathrm{d}P[X]\,\mathrm{d}s[Y] - P\,\mathrm{d}P[Y]\,\mathrm{d}s[X].$$

Substitute the identity obtained by differentiating the range condition for the section. The terms containing $P\,\mathrm{d}P[v]P$ vanish, leaving

$$R^{\nabla}(X,Y)s = P(\,\mathrm{d}P[X]\,\mathrm{d}P[Y] - \mathrm{d}P[Y]\,\mathrm{d}P[X])Ps.$$

Lean also proves that this depends only on $X(x)$, $Y(x)$ and $s(x)$, not on their extensions. The operator-valued form is alternating, additive and homogeneous, and lands in the actual fiber. Constant projector bundles have zero curvature form.

III.27.4 Geometry and scalar conventions

The main global curvature theorem uses a smooth real manifold without boundary, modeled on a complete normed real space, and bounded real-linear endomorphisms of a complete normed real space. Finite-dimensional parameter and quantum spaces fall within the corresponding real differential calculus. Complex quantum spaces can be viewed through their underlying real normed spaces. This block does not introduce a separate typeclass wrapper for complex bundles.

The atlas and global connection constructions also support the more general infrastructure for models with corners wherever their hypotheses apply. The *curvature completion claim* concerns the stated theorem for manifolds without boundary. Extending that curvature result to boundaries or corners requires further work.

III.27.5 An explicit smooth atlas

The implementation exposes the actual total space, local product homeomorphisms, linear transitions, smoothness proofs and cocycle laws. It does not register these as a `ContMDiffVectorBundle` instance. This is an interface choice. The range bundle atlas, local trivializations, overlap identities, and curvature formula are all constructed or proved from the stated inputs.

The equivalence for smooth sections and the gauge law make the atlas usable intrinsically. The connection is also defined with values in `fiber(Px)`. Six constructed objects that contain proof fields, including both local equivalences and the derivative with values in the fiber, have separate axiom audits.

III.28 Earlier compact derivations retained as alternatives

The following derivations retain valid mathematical arguments from the original manuscript. Their hypotheses and notation agree with the corrected finite core. The earlier abbreviated argument for error correction is replaced by the complete normalized and scaled recovery proofs above, and its substantive conclusions are included there.

III.28.1 Duhamel proof of leakage from a fixed packet

Let $H = H^*$ on a finite-dimensional complex Hilbert space, $P = P^* = P^2$, $Q = I - P$, and $t \in \mathbb{R}$.

Alternative proof of the commutator leakage bound. Because $QP = 0$,

$$Qe^{-itH}P = Q[e^{-itH}, P]P.$$

The Duhamel identity gives

$$[e^{-itH}, P] = -i \int_0^t e^{-i(t-s)H}[H, P]e^{-isH}\, ds.$$

Both unitary factors have norm one, so taking norms and using the integration interval's length $|t|$ yields $\|Qe^{-itH}P\| \le |t|\, \|[H, P]\|$. □

III.28.2 Proof of projected curvature with exterior forms

Let P be a smooth idempotent field and extend the projected connection to differential forms with values in the range bundle by $\nabla\omega = P\, d\omega$. Thus ∇^2 denotes the exterior covariant square, including the Lie bracket term in the exterior derivative when evaluated on vector fields.

Alternative proof of the curvature formula. For a section s with $Ps = s$,

$$\nabla^2 s = P\, d(P\, ds) = P(dP) \wedge ds.$$

Since $ds = d(Ps) = (dP)s + Pds$ and $P(dP)P = 0$, the surviving term is

$$P(dP \wedge dP)Ps.$$

□

III.28.3 Restricted low-mode proof

Let $h \neq 0$, $x = kh/2$, and $0 \leq x \leq 1$.

Alternative proof in the original low-mode regime. Since $0 \leq \sin x \leq x$, the error is nonnegative. On $[0, 1]$,

$$\sin x \geq x - \frac{x^3}{6} \geq 0.$$

Therefore

$$\sin^2 x \geq \left(x - \frac{x^3}{6}\right)^2 \geq x^2 - \frac{x^4}{3}.$$

Hence $x^2 - \sin^2 x \leq x^4/3$. Multiplication by $4/h^2$ gives

$$0 \leq k^2 - \frac{4}{h^2}\sin^2(kh/2) \leq \frac{k^4 h^2}{12}.$$

□

Part IV Worked visual atlas

V1 / HOW TO READ THIS APPENDIX

Three objects, three questions

Traditional edition: Section II.1, Section II.7, Section II.9.

A quantum calculation becomes easier to follow when its objects remain visible. This appendix follows a state vector, a density matrix, and a retained part of a dynamical system. They may describe the same experiment, but they do not answer the same question.

$\sqrt{2}\,\psi$

1
0
0
1

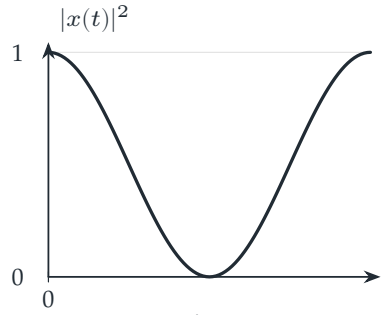
Two amplitudes one pure state

$2\rho = 2\psi\psi^*$

1	0	0	1
0	0	0	0
0	0	0	0
1	0	0	1

Off-diagonal entries retain phase.

Hidden coupling returns.



Amplitudes retain relative phase

For the Bell vector $\psi = (|00\rangle + |11\rangle)/\sqrt{2}$, the two nonzero entries are amplitudes. The density matrix $\rho = \psi\psi^*$ also records coherence in its off-diagonal entries. Measurements that compare the two addresses can detect this coherence. Deleting those entries applies a physical channel and changes the state.

How hidden dynamics returns

When a Hamiltonian couples a retained state to a hidden state, the retained amplitude can leave and later return. Its exact equation then remembers the hidden coupling. A smaller matrix obtained by deleting rows and columns does not generally reproduce that equation.

A route through the paper

Pages V3–V10 develop seeds, symmetry, and coherent circuit paths. Pages V11–V15 track leakage and moving subspaces. Pages V16–V20 distinguish measurement, channels, and recovery. Pages V21–V27 follow hidden dynamics and finite geometric diagnostics.

Read this guide alongside the traditional volume. The first 28 worked pages retain the original appendix's examples and mathematical content, with source references updated to this edition. Pages V29–V40 develop additional strengthened results. The example checks and the inherited Lean certificates have separately recorded scopes.

> **Read this as:** A packet coordinate change preserves information. A measurement, dephasing operation, or truncation may not. Always identify which operation is actually being performed.

V2 / AN ATLAS OF TYPES AND CONVENTIONS

The objects on the page

Traditional edition: Definition II.2.1, Definition II.7.1.

The same letter can stand for different kinds of data in different calculations. Keep the following types fixed while reading a formula. In this appendix, vectors are columns, operators compose from right to left, and A^* denotes the conjugate transpose.

Symbol	Object	What it records
$\mathcal{H}, \psi$	Hilbert space and state vector	They specify the space of addresses and its coherent amplitudes.
$\mathcal{A}$	Declared operator algebra	It specifies the available linear operations.
P_a	Orthogonal packet projector	It selects an entire subspace.
ρ	Positive matrix of trace one	It records populations and coherences.
E_k	Positive measurement effect	It gives the outcome probability $\mathrm{Tr}(E_k\rho)$.
K_a	Kraus operator	It describes one channel branch and need not be a projector.
H	Self-adjoint Hamiltonian	It generates evolution in real time through $e^{-\mathrm{i}tH}$.
C, ∇	Packet transport generator and connection	They describe moving subspaces and differentiation within their ranges.
P, Q	Retained and hidden projectors	They define a decomposition with $Q = I - P$.
$\Sigma(z)$	Self-energy	It records the spectral influence of the hidden sector.
$L, T(\tau)$	Nonnegative operator and Euclidean transfer	They determine decay factors and finite heat trace diagnostics.

Normalization and indexing

The tensor factors are ordered from left to right, so $X_1 = X \otimes I \otimes I$. A normalized pure state gives $\rho = \psi\psi^*$. A coefficient matrix used to count a seed orbit need not be normalized. Scaling a nonzero seed does not change its generated linear span.

A Hamiltonian and a Hadamard gate are both traditionally denoted H. Where both appear, the gate is H_{Had} and the Hamiltonian keeps the letter H. Numerical labels on a drawing are coordinates or exact example values, not observations of a physical device.

> **Read this as:** Check the type before interpreting the picture. An idempotent projector, a density matrix, and a channel matrix have different defining equations.

V3 / CYCLICITY DEPENDS ON THE GRAMMAR

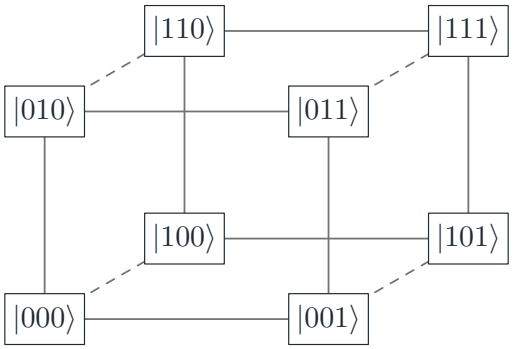
One seed, eight addresses

Traditional edition: Proposition II.2.5.

Start with $\psi_0 = |000\rangle$ and allow the three bit flip operators X_1, X_2, X_3. For a binary address $a = (a_1, a_2, a_3)$, put

$$W_a = X_1^{a_1} X_2^{a_2} X_3^{a_3}. \qquad W_a \psi_0 = |a_1 a_2 a_3\rangle .$$

The drawing shows the actual eight states reached by these words. Dashed edges connect the two squares by changing the first bit. The other edges change one of the remaining bits.



Three actual words

$$W_{101} = X_1 X_3$$

$$W_{011} = X_2 X_3$$

$$W_{110} = X_1 X_2$$

$$\dim \operatorname{span}\{W_a |000\rangle\} = 8$$

Two different meanings of “reach”

The eight vectors are orthonormal, so their *linear span* is all of $\mathbb{C}^8$. This proves cyclicity for the algebra generated by the flips. Preparing every normalized vector requires more than products of these flips alone.

For example, no such word sends $|000\rangle$ to $(|000\rangle + |001\rangle)/\sqrt{2}$. A Hadamard gate, a suitable linear combination in the observable algebra, or a larger preparation grammar is required for that operation. Counting linearly independent addressed vectors and synthesizing a physical gate sequence are separate tasks.

The exact check constructs each 8×8 word matrix, applies it to the seed, and verifies that the matrix of all eight outputs is the identity. It also tests the displayed superposition against every word output. No search over an unspecified gate set is involved.

> **Read this as:** A cyclic seed generates a vector space under an algebra. That conclusion does not automatically provide a unitary preparation procedure for every vector in it.

V4 / SCHMIDT RANK AS ACCESSIBLE MULTIPLICITY

Entanglement changes the local span

Traditional edition: Theorem II.2.2, Corollary II.2.4.

Write a bipartite vector as a coefficient matrix C, with the first subsystem indexing rows. Acting only on that subsystem transforms C to AC. Every resulting row remains in the row space of C, and every independent choice of such rows can be obtained in this way.

$$\dim \operatorname{span}\{(A \otimes I)\psi : A \in M_d(\mathbb{C})\} = d \operatorname{rank} C.$$

Product seed matrix

1	0
0	0

row rank 1
orbit dimension 2

Bell seed matrix $\sqrt{2}C$

1	0
0	1

row rank 2
orbit dimension 4

A acts on the left. It cannot invent a new direction in the row space.

The product vector $|00\rangle$ has matrix $C = \operatorname{diag}(1, 0)$. Its local orbit span allows arbitrary vectors in the first subsystem but only the second subsystem direction $|0\rangle$, so its dimension is two. The Bell vector has $C = I/\sqrt{2}$, rank two, and a four-dimensional local orbit span.

What the formula does not say

The action here allows arbitrary matrices and then takes a linear span. It is not the orbit under local unitary gates alone. Local unitary operations preserve Schmidt coefficients. They therefore cannot turn the Bell vector into an arbitrary product vector by a deterministic transformation between pure states.

For the exact calculation, apply the four matrix units E_{ab} to each seed matrix, flatten the outputs, and compute their column rank. The observed dimensions are two and four, respectively. The calculation directly exhibits the independent rows counted by the theorem.

> **Read this as:** Schmidt rank measures the remote multiplicity directions accessible to the local operator span. It is not permission for unrestricted deterministic local state preparation.

V5 / AN EXACT MULTIPLICITY LOWER BOUND

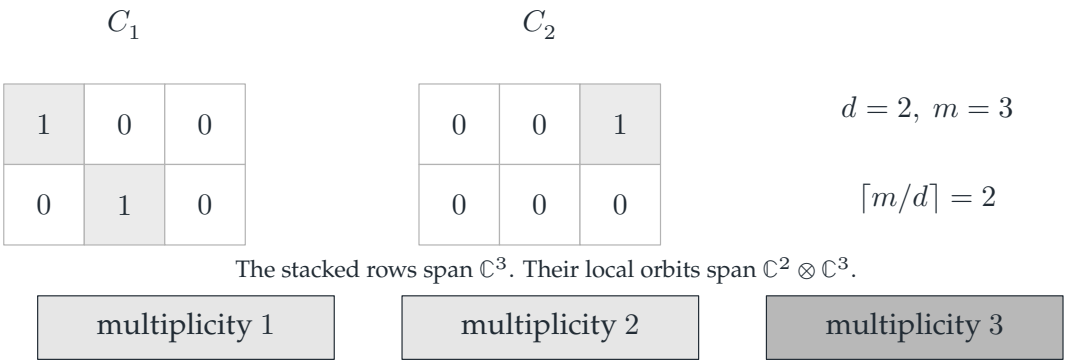
Why one seed is not always enough

Traditional edition: Theorem II.2.3.

Consider $M_2(\mathbb{C}) \otimes I_3$ acting on $\mathbb{C}^2 \otimes \mathbb{C}^3$. A seed is a 2×3 coefficient matrix. Its two rows span at most two directions in the three-dimensional multiplicity factor. Therefore no single seed is cyclic for this algebra.

$$C_1 = \begin{pmatrix} 1 & 0 & 0 \\ 0 & 1 & 0 \end{pmatrix}, \qquad C_2 = \begin{pmatrix} 0 & 0 & 1 \\ 0 & 0 & 0 \end{pmatrix}.$$

These two matrices provide a complete set of row directions. Their individual orbit dimensions are four and two, and together those spans fill the six-dimensional state space.



From the example to the finite formula

For a block $M_d(\mathbb{C}) \otimes I_m$, k seed matrices contribute at most kd independent multiplicity directions. Hence $k \geq \lceil m/d \rceil$. Partitioning a multiplicity basis into groups of size at most d attains this bound. For a direct sum of such blocks, the worst block determines the required count:

$$\operatorname{srank}_{\mathcal{A}}(\mathcal{H}) = \max_i \lceil m_i/d_i \rceil.$$

This is an invariant of the declared representation of the algebra, and depends on more than the dimension of the Hilbert space alone. If the available algebra were enlarged to the full matrix algebra on $\mathbb{C}^6$, every nonzero seed would instead be cyclic.

The example checks both the ranks of the separate coefficient matrices and the rank three of their stacked row matrix. The argument explains why the construction meets the lower bound and therefore proves minimality.

> **Read this as:** Missing multiplicity directions cannot be created by reusing the same left action. Adding seeds and enlarging the operator algebra provide different ways to supply those directions.

V6 / CHARACTER PROJECTORS YOU CAN MULTIPLY

Four phases resolve a cyclic shift

Traditional edition: Corollary II.3.3.

On four sites, let $S\,|k\rangle = |k+1 \bmod 4\rangle$ and let $\omega = \mathrm{i}$. The character projectors are the exact matrices

$$P_j = \frac{1}{4}\sum_{r=0}^{3} \mathrm{i}^{-jr} S^r, \qquad v_j(k) = \frac{1}{2}\mathrm{i}^{-jk}, \qquad P_j = v_j v_j^*.$$

All entries belong to the Gaussian rationals. Thus no approximation to a root of unity is needed in this model.

$2V$, with $V^*V = I$

	$j=0$	$j=1$	$j=2$	$j=3$
site 0	1	1	1	1
site 1	1	$-i$	-1	i
site 2	1	-1	1	-1
site 3	1	i	-1	$-i$

$$Sv_0 = 1v_0 \qquad P_0 = v_0 v_0^*$$

$$Sv_1 = iv_1 \qquad P_1 = v_1 v_1^*$$

$$Sv_2 = -1v_2 \qquad P_2 = v_2 v_2^*$$

$$Sv_3 = -iv_3 \qquad P_3 = v_3 v_3^*$$

Each column has four entries of magnitude $1/2$.

Reading the columns

Each column v_j is a normalized wave around the four sites. Advancing the address multiplies it by i^j. The entries show phase differences rather than four different probability distributions: every column has uniform site probability $1/4$.

Multiplying the actual projectors gives $P_jP_k = 0$ for $j \neq k$, $P_j^2 = P_j$, and $\sum_j P_j = I$. In particular, the complete packet tuple $(P_j\psi)_j$ retains the original vector exactly. Recording only the four packet norms is a different operation and can discard phase information between packets.

The same shift on four sites returns on V27, where it diagonalizes the Hamiltonian $L = 2I - S - S^*$, and its four character phases explain perfect transfer between opposite sites. The same fixed projectors serve as coordinates, symmetry sectors, and a complete interference ledger.

> **Read this as:** A character projector retains a complex subspace component. Its norm summarizes the size of that component while leaving its phase and direction unspecified.

V7 / TENSOR REFINEMENT BY TOTAL PARITY

A coarse packet can still contain coherence

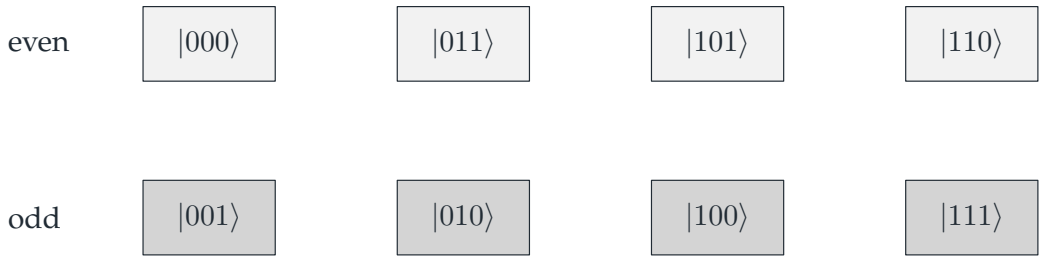
Traditional edition: Theorem II.3.7, Corollary II.3.8.

For three qubits, the eight fine projectors are $P_a = |a\rangle\langle a|$. Grouping addresses according to the parity of their Hamming weight gives

$$P_{\text{even}} = P_{000} + P_{011} + P_{101} + P_{110} = \frac{I + Z \otimes Z \otimes Z}{2}, \qquad P_{\text{odd}} = I - P_{\text{even}}.$$

This is a sum of subspaces, not an averaging of their coordinates. The rank-four even packet retains all complex amplitudes on its four children.

Each coarse projector has rank four. All eight fine projectors have rank one.



Refinement is not measurement

The fine packet description and the coarse packet description each reconstruct the full vector when every component is retained. Replacing a state by the mixture $\sum_a P_a \rho P_a$ is instead a dephasing channel. That operation removes coherence between the fine packets and can differ from dephasing only between the even and odd sectors.

For instance, a superposition of $|000\rangle$ and $|011\rangle$ lies entirely in the even packet. Its internal relative phase survives a parity measurement but is lost by a complete measurement in the computational basis if outcomes are forgotten. The two measurements use projectors from the same refinement hierarchy but expose different information.

The exact check verifies all eight addresses, their parity grouping, the rank of both coarse projectors, and equality with the tensor expression above. The general residue version replaces parity by total label modulo N and groups the tensor descendants by their summed residue.

> **Read this as:** A coarse packet is a whole subspace. Internal coherence survives a change of address description. It is lost only when an operation discards it.

V8 / INTERMEDIATE PACKETS ARE NOT FINAL PACKETS

Track the Bell state through the circuit

Traditional edition: Theorem II.4.1, Example II.4.6.

The input is $|00\rangle$. First apply a Hadamard to the first qubit, then a controlled flip:

$$|00\rangle \xrightarrow{H_{\text{Had}} \otimes I} \frac{|00\rangle + |10\rangle}{\sqrt{2}} \xrightarrow{\text{CNOT}} \frac{|00\rangle + |11\rangle}{\sqrt{2}}.$$

The displayed columns keep amplitudes, including their normalization, at every step. The middle vector occupies both parity packets. The final vector occupies only the even packet.

	seed		after $H \otimes I$		after CNOT
00	1	00	$\frac{\sqrt{2}}{2}$	00	$\frac{\sqrt{2}}{2}$
01	0	01	0	01	0
10	0	10	$\frac{\sqrt{2}}{2}$	10	0
11	0	11	0	11	$\frac{\sqrt{2}}{2}$
	even only		both parity packets		even only, with coherence

How the exact path expansion works

Insert $P_{\text{even}} + P_{\text{odd}} = I$ between the two gates. Each summand records a particular intermediate packet, while the boundary projectors select its input and output packets. Summing all terms recovers the original 4×4 circuit matrix:

$$\sum_{a,b,c} P_b \,\text{CNOT}\, P_a (H_{\text{Had}} \otimes I) P_c = \text{CNOT}(H_{\text{Had}} \otimes I).$$

This expansion is an identity even though the intermediate parity is not measured. Physically inserting a measurement would alter the problem by removing interference between its alternatives. The derivation resolves intermediate coordinates without physically measuring them.

In the finite check, all eight matrix terms indexed by parity are constructed and summed. The matrix equality is checked before specializing to the input vector. It therefore verifies the decomposition for every input of this example, not merely agreement on the Bell seed.

> **Read this as:** A final invariant packet does not imply that each preceding gate preserved it. Follow the amplitudes through the actual intermediate resolutions.

V9 / HOW TWO PATH AMPLITUDES CANCEL

Why path probabilities do not add

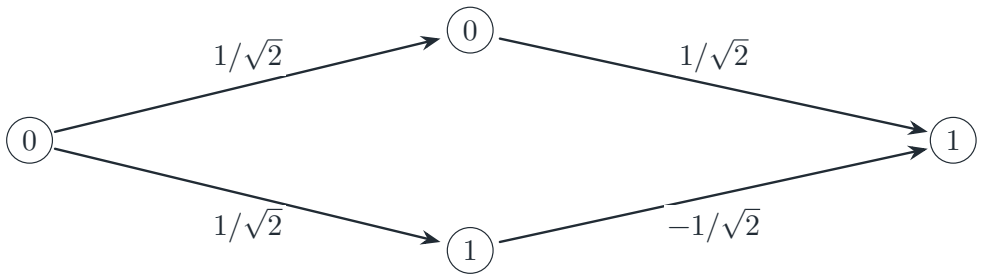
Traditional edition: Theorem II.4.2, Theorem II.4.4.

Two consecutive Hadamard gates multiply to the identity. Starting from $|0\rangle$, there are two resolved paths to output $|1\rangle$. Their signed products are

$$\langle 1|\, H_{\mathrm{Had}}\, |0\rangle\, \langle 0|\, H_{\mathrm{Had}}\, |0\rangle = \frac{1}{2}, \qquad \langle 1|\, H_{\mathrm{Had}}\, |1\rangle\, \langle 1|\, H_{\mathrm{Had}}\, |0\rangle = -\frac{1}{2}.$$

Their sum is zero. Squaring each separately gives a different answer.

Two actual Hadamard paths, not classical alternatives



$$\text{amplitude} = 1/2 - 1/2 = 0 \quad \neq \quad \text{sum of path probabilities} = 1/2$$

Where the missing term goes

For path amplitudes a, b, the outcome probability is $|a+b|^2 = |a|^2 + |b|^2 + 2\Re(a\bar{b})$. Here the last term is $-1/2$, canceling the first two terms. The path picture retains this information only if its edges carry complex amplitudes rather than unsigned reachability or probabilities.

The packetwise unitarity identity is likewise an operator identity, including the off-diagonal cancellations:

$$\sum_b U_{ba}^* U_{bc} = \delta_{ac} P_a, \qquad U_{ba} = P_b U P_a.$$

It cannot be replaced by the assertion that every path individually has unit norm. The exact checks verify all four choices of a, c for the two rank-one packets, as well as the two path products leading to the opposite output.

A measurement at the intermediate stage would remove the cross term. In that modified experiment the two alternatives really would contribute total probability $1/2$ to output one. Adding the two path probabilities would therefore describe the experiment with an intermediate measurement.

> **Read this as:** Insert projectors algebraically to resolve paths, then add amplitudes. Add probabilities only when the physical setup has actually made the alternatives incoherent.

V10 / ONE HAMILTONIAN IN TWO ORDERS

A symmetry reveals blocks, not approximations

Traditional edition: Theorem II.5.1.

Take the exact rational Hamiltonian

$$H = X \otimes X + \frac{3}{8}(Z \otimes I + I \otimes Z).$$

It commutes with total parity $Z \otimes Z$. Reordering the computational basis into even addresses $(00, 11)$ and odd addresses $(01, 10)$ displays the invariant subspaces explicitly.

Computational order

	00	01	10	11
00	$\frac{3}{4}$	0	0	1
01	0	0	1	0
10	0	1	0	0
11	1	0	0	$-\frac{3}{4}$

same operator
different order

Parity order

	00	11	01	10
00	$\frac{3}{4}$	1	0	0
11	1	$-\frac{3}{4}$	0	0
01	0	0	0	1
10	0	0	1	0

Even eigenvalues: $\pm 5/4$. Odd eigenvalues: ± 1.

$$H_{\text{even}} = \begin{pmatrix} 3/4 & 1 \\ 1 & -3/4 \end{pmatrix}, \qquad H_{\text{odd}} = \begin{pmatrix} 0 & 1 \\ 1 & 0 \end{pmatrix}.$$

The even block squares to $(25/16)I$, so its eigenvalues are $\pm 5/4$. The odd block squares to I, so its eigenvalues are ± 1. Exponentiating either block gives the corresponding part of the exact evolution. Transfer between the packets remains zero for every real time.

What has changed?

Only the order of basis vectors has changed. No matrix entries, amplitudes, or energy levels were discarded. This is why the decomposition is exact. Keeping just the even block would be a separate restriction of the state space, justified for initial data known to be even and for dynamics that preserve it.

The next page breaks a symmetry in a smaller model. There the entries coupling the packets no longer vanish, so their effect needs an explicit bound. The exact tests here multiply the commutator, verify the displayed permutation, and compute all four eigenvalues symbolically.

> **Read this as:** Block diagonalization uses an invariant decomposition already present in the operator. It is not evidence that an arbitrary chosen packet is invariant.

V11 / COMMUTATORS AND PROBABILITY BOUNDS

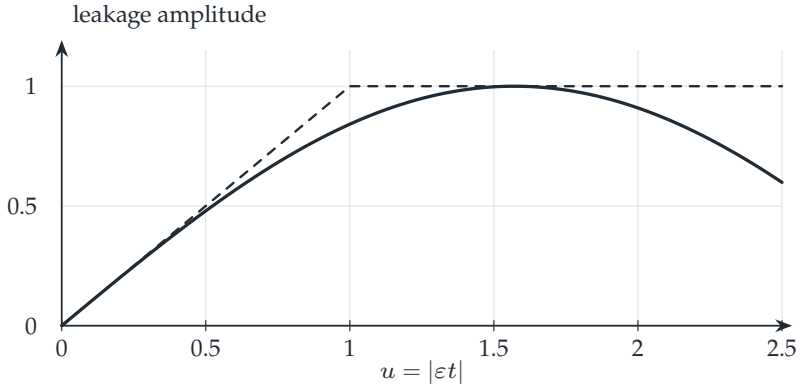
Quantify the amplitude that escapes

Traditional edition: Theorem II.5.3, Corollary II.5.4.

For a two-level system, choose $H = \varepsilon X$, $P = |0\rangle\langle 0|$, and $Q = I - P$. Direct exponentiation gives

$$e^{-\mathrm{i}tH} = \cos(\varepsilon t) I - \mathrm{i}\sin(\varepsilon t) X, \quad \left\| Q e^{-\mathrm{i}tH} P \right\| = |\sin(\varepsilon t)|, \quad \|[H, P]\| = |\varepsilon|.$$

The general commutator estimate becomes the elementary bound $|\sin u| \le |u|$. Unitarity also bounds the amplitude by one.



$H = \varepsilon X$

solid: $|\sin u|$
dashed: $\min(1, u)$

Probability is $\sin^2 u$,
not $|\sin u|$.

From a norm to a probability

For this initial state, the escape probability is $\sin^2(\varepsilon t)$, not $|\sin(\varepsilon t)|$. Consequently

$$\Pr(\text{hidden packet at } t) \le \min\{1, \varepsilon^2 t^2\}.$$

At $\varepsilon t = \pi/6$, the amplitude is $1/2$ and the probability is $1/4$. Near zero, amplitudes are first order while escape probabilities are second order. Mixing those two quantities produces an incorrect interpretation of a leakage plot.

The figure displays samples of the explicit functions above. The supporting check verifies the exact exponential identity, its unitarity, the squared leakage matrix, and the special-time value. The paper's theorem supplies the bound for all times within its stated scope.

At larger times amplitude can return from the hidden packet. The commutator bound therefore limits the largest possible leakage without predicting that it must rise monotonically.

> **Read this as:** The norm estimate controls amplitude. For a normalized state, square it to obtain a probability bound, and retain the distinction between a bound and the actual oscillatory dynamics.

V12 / NOT ALL MOTION IS PHYSICAL EVOLUTION

A moving frame creates a connection term

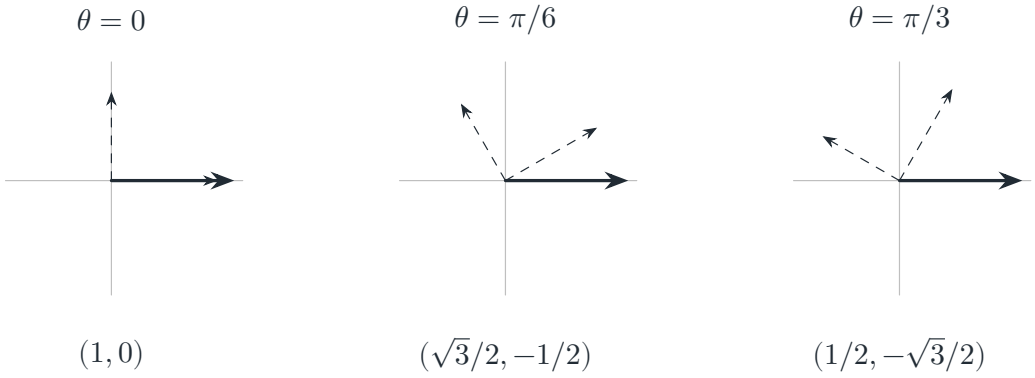
Traditional edition: Theorem II.6.3.

Set the laboratory Hamiltonian to zero and keep $\psi(t) = |0\rangle$ fixed. Describe it in rotating coordinates,

$$U(t) = \begin{pmatrix} \cos t & -\sin t \\ \sin t & \cos t \end{pmatrix}, \qquad y(t) = U(t)^* \psi(t) = \begin{pmatrix} \cos t \\ -\sin t \end{pmatrix}.$$

The vector has not moved in the laboratory, but its coordinate entries have changed.

Solid vector: fixed in the laboratory. Dashed axes: rotating frame.



The missing term can be computed exactly

Let $J = \begin{pmatrix} 0 & -1 \\ 1 & 0 \end{pmatrix}$. Since $U^*\dot{U} = J$, the coordinate Hamiltonian is

$$H_{\text{frame}} = -\mathrm{i}J = \begin{pmatrix} 0 & \mathrm{i} \\ -\mathrm{i} & 0 \end{pmatrix}, \qquad \mathrm{i}\dot{y} = H_{\text{frame}} y.$$

This matrix is Hermitian. Omitting it would predict a constant y, contradicting the displayed coordinates. In this example the norm of the omitted time derivative is exactly one, so the failure is not a small numerical residual.

For a nonzero laboratory Hamiltonian, the same product rule adds the transformed physical term U^*HU. Thus $U^*HU - \mathrm{i}U^*\dot{U}$ separates the physical generator from the coordinate correction. Both pieces belong to the same equation but have different origins.

The drawing shows actual rotated axes at three angles, not three different laboratory trajectories. The check differentiates the exact matrices and verifies the coordinate Schrödinger equation symbolically. The explicit derivatives make a numerical difference approximation unnecessary.

> **Read this as:** When coordinates move, even a stationary physical vector acquires changing components. The connection term accounts for that change without adding a force to the laboratory system.

V13 / THE CANONICAL PACKET CONNECTION

Differentiate the subspace itself

Traditional edition: Theorem II.6.1, Theorem II.6.2.

Continue with $P(t) = U(t)\,\mathrm{diag}(1,0)U(t)^*$ and $Q(t) = I - P(t)$. Differentiating $P^2 = P$ gives

$$\dot{P}P + P\dot{P} = \dot{P}, \qquad P\dot{P}P = 0.$$

The second identity says that the derivative has no component entirely inside the current packet. It moves the subspace relative to its complement.

$P(0)$

1	0
0	0

$\dot{P}(0)$

0	1
1	0

C

0	-1
1	0

$$P\dot{P}P = 0, \qquad C^* = -C, \qquad [C, P] = \dot{P}.$$

For this complete pair of packets, define

$$C = \dot{P}P + \dot{Q}Q.$$

Exact calculation yields the constant matrix $C = J$, with $C^* = -C$ and $[C, P] = \dot{P}$. At $t = 0$, the displayed small matrices allow these identities to be checked by direct multiplication.

From two packets to a complete family

For differentiable orthogonal projectors P_a summing to the identity, the paper constructs

$$C = \sum_a \dot{P}_a P_a = \frac{1}{2}\sum_a [\dot{P}_a, P_a].$$

This single connection reproduces the motion of every packet in the family. No basis within a packet is needed for this formula. A basis choice would add internal coordinate data without changing which subspaces are selected.

The completeness of the family matters in deriving skew-Hermiticity and the simultaneous transport identities. Using only one summand of an incomplete list is not automatically the same connection. The example retains both P and Q throughout, even when the picture emphasizes only the first line.

> **Read this as:** The projector derivative describes motion between subspaces. The canonical connection reconstructs that motion from the complete family without choosing internal packet bases.

V14 / THE RANGE BUNDLE IS CONSTRUCTED LOCALLY

A chart failure is not a singular fiber

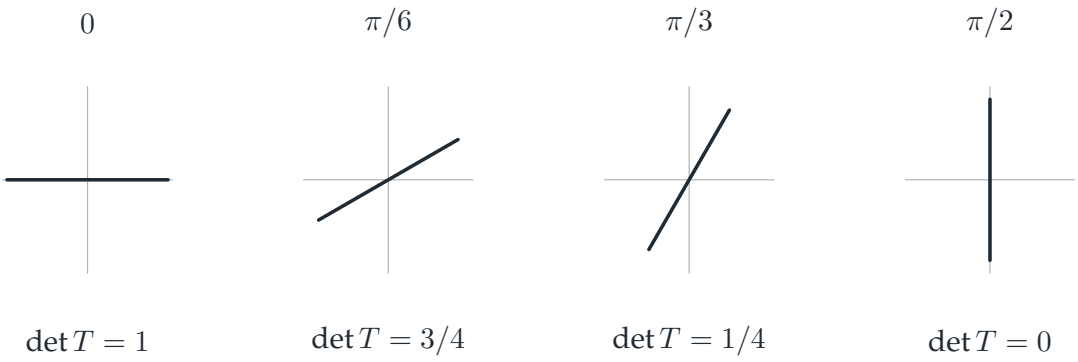
Traditional edition: Theorem II.6.7. Details of the range atlas: saved v0.6.0 supplement, pp. 2–4.

The fiber of a projector field is the actual fixed subspace $E_x = \{v : P(x)v = v\}$. To compare it with a nearby anchor fiber E_a, the completion proof constructs

$$T_a(x) = P(x)P(a) + (I - P(x))(I - P(a)).$$

It equals the identity at the anchor and intertwines the two projectors. Where it is invertible, its restriction provides local fiber coordinates.

The ranges of $P(\theta)$ are shown with a horizontal anchor.



At the last position, use a new anchor. The fiber still has dimension one.

An exact example of the domain restriction

For the rotating line and anchor $P(0)$,

$$T_0(t) = \cos t\, U(t), \qquad \det T_0(t) = \cos^2 t.$$

The chart fails at $t = \pi/2$, but $P(\pi/2) = \operatorname{diag}(0, 1)$ is a perfectly regular rank-one projector. Choosing a vertical anchor supplies a new chart there. What failed was the comparison with one reference fiber, not the fiber itself.

In general, the open sets where $T_a(x)$ is invertible cover the base. The inverse chart maps and smooth overlap maps are constructed from the actual matrices. Their cocycle identities express consistent coordinate changes, rather than assuming a global basis exists.

The v0.6.0 supplement proves the intrinsic connection and its curvature using actual manifold derivatives. Its scope includes bounded idempotents, not only orthogonal ones. The illustration uses a finite-dimensional orthogonal projector to make the construction visible. Those simplifying choices do not restrict the recorded theorem.

> **Read this as:** A smooth bundle is built from compatible local charts. The singularity of one chart determinant can be harmless, provided another anchor covers the same smooth fiber.

V15 / AN EXACT BLOCH PROJECTOR CALCULATION

Curvature measures a local area response

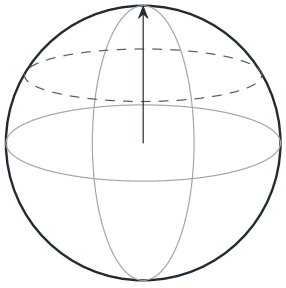
Traditional edition: Theorem II.6.7, Corollary II.6.8.

On the unit sphere, set $n = (\sin\theta\cos\phi, \sin\theta\sin\phi, \cos\theta)$ and

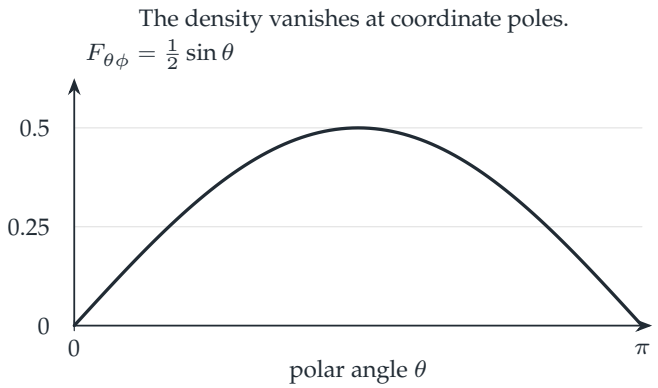
$$P(\theta,\phi) = \frac{1}{2}(I + n\cdot\sigma).$$

This is a smooth rank-one orthogonal projector. The intrinsic curvature is the endomorphism-valued two-form $P(\,\mathrm{d}P \wedge \mathrm{d}P)P$. With the paper's scalar convention, its component is

$$F_{\theta\phi} = -\mathrm{i}\,\mathrm{Tr}\big(P[\partial_\theta P, \partial_\phi P]\big) = \frac{1}{2}\sin\theta.$$



Cap flux at $\theta = \pi/3$ is $\pi/2$.



A local frame gives the same answer

Away from the south pole, use $u_N = (\cos(\theta/2), e^{\mathrm{i}\phi}\sin(\theta/2))^T$. Then $P = u_N u_N^*$ and the scalar one-form is

$$A_N = -\mathrm{i}u_N^*\,\mathrm{d}u_N = \frac{1-\cos\theta}{2}\,\mathrm{d}\phi, \qquad \mathrm{d}A_N = \frac{1}{2}\sin\theta\,\mathrm{d}\theta\wedge\mathrm{d}\phi.$$

Thus the curvature flux through the cap $0 \le \theta \le \theta_0$ is $\pi(1-\cos\theta_0)$. At $\theta_0 = \pi/3$, it is exactly $\pi/2$. The latitude drawn in the plate illustrates this cap. The exact flux comes from the formula above.

The vanishing of the coordinate density at a pole does not mean the geometric curvature disappears there. The spherical area form also carries the factor $\sin\theta$. Assigning a phase to parallel transport also requires an orientation and a sign convention for the connection. These choices determine how flux relates to phase.

> **Read this as:** The projector formula and a local frame calculation agree. Curvature is intrinsic even when no single smooth frame covers the whole sphere.

V16 / THE ANSWER DEPENDS ON ITS EFFECTS

Which coherence can a measurement see?

Traditional edition: Theorem II.7.2, Theorem II.7.4, Corollary II.7.5.

For the Bell density matrix $\rho = |\Phi^+\rangle\langle\Phi^+|$, parity dephasing does nothing: both nonzero amplitudes already lie in the even subspace. Dephasing in the computational basis removes the entries between addresses 00 and 11.

2ρ, also $2D_{\text{parity}}(\rho)$

	00	01	10	11
00	1	0	0	1
01	0	0	0	0
10	0	0	0	0
11	1	0	0	1

same diagonal
different coherence

$2D_{\text{computational}}(\rho)$

	00	01	10	11
00	1	0	0	0
01	0	0	0	0
10	0	0	0	0
11	0	0	0	1

Bell-projector outcome: 1 on the left, $1/2$ on the right.

Every effect in the computational basis $E_a = |a\rangle\langle a|$ has the same expectation on both matrices, namely $1/2$ at 00 and 11 and zero elsewhere. These measurements read only the diagonal. They cannot distinguish the pure Bell state from this incoherent mixture.

A measurement that resolves the difference

Use the valid two-outcome measurement with effects $E = \rho$ and $I - E$. Then

$$\operatorname{Tr}(E\rho) = 1, \qquad \operatorname{Tr}\Big(ED_{\text{computational}}(\rho)\Big) = \frac{1}{2}.$$

The effect itself is not diagonal in the fine computational packets. It compares their coherent combination, so it falls outside the paper's invariance result for block-diagonal effects.

This example contains three operations that should not be conflated: representing a state by all of its packet matrix blocks, applying a dephasing channel, and reading one specified measurement. Only the second discards the off-diagonal blocks. The third may or may not notice that loss, depending on its effects.

The exact checks construct all four fine projectors, both parity projectors, both dephased states, and the outcome traces. They reject the stronger statement that *every* measurement is invariant under dephasing.

> **Read this as:** A measurement's inability to see a coherence does not make that coherence absent. It states a restriction on the observable, not an equality of the underlying states.

V17 / POPULATIONS AND COHERENCES TRANSFORM DIFFERENTLY

A channel acts on four matrix entries

Traditional edition: Theorem II.7.6, Example II.7.12.

Choose amplitude damping with $\gamma = 9/25$:

$$K_0 = \begin{pmatrix} 1 & 0 \\ 0 & 4/5 \end{pmatrix}, \qquad K_1 = \begin{pmatrix} 0 & 3/5 \\ 0 & 0 \end{pmatrix}, \qquad K_0^* K_0 + K_1^* K_1 = I.$$

The channel $\Phi(\rho) = \sum_a K_a \rho K_a^*$ is trace preserving and completely positive. The special parameter keeps every displayed coefficient rational.

Superoperator on matrix entries

	00	01	10	11
00	1	0	0	$\frac{9}{25}$
01	0	$\frac{4}{5}$	0	0
10	0	0	$\frac{4}{5}$	0
11	0	0	0	$\frac{16}{25}$

$\gamma = 9/25$

coherence factor $4/5$

Output from $|+\rangle$

$\frac{17}{25}$	$\frac{2}{5}$
$\frac{2}{5}$	$\frac{8}{25}$

$$\operatorname{Tr}\rho = 1, \quad \det\rho = 36/625 > 0$$

The superoperator uses the entry order $(\rho_{00}, \rho_{01}, \rho_{10}, \rho_{11})$. Population leaves the excited state with factor $9/25$, while coherences contract by $4/5$. These are not the same rate or the same coordinate.

For $\rho_+ = \frac{1}{2}\begin{pmatrix} 1 & 1 \\ 1 & 1 \end{pmatrix}$, the exact output is

$$\Phi(\rho_+) = \begin{pmatrix} 17/25 & 2/5 \\ 2/5 & 8/25 \end{pmatrix}.$$

Its trace is one and determinant is $36/625 > 0$, so it is a mixed positive state. Arrows that show population transfer alone would leave its off-diagonal entries unspecified.

How complete positivity is certified

The Choi matrix is an explicit sum of two outer products of vectorized Kraus operators. Its eigenvalues are $41/25, 9/25, 0, 0$, all nonnegative. This gives an independent finite certificate in addition to Kraus normalization. The Choi matrix has trace two under the convention used by the check, which leaves the maximally entangled vector unnormalized.

> **Read this as:** A packet channel acts on pairs of packet addresses, because density matrices have two indices. Population transfer alone does not reconstruct a quantum channel.

V18 / WHY COMPLETE POSITIVITY IS THE RELEVANT CONDITION

An ancilla tests more than positivity

Traditional edition: Classical input II.7.7.

Ordinary transpose T sends a positive matrix on one system to another positive matrix and preserves its trace. Those properties are insufficient for a quantum channel on a subsystem of an entangled state. The test must include id ⊗ T on the larger system.

$$2(\mathrm{id} \otimes \mathsf{T})(\rho_{\mathrm{Bell}})$$

00	1	0	0	0
01	0	0	1	0
10	0	1	0	0
11	0	0	0	1

$$w = (|01\rangle - |10\rangle)/\sqrt{2}$$

$$w^*(\mathrm{id} \otimes \mathsf{T})(\rho)w = -1/2$$

Transpose is positive on one system.
It is not completely positive.

Apply this extended map to the Bell density matrix. The result is

$$(\mathrm{id} \otimes \mathsf{T})(\rho_{\mathrm{Bell}}) = \frac{1}{2}\begin{pmatrix} 1 & 0 & 0 & 0 \\ 0 & 0 & 1 & 0 \\ 0 & 1 & 0 & 0 \\ 0 & 0 & 0 & 1 \end{pmatrix}.$$

Its middle block has one negative eigenvalue. More concretely, the normalized vector $w = (|01\rangle - |10\rangle)/\sqrt{2}$ satisfies

$$w^*(\mathrm{id} \otimes \mathsf{T})(\rho_{\mathrm{Bell}})w = -\frac{1}{2}.$$

This exact negative value of the quadratic form certifies failure of positivity on the composite system. No numerical eigenvalue tolerance is needed.

Why the Kraus form avoids this problem

For every auxiliary dimension and positive X, each term $(I \otimes K_a)X(I \otimes K_a)^*$ is positive. Their sum is positive as well. This argument explains the word *completely*. The conclusion holds for every auxiliary dimension, which a test of one input density matrix on the original system cannot establish.

The transpose counterexample is an explanatory finite calculation, not a new addition to the formal theorem count. It makes visible the hypothesis that the manuscript's Kraus result already supplies. The exact check constructs the partial transpose with the stated tensor indexing and evaluates its negative witness directly.

> **Read this as:** A map can look harmless on an isolated system and fail on an entangled extension. Complete positivity retains compatibility with every auxiliary system.

V19 / FOUR EXACT SYNDROME PACKETS

Find the error without reading the logical state

Traditional edition: Theorem II.8.2, Theorem II.8.4, Example II.8.8.

Encode a qubit by $|0_L\rangle = |000\rangle$ and $|1_L\rangle = |111\rangle$. Let P project onto this code and take errors $E_a \in \{I, X_1, X_2, X_3\}$. Their images are four orthogonal rank-two packets $Q_a = E_a P E_a^*$ that sum to the full identity.

Channel probabilities: $1/10,\ 2/10,\ 3/10,\ 4/10$.

no error	X_1	X_2	X_3
$\|000\rangle$	$\|100\rangle$	$\|010\rangle$	$\|001\rangle$
$\|111\rangle$	$\|011\rangle$	$\|101\rangle$	$\|110\rangle$
ratio $3:4$	ratio $3:4$	ratio $3:4$	ratio $3:4$

Use the logical state $\psi = (3\,|0_L\rangle + 4\,|1_L\rangle)/5$ and channel probabilities $w = (1, 2, 3, 4)/10$. The noisy state is $\sum_a w_a E_a \psi\psi^* E_a^*$. A syndrome measurement returns label a with probability w_a, independent of the logical amplitudes.

The recovery is an actual channel

The operators $R_a = E_a^* Q_a$ satisfy $\sum_a R_a^* R_a = I$. Applying the recovery $\mathcal{R}(X) = \sum_a R_a X R_a^*$ to the noisy state gives exactly $\psi\psi^*$. The off-diagonal logical coherence $12/25$ is recovered as well as the populations $9/25$ and $16/25$.

The Knill–Laflamme compressions are $P E_a^* E_b P = \delta_{ab} P$. Their scalar form says that the error labels do not resolve the encoded vector. The exact checks evaluate all sixteen compressions, all sixteen syndrome products, the four probabilities, the recovery normalization, and the full recovered matrix.

This code corrects the specified flips of individual bits. That result does not cover arbitrary errors on three qubits or arbitrary errors on a single qubit. The next example exhibits an error outside its protected family.

> **Read this as:** A syndrome identifies an error subspace while leaving a two-dimensional logical subspace intact. Measuring the two logical basis states separately would destroy the information the recovery must preserve.

V20 / THE SCALAR COMPRESSION TEST MATTERS

An unchanged syndrome can hide a logical error

Traditional edition: Theorem II.8.2, Proposition II.8.7.

Apply $Z_1 = Z \otimes I \otimes I$ to the same repetition code. It sends $|000\rangle$ to itself and $|111\rangle$ to its negative. Both states remain inside the original code, so the previous syndrome partition reports no bit flip.

$$\frac{3\,|000\rangle + 4\,|111\rangle}{5} \longmapsto \frac{3\,|000\rangle - 4\,|111\rangle}{5}.$$

The populations are unchanged, but the relative phase is not.

$V^* Z_1 V$

1	0
0	-1

before: $(3, 4)/5$

after: $(3, -4)/5$

same code support
different relative phase

Required scalar form cI

c	0
0	c

A trace of zero does not make $\mathrm{diag}(1, -1)$ the zero operator.

Let V be the code isometry with columns $|000\rangle, |111\rangle$. For the proposed error family $\{I, Z_1\}$, its off-diagonal error compression is

$$V^* I^* Z_1 V = \begin{pmatrix} 1 & 0 \\ 0 & -1 \end{pmatrix}.$$

This matrix is not cI for any scalar c. Thus the Knill–Laflamme condition fails for that family. Its trace is zero even though its action on the code is nonzero. A trace test alone would miss the obstruction.

Known correction versus family recovery

If it is known with certainty that Z_1 occurred, applying Z_1 again reverses it. The failed criterion concerns a *single recovery valid for every unknown error in the declared family*, not invertibility of each error considered separately. This distinction prevents a misleading conclusion that no phase error can ever be undone.

The finite calculation checks the actual compressed matrix and rejects its equality to zero. The scalar obstruction is then transparent from the two unequal diagonal entries.

> **Read this as:** Correction must preserve all logical superpositions for the declared error family. Staying in the code and preserving basis probabilities are not sufficient.

V21 / TWO INVERTIBILITY CONDITIONS, NOT ONE

Hidden states return as spectral dependence

Traditional edition: Theorem II.9.2, Theorem II.9.3.

Take $H = \begin{pmatrix} 0 & 1 \\ 1 & 2 \end{pmatrix}$ and retain its first coordinate. The eliminated block is $H_{QQ} = 2$. Whenever $z - 2$ and the full $zI - H$ are invertible,

$$H_{\text{eff}}(z) = \frac{1}{z-2}, \qquad \left[(zI - H)^{-1}\right]_{00} = \frac{1}{z - 1/(z-2)} = \frac{z-2}{z^2 - 2z - 1}.$$

This is the corrected hypothesis set recorded in the formal release.

Filled: full resolvent poles. Open at 2: only the eliminated inverse fails.



At $z = 3$: exact retained resolvent $1/2$, bare truncation $1/3$.

At $z = 3$, the exact retained resolvent is $1/2$. Bare truncation uses only $H_{PP} = 0$ and gives $1/3$, an error of $1/6$. The omitted coupling has changed the response even though the retained diagonal entry did not change.

A pole can belong to the elimination chart

At $z = 2$, the eliminated inverse does not exist, so the displayed Schur formula cannot be applied there as written. Nevertheless, the full resolvent exists and its retained entry is zero. The rational expression has a continuation to this value. By contrast, $1 \pm \sqrt{2}$ are poles of the full resolvent.

Invertibility of the full matrix is an independent requirement. At $z = 0$, $H = \operatorname{diag}(0, -1)$ has an invertible eliminated block in $zI - H$, but the full matrix is singular. The original prose omitted this condition. The preserved amendments restore it. This appendix uses the corrected form throughout.

> **Read this as:** An exact elimination formula has a spectral domain. Check both inverses before evaluating it, and distinguish poles of an intermediate inverse from poles of the full physical resolvent.

V22 / AN EXACT QUANTUM MEMORY EQUATION

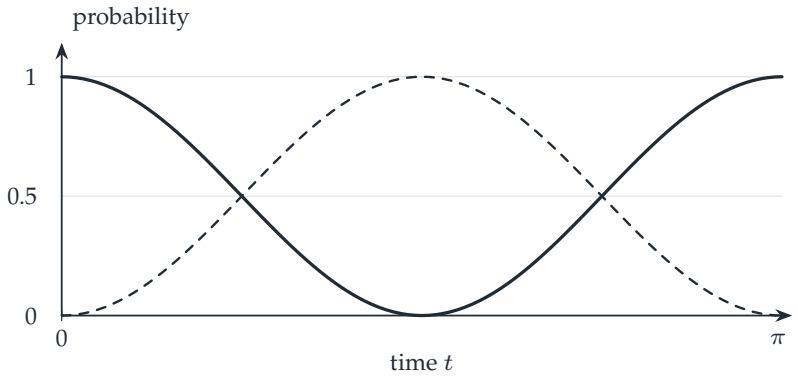
The smaller system remembers the discarded one

Traditional edition: Theorem II.9.8, Theorem II.9.11.

Choose $H = X$, initial state $(1, 0)^T$, and retain the first coordinate. The coupled equations and their solution are

$$\mathrm{i}\dot{x} = y, \qquad \mathrm{i}\dot{y} = x, \qquad x(t) = \cos t, \quad y(t) = -\mathrm{i}\sin t.$$

The hidden probability returns periodically. Deleting the hidden row and column would instead leave the zero Hamiltonian and predict $x(t) = 1$.



solid: retained
dashed: hidden

$$K(t) = 1$$

The two probabilities sum to one.

Eliminate exactly, not approximately

Integrating the second equation with $y(0) = 0$ gives $y(t) = -\mathrm{i}\int_0^t x(s)\,ds$. Substitution produces

$$\dot{x}(t) = -\int_0^t x(s)\,ds.$$

The memory kernel is the constant function one. Differentiating once more recovers $\ddot{x} = -x$ with $x(0) = 1$ and $\dot{x}(0) = 0$, explaining the cosine solution. A nonzero hidden initial state would add a forcing term that must also be retained.

The full propagator is a unitary group, but its retained scalar entry is not a semigroup. At $t = s = \pi/4$,

$$x(t + s) - x(t)x(s) = 0 - \frac{1}{2} = -\frac{1}{2}.$$

There is no contradiction: compression of a product need not equal the product of the compressed factors when the hidden subspace carries intermediate amplitude.

The check verifies the differential and integral equations symbolically and the displayed nonzero semigroup defect exactly. The curves visualize the explicit solution and its periodic return of amplitude.

> **Read this as:** Exact elimination replaces a hidden coordinate with memory and forcing from the initial data. Replacing that memory by a constant generator is an additional approximation, not part of the exact theorem.

V23 / SPECTRAL POSITIVITY IS BASIS INDEPENDENT

Positive transfer is not a stochastic matrix

Traditional edition: Theorem II.10.1, Theorem II.10.3.

For $H = I - X$, the two eigenvalues are zero and two. Its Euclidean transfer is

$$T(\tau) = e^{-\tau H} = \frac{1}{2}\begin{pmatrix} 1+q & 1-q \\ 1-q & 1+q \end{pmatrix}, \qquad q = e^{-2\tau}.$$

For $\tau \geq 0$, the eigenvalues $1, q$ lie in $(0, 1]$, and multiplying two such matrices replaces q, r by qr. This is the semigroup law in spectral coordinates.

T at $e^{-2\tau} = 1/2$

$\frac{3}{4}$	$\frac{1}{4}$
$\frac{1}{4}$	$\frac{3}{4}$

Both have spectrum $\{1, 1/2\}$.

ZTZ in another basis

$\frac{3}{4}$	$-\frac{1}{4}$
$-\frac{1}{4}$	$\frac{3}{4}$

Positive-definite operator: $v^* T v > 0$ for $v \neq 0$. Not an entrywise test.

At $q = 1/2$, the displayed T happens also to have nonnegative entries and column sums one. Conjugate by the unitary Z. The spectrum and positivity of the quadratic form are preserved, but both off-diagonal entries become $-1/4$. Thus positivity as an operator is not entrywise positivity and does not by itself give a Markov interpretation.

A useful finite positive kernel

For this nonnegative H, vectors u_a and times $t_a \geq 0$ satisfy

$$\sum_{a,b} \langle u_a, e^{-(t_a+t_b)H} u_b \rangle = \left\| \sum_a e^{-t_a H} u_a \right\|^2 \geq 0.$$

The factorization makes positivity transparent. It remains a finite operator identity. A continuum reconstruction theorem requires a compatible field structure, limits, positivity hypotheses, and the other assumptions of the chosen reconstruction framework. Each of these assumptions requires its own justification beyond the two positive eigenvalues.

The exact check verifies the matrix semigroup law as a polynomial identity in q, r and verifies the unchanged spectrum after conjugation. It rejects entrywise nonnegativity for the conjugated matrix.

> **Read this as:** Euclidean positivity refers to quadratic forms and spectral values. A stochastic interpretation or a continuum physical reconstruction needs additional structure.

V24 / THE EXACT HEAT TRACE ON FOUR SITES

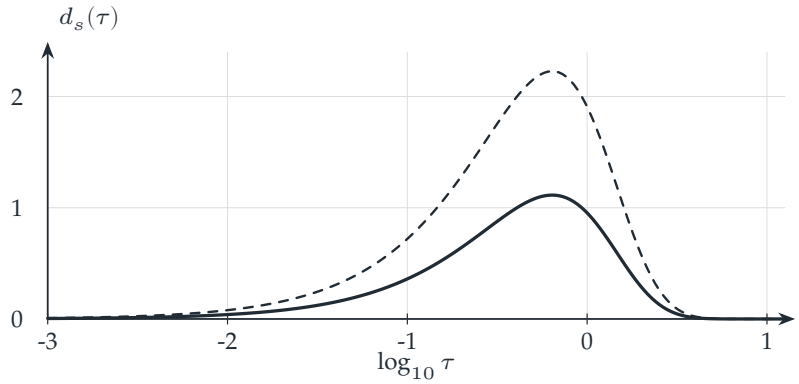
A dimension curve is a scale diagnostic

Traditional edition: Definition II.11.1, Proposition II.11.2.

For the Laplacian on a cycle with four sites $L = 2I - S - S^*$, the eigenvalues are $0, 2, 2, 4$. The normalized heat trace and its diagnostic of spectral dimension are therefore

$$K(\tau) = \frac{1 + 2e^{-2\tau} + e^{-4\tau}}{4} = \frac{(1 + e^{-2\tau})^2}{4}, \qquad d_s(\tau) = -2\tau \frac{K'(\tau)}{K(\tau)} = \frac{8\tau}{e^{2\tau} + 1}.$$

No numerical differentiation is needed for this finite example.



solid: four-cycle
dashed: product of two

No broad plateau is promised at four sites.

Finite diagnostic, not a dimension proof.

Both ends reflect the finite size of the system

As $\tau \to 0$, every eigenmode contributes approximately one and the dimension diagnostic tends to zero. As $\tau \to \infty$, the zero mode dominates, so it again tends to zero. A finite spectrum cannot sustain a nonzero plateau at all scales.

For the Cartesian product of two identical cycles with four sites, the Laplacian eigenvalues add and the heat traces multiply: $K_2 = K^2$. Consequently $d_{s,2} = 2d_s$ exactly. The product identity determines the second curve exactly from the first.

At $\tau = \log 2/2$, the first curve equals $4 \log 2/3$. This noninteger value is a spectral quantity that depends on scale, not a claim that the graph has a fractional topological dimension. Four sites are too few to promise a broad geometric plateau. Experiments on larger grids remain finite diagnostics. Convergence requires the analytic hypotheses developed on V37.

> **Read this as:** A convincing continuum dimension needs a stable scale window that persists under controlled refinement. One appealing finite curve is not that theorem.

V25 / AN EXACT ERROR ENCLOSURE, NOT A FITTED SLOPE

Refine the grid while holding the mode fixed

Traditional edition: Theorem II.11.4.

For the circle symbol, the continuum value is k^2 and the grid value is

$$\lambda_{k,h} = \frac{4}{h^2}\sin^2\left(\frac{kh}{2}\right), \qquad h \neq 0.$$

For a fixed low mode, the paper bounds the error by $0 \leq k^2 - \lambda_{k,h} \leq k^4 h^2/12$. The spacing condition matters because the displayed expression divides by h^2.

$h = \frac{1}{4}$	$h = \frac{1}{8}$	$h = \frac{1}{16}$
error (approx.)	error (approx.)	error (approx.)
$\simeq 0.005197495$	$\simeq 0.001301405$	$\simeq 0.000325478$
bound $h^2/12$	bound $h^2/12$	bound $h^2/12$
$\frac{1}{192}$	$\frac{1}{768}$	$\frac{1}{3072}$

Successive error ratios lie strictly between 3.99 and 4.

What is certified in the displayed table?

Take $k = 1$ and $h = 1/4, 1/8, 1/16$. For $x = h/2 \in [0, 1]$, alternating Taylor sums give rational lower and upper bounds for $\sin x$. Squaring these positive endpoints and multiplying by $4/h^2$ yields exact rational enclosures for each error. The displayed decimals only locate those much narrower rational intervals.

Each interval lies strictly inside $(0, h^2/12)$. Dividing successive interval endpoints proves that both error ratios are between 3.99 and 4. The check verifies these inequalities by rational arithmetic, without relying on approximate sine values or a fitted logarithmic slope.

Why the mode regime matters

If instead $k = \pi/h$ moves with the grid, the ratio $\lambda_{k,h}/k^2 = 4/\pi^2$ stays constant, not one. The bound's factor k^4 warns that it is not uniform in arbitrary moving high modes. The displayed rational test evaluates the analytic symbol. It does not assert that every chosen spacing defines an integer periodic grid.

> **Read this as:** Second-order convergence is a quantified statement with a specified mode regime. Keep that regime fixed when reading an error curve or comparing refinements.

V26 / TEST THE CONSTRAINTS BEFORE THE PROJECTION

A zero compressed anomaly can be automatic

Traditional edition: Theorem II.12.2, Proposition II.12.3.

Take the self-adjoint matrices

$$C_1 = \operatorname{diag}(0, 1, -1), \qquad C_2 = \begin{pmatrix} 0 & 0 & 0 \\ 0 & 0 & 1 \\ 0 & 1 & 0 \end{pmatrix}, \qquad P = \operatorname{diag}(1, 0, 0).$$

Both constraints annihilate $P\mathbb{C}^3$, and their common kernel is exactly that one-dimensional space. Nevertheless, their full commutator is nonzero.

$[C_1, C_2]$

0	0	0
0	0	2
0	−2	0

$P = \operatorname{diag}(1, 0, 0)$

$C_1 P = C_2 P = 0$

$P[C_1, C_2]P$

0	0	0
0	0	0
0	0	0

The right matrix is zero by the common-kernel choice, not by operator closure.

Why the compressed test cannot decide closure

Since $C_1 P = C_2 P = 0$, each product $C_1 C_2 P$ and $C_2 C_1 P$ vanishes. Therefore $P[C_1, C_2]P = 0$ without any requirement that the unprojected commutator close in the chosen constraint span. In this example the skew off-diagonal commutator is not a linear combination of the two displayed symmetric constraints.

More generally, an anomaly expression made from their commutators and linear combinations of constraints also kills an exact projector onto the common kernel on the right. The formal release records this limit of the diagnostic. A nonzero compressed residual can reveal inconsistent proposed data, but an automatic zero does not construct an anomaly-free constraint algebra.

A substantive closure analysis must inspect the operator relations, their domains, the actual physical subspace, and compatibility under refinement. For infinite systems, these questions also involve domain and limit control that finite matrix arithmetic cannot replace.

The exact example computes both constraint products, the full commutator, and its compression. It deliberately rejects the inference from compressed zero to unprojected zero.

> **Read this as:** Before interpreting a vanishing residual, check whether the definition of its projector already forces it to vanish. A tautological diagnostic cannot supply the missing existence or closure theorem.

V27 / SEEDS, CHARACTERS, INTERFERENCE, AND DEPHASING

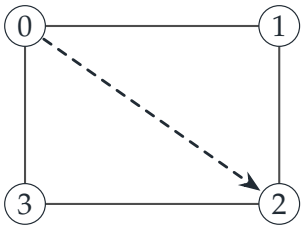
One calculation of transfer to the opposite site

Traditional edition: Corollary II.3.3, Theorem II.4.4, Theorem II.7.4.

Return to the shift on four sites S and Laplacian $L = 2I - S - S^*$. The same character projectors have energies $(0, 2, 4, 2)$. At time $t = \pi/2$, their evolution phases are $(1, -1, 1, -1)$, exactly the character eigenvalues of S^2. Hence

$$e^{-\mathrm{i}\pi L/2} = S^2, \qquad |0\rangle \longmapsto |2\rangle .$$

$e^{-\mathrm{i}\pi L/2} = S^2$



start

1
0
0
0

time $\pi/2$

0
0
1
0

Target probability after partial momentum dephasing: $1 - 3\eta/4$.

At halfway time $\pi/4$, the actual amplitude vector is $(-\mathrm{i}, 1, \mathrm{i}, 1)^T/2$, giving uniform site probabilities. The subsequent phases recombine those four amplitudes into a single output at the opposite site. Uniform intermediate probabilities do not imply an incoherent intermediate state.

A channel changes the conclusion predictably

Before evolving, mix the seed density matrix with its complete momentum dephasing:

$$\rho_\eta = (1-\eta)\,|0\rangle\langle 0| + \eta \sum_j P_j\,|0\rangle\langle 0|\,P_j = (1-\eta)\,|0\rangle\langle 0| + \eta I/4, \quad 0 \le \eta \le 1.$$

At transfer time, the probability at the opposite site is exactly $1 - 3\eta/4$. Complete momentum dephasing reduces it to $1/4$. This calculation isolates how discarded coherence changes the interference result.

Finally, the shift grammar generates four independent vectors from $|0\rangle$, while the Hamiltonian powers generate only three: its repeated energy links two momentum directions. The same seed can therefore be cyclic for the shift algebra and noncyclic for the Hamiltonian algebra, even though perfect transfer occurs at one time.

> **Read this as:** Perfect transfer is an exact finite interference statement. It neither implies cyclicity for every operator grammar nor survives an unaccounted dephasing operation.

V28 / AN EVIDENCE GUIDE FOR THE READER

What these pictures establish

Traditional edition: Section II.14. Saved formal scope: v0.6.0 ledger and completion supplement.

The appendix uses small objects to make the paper's constructions inspectable. Every matrix and finite example is supplied in editable source, with a separate check record. The plates make those calculations visible. Their appearance helps explain the result, while the equations and check records supply its evidence.

Evidence	What it supports	What it does not supply
Exact matrices	The displayed finite identities, witnesses, and counterexamples.	A classification of arbitrary systems.
Symbolic derivatives	The explicit rotating and Bloch examples.	A proof inferred from numerical differentiation.
Rational enclosures	The three displayed dispersion intervals and ratio inequalities.	A continuum theorem from three sample points.
Saved Lean release	Its 19 registered finite items under their recorded hypotheses.	A fresh kernel run for this appendix.
Numerical record	The original finite software examples in the tested environment.	Physical experiments or unrestricted convergence.

Which source is authoritative?

The saved formal checkpoint is v0.6.0: 323 recorded theorem declarations in 25 current modules, including supporting lemmas. These counts describe the inherited checkpoint. This prose revision includes no new Lean kernel execution. The final traditional edition supplies the current reading references. The original proof sources and the separate v0.5.1 editorial sibling retain their own identities.

The five research boundaries remain separate: an anomaly-free coherent refinement, uniform control of effective operators, Lorentzian reconstruction, an Einstein infrared limit, and a positive physical massless spin-two sector. A finite projector bundle, positive transfer matrix, or spectral diagnostic does not settle them.

A practical way to use the appendix

Choose one page, reproduce its matrix calculation, and then read the cited theorem with its hypotheses. The retained execution records give the exact assertions, tested ranges, and rejected controls for the finite and symbolic suites. The additional examples and their recorded bounds are described on V40. In particular, retain the two resolvent assumptions on V21, the distinction between a known error and an error family on V20, and the limitation of testing only the common kernel on V26.

> **Read this as:** Exact finite structure is valuable because its boundary is explicit. The appendix adds understanding and reproducibility, not unproved continuum claims or a new theorem count.

V29 / A SIX-DIMENSIONAL REGULAR REPRESENTATION

Nonabelian packets carry multiplicity

Traditional edition: Theorem II.3.1, Theorem II.3.2.

Let $\mathcal{H} = \mathbb{C}[S_3]$ have the six orthonormal basis vectors $|g\rangle$, with left action $U(h)\,|g\rangle = |hg\rangle$. The irreducible characters on the identity, transposition, and three-cycle classes are

	e	(12)	(123)	d_λ
trivial	1	1	1	1
sign	1	-1	1	1
standard	2	0	-1	2

$$P_\lambda = \frac{d_\lambda}{6} \sum_{g \in S_3} \chi_\lambda(g^{-1}) U(g).$$

All matrices in this example are rational. Multiplying them gives self-adjoint idempotents of ranks $1, 1, 4$, with pairwise zero products and sum I_6.



$$\mathbb{C}[S_3] \cong \mathbb{C} \oplus \mathbb{C} \oplus (\mathbb{C}^2 \otimes \mathbb{C}^2)$$

The standard packet has dimension four

The standard representation occurs twice in the regular representation. Its isotypic component therefore has dimension $2 \cdot 2 = 4$: one factor carries the two-dimensional irreducible action and the other records multiplicity. A character projector selects the whole isotypic component. It does not select a particular copy or a particular internal vector.

Representation matrix units refine the irreducible factor, while leaving the multiplicity factor untouched. Their multiplication law is stronger information than a list of packet ranks. A basis chosen inside this packet supplies coordinates. It does not canonically distinguish the two copies of the standard representation.

What the retained check establishes

The retained exact check constructs all six permutation matrices, tests all 36 multiplication relations, computes the character averages, and checks ranks independently by Gaussian elimination and traces. It rejects the claim that the standard isotypic projector has rank two. This is one specified representation of S_3, not a computational classification of all finite group representations.

> **Read this as:** For a nonabelian symmetry, distinguish irreducible dimension from multiplicity. A central character projector retains both.

V30 / AN EXACT LOCAL CHART AND ITS FAILURE

Rotate whole packets by a polar factor

Traditional edition: Theorem II.6.5, Theorem II.6.6.

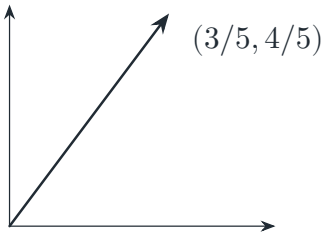
On $\mathcal{H} = \mathbb{C}^2$, put $P_0 = \operatorname{diag}(1,0)$, $P_1 = I - P_0$, and

$$R = \begin{pmatrix} 3/5 & -4/5 \\ 4/5 & 3/5 \end{pmatrix}, \qquad Q_a = RP_aR^*, \qquad S = \sum_{a=0}^{1} Q_aP_a = \frac{3}{5}R.$$

The exact Gram matrices give

$$(S-I)^*(S-I) = \frac{16}{25}I, \quad S^*S = \frac{9}{25}I, \quad \|S-I\| = \frac{4}{5} < 1.$$

Consequently the unitary polar factor is $S(S^*S)^{-1/2} = R$, and $Q_aR = RP_a$ for both complete packets.



$$S = (3/5)R$$
$$S^*S = (9/25)I$$
$$\downarrow$$
$$S(S^*S)^{-1/2} = R$$

The norm condition selects a chart

If the target rank-one packet is orthogonal to the initial one, the two labels are exchanged and $S = 0$. Its polar inverse square root is undefined. This is a failure of this direct local construction, although a unitary carrying one packet system to the other still exists. The strict norm assumption is sufficient, not a global existence criterion for all packet rotations.

Short steps can be composed before reaching a distant endpoint. For example, the rational step $R_1 = \begin{pmatrix} 4/5 & -3/5 \\ 3/5 & 4/5 \end{pmatrix}$ obeys

$$R_1^2 = \begin{pmatrix} 7/25 & -24/25 \\ 24/25 & 7/25 \end{pmatrix}.$$

The multiplication is exact and each step has a valid local overlap. The convergence theorem has a separate analytic contract: a twice continuously differentiable complete projector path on a compact time interval, sufficiently fine partitions, and a constant depending on the path in an $O(|\pi|)$ estimate in operator norm.

Evidence boundary

The retained run checks the Gram identities, polar factor, intertwining, and product of two rational steps. It also checks that the overlap has rank zero when the endpoint packets are orthogonal. It does not certify the analytic convergence theorem by sampling a path.

> **Read this as:** A local polar chart can fail while the subspaces remain regular. Use the stated chart hypothesis and the separate convergence theorem when composing small rotations.

V31 / CHANNEL, CHOI, AND GENERATOR CHECKS

Coherence order survives a covariant channel

Traditional edition: Theorem II.7.8, Theorem II.7.10, Theorem II.7.14.

Take $S = Z = \operatorname{diag}(1, -1)$ on $\mathbb{C}^2$. Under conjugation $X \mapsto ZXZ$, diagonal matrices have coherence order zero and off-diagonal matrices have coherence order one modulo two. Its projectors on Hilbert–Schmidt operator space are $\mathcal{L}_0(X) = (X + ZXZ)/2$ and $\mathcal{L}_1(X) = (X - ZXZ)/2$.

Choose amplitude damping with $K_0 = \operatorname{diag}(1, 4/5)$ and $K_1 = (3/5)\,|0\rangle\langle 1|$. The channel is trace preserving, population flows from state one to state zero, and each coherence contracts by $4/5$.

even Choi addresses $00, 11$	odd Choi addresses $01, 10$
$\begin{pmatrix} 1 & 4/5 \\ 4/5 & 16/25 \end{pmatrix}$	$\operatorname{diag}(9/25, 0)$

$$\Phi(|0\rangle\langle 1|) = (4/5)\,|0\rangle\langle 1|$$

With the unnormalized Choi convention $J = \sum_{a,b} \Phi(|a\rangle\langle b|) \otimes |a\rangle\langle b|$ and basis $(00, 01, 10, 11)$, the exact matrix is

$$J = \begin{pmatrix} 1 & 0 & 0 & 4/5 \\ 0 & 9/25 & 0 & 0 \\ 0 & 0 & 0 & 0 \\ 4/5 & 0 & 0 & 16/25 \end{pmatrix}, \qquad [J, Z \otimes Z] = 0.$$

The $00, 11$ block is positive and has rank one. The other nonzero eigenvalue is $9/25$. The retained check also verifies that every principal minor is nonnegative.

Symmetry in continuous time has its own hypotheses

For the Lindblad generator with Hamiltonian $H = \operatorname{diag}(0, 2)$ and jump $L = (3/5)\,|0\rangle\langle 1|$, H has charge zero and L has charge one. Each matrix unit stays within its coherence order under the generator. Replacing H by X breaks that conclusion: the generator then sends a diagonal matrix to off-diagonal entries.

All four input matrix units are checked exactly for channel covariance, generator order preservation, and zero generator trace. The paper uses the finite exponential series to extend generator invariance to the semigroup. The retained calculation uses no numerical solver for the master equation. Symmetry alone does not close the scalar population equations inside packets of higher rank.

> **Read this as:** Charge is a property of operator space. Covariance preserves its coherent sectors, while complete positivity is checked separately through Kraus or Choi data.

V32 / A TOTAL CHANNEL FROM SINGULAR ERROR DATA

Null Gram directions are removed before recovery

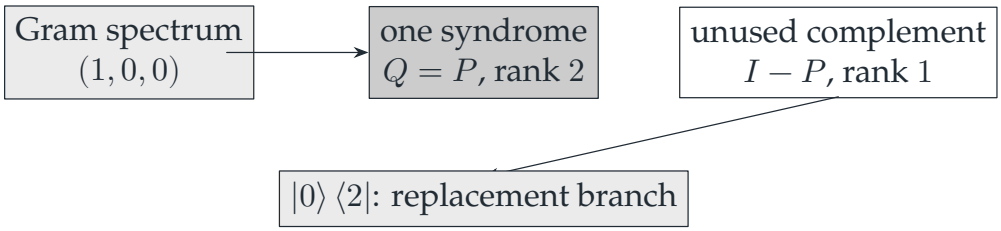
Traditional edition: Theorem II.8.3, Theorem II.8.4.

Let $\mathcal{H} = \mathbb{C}^3$, with nonzero code projector $P = \mathrm{diag}(1, 1, 0)$. On the code use the error family $E_1 = (3/5)P$, $E_2 = (4/5)P$, and $E_3 = 0$. Its Knill–Laflamme Gram matrix is

$$c = \frac{1}{25}\begin{pmatrix} 9 & 12 & 0 \\ 12 & 16 & 0 \\ 0 & 0 & 0 \end{pmatrix}, \qquad PE_a^* E_b P = c_{ab} P.$$

The errors are redundant rather than three distinct syndromes. A real unitary change of error coordinates gives

$$W = \begin{pmatrix} 3/5 & 4/5 & 0 \\ -4/5 & 3/5 & 0 \\ 0 & 0 & 1 \end{pmatrix}, \quad WcW^* = \mathrm{diag}(1, 0, 0), \quad (F_1, F_2, F_3) = (P, 0, 0).$$



Normalize only positive eigenvalues

The positive branch has $V_1 = P$ as an isometry *on the code*, and syndrome support $Q = P$. No factor $\lambda^{-1/2}$ is formed on either zero branch: those branches vanish on the code. Treating them as extra recoverable packets would divide by zero.

The syndrome support is smaller than the ambient space. Define a total recovery with Kraus operators

$$R_1 = P, \qquad R_2 = |0\rangle\langle 2|, \qquad R_1^* R_1 + R_2^* R_2 = I_3.$$

It acts as the identity on operators supported on the code and sends the unused complement population into a chosen code state. The declared error map preserves the trace of code states, so recovery returns every code matrix unit, including both off-diagonal units, exactly. It need not preserve states on the unused complement.

Exceptional cases and scope

This construction assumes a nonzero code so that a complement replacement state exists. The case of a zero code is vacuous and has its own formal statement in the saved ledger. The retained exact run verifies all nine Gram compressions, the diagonalization, both null branches, total channel normalization, and all four code matrix units. It adds no Lean coverage and does not implement a numerical spectral decoder for arbitrary Gram data.

> **Read this as:** Positive Gram support defines genuine syndrome isometries. Null branches vanish. Specifying the action on the complement makes the recovery a total channel.

V33 / THE OPTIMAL SCALAR FOR TWO SPECTRAL POINTS

An approximate defect has a precise norm meaning

Traditional edition: Definition II.8.6, Proposition II.8.7.

On a two-dimensional code, consider the overlap compression

$$A = PE_a^* E_b P = \operatorname{diag}(11/10, 9/10).$$

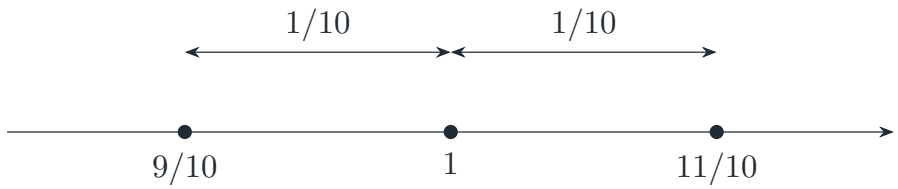
For instance, within the code take $E_a = I$ and $E_b = A$. This declares an error family, not by itself a normalized noise channel. The optimal scalar compression has

$$\inf_{c\in\mathbb{C}} \|A - cI\| = \frac{1}{10}, \qquad c = 1 \text{ attains it.}$$

Indeed, for every complex c, the triangle inequality gives

$$\frac{1}{5} = \left|\frac{11}{10} - \frac{9}{10}\right| \le \left|\frac{11}{10} - c\right| + \left|\frac{9}{10} - c\right|.$$

Thus the larger of the two distances is at least $1/10$, while both distances equal $1/10$ at $c = 1$.



one pair: $1/10$, full family $\{I, A\}$: $1/5$

What one pair contributes to the family defect

For unit code vectors ψ, ϕ, this pair therefore satisfies

$$|\langle E_a\psi, E_b\phi\rangle - \langle\psi, \phi\rangle| \le \frac{1}{10}.$$

The bound is attained on either coordinate vector. For the *whole* declared family $\{I, A\}$, the A^*A compression also enters the maximum: its diagonal entries are $121/100, 81/100$, giving pair defect $1/5$. Hence the full family value is $\varepsilon_{\mathrm{KL}} = 1/5$, not $1/10$.

This distinction prevents a tempting shortcut from one favorable overlap to an approximate correction claim. The quantity measures how close all overlap operators are to scalar action on the code. A recovery fidelity bound requires a declared normalized channel, a metric, and a separate continuity result.

What is checked exactly

For $\varepsilon \in \{0, 1/10, 1/4, 1\}$ the script checks $(A - I)^*(A - I) = \varepsilon^2 I$ for $A = \operatorname{diag}(1 + \varepsilon, 1 - \varepsilon)$ and several rational scalar controls. The triangle argument proves the lower bound for every complex scalar. Checking a finite list of candidates would not establish that conclusion. The family maximum above is also recorded separately.

> **Read this as:** An overlap norm has a useful operational interpretation. Evaluate every error pair, then keep that statement separate from an unproved recovery fidelity estimate.

V34 / SIGN, STABILITY, AND A CONVERGENT EXPANSION

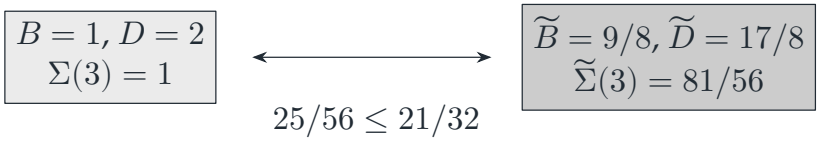
Control the hidden spectral response

Traditional edition: Theorem II.9.4, Proposition II.9.5, Theorem II.9.12.

Retain one coordinate in $H = \begin{pmatrix} 0 & 1 \\ 1 & 2 \end{pmatrix}$, so $A = 0$, $B = 1$, and $D = 2$. In its elimination domain, $\Sigma(z) = 1/(z-2)$. At $z = 3 + \mathrm{i}$,

$$\Sigma(3+\mathrm{i}) = \frac{1-\mathrm{i}}{2}, \qquad \Im\Sigma(z) = -(\Im z)\left|(z-2)^{-1}\right|^2 \le 0.$$

The sign in the upper half plane comes from self-adjoint hidden data. It is not an entrywise sign condition on an arbitrary effective matrix.



common hypotheses: $g = 9/8$, $\delta = 3/4$

A stability estimate with a common spectral gap

Compare $(B, D) = (1, 2)$ with $(\widetilde{B}, \widetilde{D}) = (9/8, 17/8)$ at $z = 3$. Both hidden spectral distances are at least $\delta = 3/4$, and both couplings are bounded by $g = 9/8$. Then

$$|\Sigma - \widetilde{\Sigma}| = \left|1 - \frac{81}{56}\right| = \frac{25}{56}, \qquad \frac{2g}{\delta}|B - \widetilde{B}| + \frac{g^2}{\delta^2}|D - \widetilde{D}| = \frac{21}{32}.$$

The theorem bounds the difference using a common spectral gap. Applying the bound uniformly to a refinement family requires uniform spectral separation and control of the couplings.

A series near zero energy and its exact remainder

At $z = 1/2$, $|z|\,|D^{-1}| = 1/4 < 1$, so

$$\Sigma(z) = -\sum_{n=0}^{\infty} \frac{z^n}{2^{n+1}}.$$

After the first four terms, the exact remainder has magnitude $1/384$. The geometric series controls the infinite tail. The retained check verifies that remainder, the complex sign identity, and the identities for the projected resolvent and bare truncation at four specified real spectral parameters.

At $z = 2$ the hidden inverse fails. At an eigenvalue of the full Hamiltonian, the retained Feshbach inverse fails. Neither point belongs to the resolvent identity's domain. Analytic continuation of a scalar expression does not erase its theorem hypotheses.

> **Read this as:** A uniform effective response requires a uniform gap and coupling bound. Exact small examples show how those hypotheses enter each estimate.

V35 / TWO HIDDEN FREQUENCIES AND A TEST OF LOCAL CLOSURE

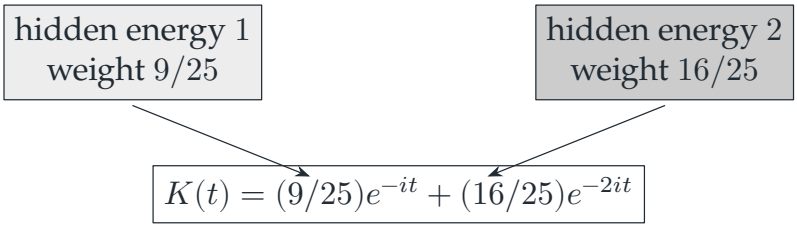
Memory positivity is a Gram identity

Traditional edition: Theorem II.9.9, Theorem II.9.11.

Use retained space $\mathbb{C}$ and hidden space $\mathbb{C}^2$, with $A = 0$, $B = (3/5, 4/5)$, and $D = \operatorname{diag}(1, 2)$. The full Hamiltonian is $\begin{pmatrix} 0 & 3/5 & 4/5 \\ 3/5 & 1 & 0 \\ 4/5 & 0 & 2 \end{pmatrix}$. Its memory kernel is

$$K(t) = \frac{9}{25}e^{-\mathrm{i}t} + \frac{16}{25}e^{-2\mathrm{i}t}, \qquad K(0) = 1.$$

Each oscillatory coefficient is positive although $K(t)$ need not be real or pointwise nonnegative. At $t = \pi/2$, it equals $-16/25 - 9\mathrm{i}/25$.



Positive definite means a matrix test at arbitrary times

For retained scalars v_j and real times t_j, the structural identity is

$$\sum_{j,k} \overline{v}_j K(t_j - t_k) v_k = \left\| \sum_k e^{\mathrm{i}t_k D} B^* v_k \right\|^2 \geq 0.$$

The exact worked check specializes to $t = (0, \pi/2, \pi)$ and $v = (1, 2, -1)$. Its phases lie in $\mathbb{Q}(\mathrm{i})$, so both sides are computed without evaluating trigonometric functions. This Gram test illustrates the factorization. The written identity proves positivity for all choices of times and vectors.

Why this does not close to a bare local equation

With hidden initial state zero, the full system has $\ddot{x}(0) = -(A^2 + BB^*)x(0) = -x(0)$. The bare retained equation $\mathrm{i}\dot{x} = Ax$ would instead give zero acceleration. Therefore exact local closure for every retained initial state fails. More generally, equality of these accelerations forces $BB^* = 0$ and hence $B = 0$.

A nonzero initial hidden vector also supplies the forcing term $Be^{-\mathrm{i}tD}y(0)$. It is additional data, not part of the convolution kernel. The retained checks cover the displayed kernel values, exact Gram factorization, and acceleration defect. The integral equation follows from the written elimination argument.

> **Read this as:** Memory is positive definite through a Gram factorization, not through pointwise signs. Exact bare local closure requires the coupling to vanish.

V36 / STRICT POSITIVITY AND THE GROUND GAP

A positive transfer determines its Hamiltonian

Traditional edition: Theorem II.10.2, Proposition II.10.5.

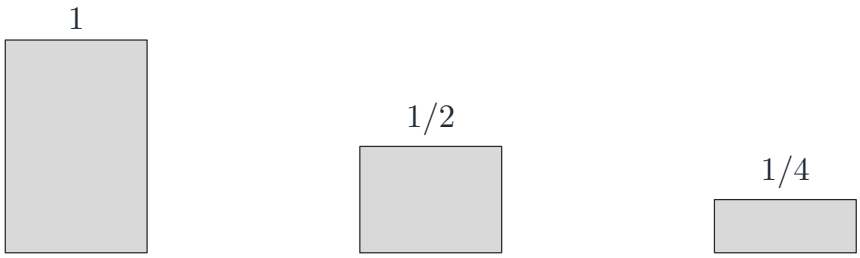
On $\mathcal{H} = \mathbb{C}^3$, take the strictly positive contraction

$$T = \operatorname{diag}(1, 1/2, 1/4), \qquad H = -\log T = \operatorname{diag}(0, \log 2, 2\log 2).$$

At unit Euclidean time, $T = e^{-H}$. The self-adjoint logarithm is unique because the logarithm acts on positive spectral values. At integer time $n \geq 0$,

$$T^n = \operatorname{diag}(1, 2^{-n}, 4^{-n}), \qquad P_0 = \operatorname{diag}(1, 0, 0), \qquad \|T^n - P_0\| = 2^{-n}.$$

The gap $\Delta = \log 2$ determines the rate $e^{-n\Delta}$ exactly in this example.



T^n : $1,\ 2^{-n},\ 4^{-n}$ $\|T^n - P_0\| = 2^{-n}$

Strict positivity is an essential finite hypothesis

For $T' = \operatorname{diag}(1, 0)$, the operator is positive semidefinite, but there is no finite self-adjoint H' on all of $\mathbb{C}^2$ with $T' = e^{-H'}$: every finite eigenvalue of H' exponentiates to a strictly positive value. One may restrict to the positive support, but that changes the space on which the logarithm is defined.

For a family with nontrivial excited spectra, a uniform exponential rate needs a common positive lower bound on the gap. Ground multiplicity does not cause a problem: P_0 selects the entire eigenspace at the minimum energy. For a Hamiltonian whose minimum is $E_0 \neq 0$, the normalized transfer is $e^{-t(H - E_0 I)}$ before taking the limit.

Positivity is retained at several Euclidean times

For arbitrary vectors u_j and nonnegative integer times n_j, the reflected kernel obeys

$$\sum_{j,k} \langle u_j, T^{n_j + n_k} u_k \rangle = \left\| \sum_j T^{n_j} u_j \right\|^2 .$$

This is a finite Gram factorization. The retained run checks the integer semigroup and diagonal ground error for $n = 0, \ldots, 12$, and rejects a logarithm on the full space for the singular control. The written spectral argument justifies the logarithms and extends the functional calculus statement to all times.

> **Read this as:** A positive definite transfer can be logarithmically reconstructed. Ground convergence needs a declared normalization and gap, while continuum reconstruction still needs its own structure.

V37 / FINITE HEAT DATA AND THE QUANTIFIERS

The dimension window has an order of limits

Traditional edition: Theorem II.11.5, Corollary II.11.8.

For the unit circle grid with N sites, the scaled eigenvalues are $\lambda_N(k) = 4N^2 \sin^2(\pi k/N)$. Put $Z_N(t) = \sum_k e^{-t\lambda_N(k)}$ and $d_N(t) = 2t \sum_k \lambda_N(k) e^{-t\lambda_N(k)} / Z_N(t)$.

At the single time $t = \log 2/16$, two small grids admit exact rational heat weights:

N	spectrum	Z_N	$\sum \lambda e^{-t\lambda}$	$d_N/\log 2$
2	$(0, 16)$	$3/2$	8	$2/3$
4	$(0, 32, 32, 64)$	$25/16$	20	$8/5$

These are unnormalized traces. Normalizing by N changes Z_N but leaves the logarithmic derivative at that fixed grid unchanged.



The theorem uses two separate choices

For each $\varepsilon > 0$, first choose a fixed positive time t_ε so that the continuum torus dimension differs from one by less than $\varepsilon/2$. Then choose N_ε so that every $N \geq N_\varepsilon$ differs from that continuum value by less than $\varepsilon/2$ at the *same time*. This proves one controlled intermediate time for all sufficiently fine grids.

It does not assert a uniform interval width from that argument, a moving time t_N with no extra estimates, or a dimension plateau at every scale. At fixed finite N, $d_N(t) \to 0$ as $t \downarrow 0$ and as $t \to \infty$. By contrast, first taking $N \to \infty$ at positive t and then taking $t \downarrow 0$ yields the continuum dimension.

Where the infinite tail is controlled

At a fixed time, the proof bounds centered modes below by $16k^2$ and above by $4\pi^2 k^2$. The summable Gaussian dominators control both the heat trace and its first moment. A finite grid table supplies neither those tails nor the quantifiers. The retained check verifies the two displayed spectra, rational weights, traces, and dimension coefficients. It also distinguishes the unscaled cycle with four sites from the scaled unit circle grid.

> **Read this as:** The strengthened window result proves convergence after fixing a suitable time. The exact table is a worked calculation, not its proof.

V38 / THE IMAGE OF AN ISOMETRY IS NOT THE WHOLE LEVEL

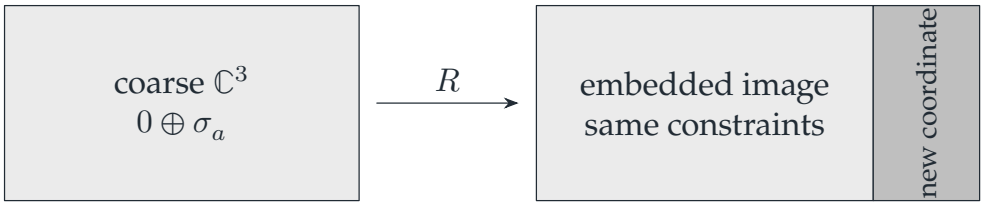
Transport constraints without hiding closure

Traditional edition: Theorem II.12.2, Theorem II.12.5, Proposition II.12.6.

On $\mathbb{C}^3 = \mathbb{C}\,|0\rangle \oplus \mathbb{C}^2$, use $C_a = 0 \oplus \sigma_a$ for $a = x, y, z$. The common kernel is $\mathbb{C}\,|0\rangle$, and the full algebra closes:

$$[C_x, C_y] = 2\mathrm{i}C_z, \qquad [C_y, C_z] = 2\mathrm{i}C_x, \qquad [C_z, C_x] = 2\mathrm{i}C_y.$$

These are uncompressed identities. They supply an actual closure test in the quotient by the constraint span, unlike the automatic compressed zero on the physical kernel.



closure on im R transfers, and the new complement needs its own test

Exact transport holds on the coarse image

Embed by the coordinate isometry $R : \mathbb{C}^3 \to \mathbb{C}^4$ and set $\widetilde{C}_a = C_a \oplus 1$. Then $\widetilde{C}_a R = RC_a$, so

$$[\widetilde{C}_a, \widetilde{C}_b]R = R[C_a, C_b].$$

The coarse physical vector maps into the fine common kernel. However, the same prescribed Pauli structure does *not* close on the whole fine level: on the added coordinate the commutator is zero, whereas $2\mathrm{i}\widetilde{C}_z$ is $2\mathrm{i}$. Exact transport constrains the image of R and leaves its orthogonal complement as separate data.

An approximate residual is also explicit

Perturb only $\widetilde{C}_x$ by $(1/10)\,|0\rangle\langle 0|$. For the unit coarse physical vector, the fine constraint residual is exactly $1/10$. The intertwining defect has the same norm. The general result for approximate transport controls these residuals and commutator errors using the defect sizes and a common bound on the constraint norms. A nonzero anomaly remains an error that must be controlled.

The retained checks verify all three coarse commutators, the isometry, each constraint intertwining, all nine commutator transports, and the residual. The added coordinate provides a counterexample to extending the identity on the image to the whole space. Unbounded constraints would additionally require a common invariant domain.

> **Read this as:** Closure is a statement about the operator algebra. Refinement intertwining transports it to the embedded image. The new degrees of freedom require their own control.

V39 / EXACT EMBEDDINGS AND A SUMMABLE TAIL

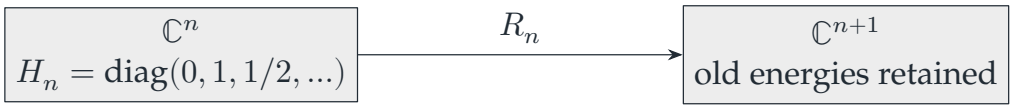
Two routes to a bounded Hamiltonian limit

Traditional edition: Theorem II.13.2, Theorem II.13.4, Corollary II.13.5.

For the exact route, let $\mathcal{H}_n = \mathbb{C}^n$ with coordinate inclusions and

$$H_n = \operatorname{diag}(0, 1, 1/2, \dots, 1/(n-1)), \qquad H_1 = (0).$$

The old energies are retained at every level, $H_{n+1}R_n = R_nH_n$, and $\|H_n\| \le 1$. On the Hilbert space of the direct limit $\ell^2(\mathbb{N}_0)$, the diagonal sequence defines a bounded self-adjoint H_∞. Projectors onto even addresses also intertwine and give a fixed complete system of two packets in the limit.



fixed $\mathbb{C}^2$: $H_n = \operatorname{diag}(0, 1 + 2^{-n})$
tail $\|H_n - H\| = 2^{-n}$

Compatibility and boundedness are different assumptions

The equally compatible tower $\operatorname{diag}(0, 1, 2, \dots, n-1)$ has growing norms. It does not satisfy the bounded direct limit theorem. Its natural diagonal operator needs a separately specified domain. Dropping the uniform norm hypothesis does not supply that domain argument.

For the norm route, work instead on the *single fixed space* $\mathbb{C}^2$ and set

$$H_n = \operatorname{diag}(0, 1 + 2^{-n}), \qquad H = \operatorname{diag}(0, 1).$$

Here $\|H_{n+1} - H_n\| = 2^{-(n+1)}$ and $\|H_n - H\| = 2^{-n}$. The summable tail supplies an error bound for every n. For $|t| \le T$, the paper's Duhamel estimate gives

$$\left\|e^{-\mathrm{i}tH_n} - e^{-\mathrm{i}tH}\right\| \le T2^{-n}.$$

The Euclidean counterpart holds on $0 \le t \le T$ because both Hamiltonians are nonnegative. If packet projectors also converge in norm, leakage operators converge uniformly on these time intervals.

Execution scope

Exact inclusions and projector compatibility are checked through level eight. The two-dimensional tail identities are checked for $n = 0, \dots, 12$. Their infinite conclusion uses the displayed geometric series and the theorem's analytic estimate. A finite prefix cannot certify an unspecified continuation of a tower.

> **Read this as:** Exact embedded compatibility uses a uniform norm bound. Approximate convergence uses a common space and summable defects. Keep the hypotheses of these two routes explicit.

V40 / REFLECTION GRAMS, TRACES, AND FINAL SCOPE

Choose the topology that preserves the quantity

Traditional edition: Theorem II.13.6, Theorem II.13.8, Section II.14.

Let $q_n = 1/2+2^{-(n+2)}$ and define the scalar reflected kernel $C_n(j,k) = 1+q_n^{j+k}$ on nonnegative integers. Each finite Gram matrix is a sum of two positive rank-one matrices, and pointwise convergence gives $C(j,k) = 1 + (1/2)^{j+k}$. For times $(0,1,2)$ and coefficients $(1,-2,1)$,

$$\sum_{j,k} v_j C_n(j,k) v_k = (1-q_n)^4 \geq 0.$$

This exact check illustrates how finite quadratic forms pass positivity to the limit.



positive trace-class control: norm convergence alone does not preserve a trace

Operator norm does not preserve trace in growing rank

On ℓ^2, let P_n select the first n coordinates and set $A_n = P_n/n$. Then $\|A_n\| = 1/n \to 0$ while $\operatorname{Tr} A_n = 1$ for every n. These positive trace-class operators show why the choice of topology matters. Their zero limit is not the heat operator of a finite Hamiltonian.

For transfers on two states $T_n = \operatorname{diag}(1, q_n) = e^{-H_n}$, with $H_n = \operatorname{diag}(0, -\log q_n)$ at unit time, the error in trace norm is $2^{-(n+2)}$ and the heat traces converge to $3/2$. The criterion for convergence of spectral dimension additionally assumes convergence of the first heat moments in trace norm and a nonzero limiting heat trace. Convergence of the heat trace alone does not determine that quotient.

The retained evidence and the remaining open targets

The extension includes retained exact checks over specified finite ranges in $\mathbb{Q}(\mathrm{i})$ using `Fraction` from Python's standard library. The original appendix's record of 180 checks, including symbolic derivatives, is also retained. Both records come from earlier executions. This prose revision adds no symbolic or Lean kernel run. All model and vector sources remain supplied.

The saved v0.6.0 ledger lists 19 finite items with their recorded hypotheses. Its five original targets for continuum and physical reconstruction remain open. The strengthened edition supplies analytic proofs and criteria for bounded limits. These results and examples do not establish the unresolved physical existence claims.

> **Read this as:** Use pointwise convergence for finite positivity tests, operator norm for bounded dynamics and constraints, and trace norm for heat traces. Every conclusion keeps its own hypotheses and evidence scope.

References

[1] Cédric Bény, Achim Kempf, and David W. Kribs, *Generalization of quantum error correction via the Heisenberg picture*, Physical Review Letters **98** (2007), no. 10, 100502.

[2] Michael V. Berry, *Quantal phase factors accompanying adiabatic changes*, Proceedings of the Royal Society of London. Series A **392** (1984), no. 1802, 45–57.

[3] Rajendra Bhatia, *Matrix analysis*, Graduate Texts in Mathematics, vol. 169, Springer, New York, 1997.

[4] Sergey Bravyi, David P. DiVincenzo, and Daniel Loss, *Schrieffer Wolff transformation for quantum many body systems*, Annals of Physics **326** (2011), no. 10, 2793–2826.

[5] Man Duen Choi, *Completely positive linear maps on complex matrices*, Linear Algebra and its Applications **10** (1975), no. 3, 285–290.

[6] Alain Connes, *Noncommutative geometry*, Academic Press, San Diego, 1994.

[7] Paul A. M. Dirac, *Lectures on quantum mechanics*, Yeshiva University, New York, 1964.

[8] Herman Feshbach, *Unified theory of nuclear reactions*, Annals of Physics **5** (1958), no. 4, 357–390.

[9] William Fulton and Joe Harris, *Representation theory: A first course*, Graduate Texts in Mathematics, vol. 129, Springer, New York, 1991.

[10] James Glimm and Arthur Jaffe, *Quantum physics: A functional integral point of view*, second ed., Springer, New York, 1987.

[11] Marc Henneaux and Claudio Teitelboim, *Quantization of gauge systems*, Princeton University Press, Princeton, New Jersey, 1992.

[12] Tosio Kato, *On the adiabatic theorem of quantum mechanics*, Journal of the Physical Society of Japan **5** (1950), 435–439.

[13] ———, *Perturbation theory for linear operators*, Springer, Berlin, 1995.

[14] Emanuel Knill and Raymond Laflamme, *Theory of quantum error correcting codes*, Physical Review A **55** (1997), no. 2, 900–911.

[15] Karl Kraus, *States, effects, and operations*, Lecture Notes in Physics, vol. 190, Springer, Berlin, 1983.

[16] Goran Lindblad, *On the generators of quantum dynamical semigroups*, Communications in Mathematical Physics **48** (1976), no. 2, 119–130.

[17] Sadao Nakajima, *On quantum theory of transport phenomena: steady diffusion*, Progress of Theoretical Physics **20** (1958), no. 6, 948–959.

[18] Michael A. Nielsen and Isaac L. Chuang, *Quantum computation and quantum information*, tenth anniversary ed., Cambridge University Press, Cambridge, 2010.

[19] Konrad Osterwalder and Robert Schrader, *Axioms for Euclidean Green functions*, Communications in Mathematical Physics **31** (1973), no. 2, 83–112.

[20] ———, *Axioms for Euclidean Green functions. II*, Communications in Mathematical Physics **42** (1975), no. 3, 281–305.

[21] Michael Reed and Barry Simon, *Methods of modern mathematical physics. I: Functional analysis*, Academic Press, New York, 1972.

[22] Benjamin Schumacher and Michael A. Nielsen, *Quantum data processing and error correction*, Physical Review A **54** (1996), no. 4, 2629–2635.

[23] Jean Pierre Serre, *Linear representations of finite groups*, Graduate Texts in Mathematics, vol. 42, Springer, New York, 1977.

[24] W. Forrest Stinespring, *Positive functions on C star algebras*, Proceedings of the American Mathematical Society **6** (1955), no. 2, 211–216.

[25] John C. Strikwerda, *Finite difference schemes and partial differential equations*, second ed., Society for Industrial and Applied Mathematics, Philadelphia, 2004.

[26] Dmitri V. Vassilevich, *Heat kernel expansion: user's manual*, Physics Reports **388** (2003), no. 5, 279–360.

[27] John Watrous, *The theory of quantum information*, Cambridge University Press, Cambridge, 2018.

[28] Frank Wilczek and A. Zee, *Appearance of gauge structure in simple dynamical systems*, Physical Review Letters **52** (1984), no. 24, 2111–2114.

[29] Robert Zwanzig, *Ensemble method in the theory of irreversibility*, The Journal of Chemical Physics **33** (1960), no. 5, 1338–1341.